

MOLECULAR DYNAMIC SIMULATION OF
PATCHOULOL BIOTRANSFORMATION



NORUL AFWAN BINTI KAMARUDIN

MASTER OF ENGINEERING (CHEMICAL)

UNIVERSITI MALAYSIA PAHANG

MOLECULAR DYNAMIC SIMULATION OF PATCHOULOL
BIOTRANSFORMATION

The logo of the University of Malaysia Pahang is a shield-shaped emblem. It features a central white diamond with a yellow diamond inside it. Two curved lines, one light blue and one light green, arch over the central diamond. The shield is divided into four quadrants: top-left is light blue, top-right is light purple, bottom-left is light purple, and bottom-right is light blue.

NORUL AFWAN BINTI KAMARUDIN

Thesis submitted in fulfilment of the requirements for the award of the degree of
Master of Engineering (Chemical)

Faculty of Chemical Engineering and Natural Resources
UNIVERSITI MALAYSIA PAHANG

MARCH 2016

UNIVERSITI MALAYSIA PAHANG

DECLARATION OF THESIS AND COPY RIGHT

Author's Full Name : NORUL AFWAN BINTI KAMARUDIN
Date of birth : 23 MAY 1984
Title : MOLECULAR DYNAMIC SIMULATION OF
PATCHOULOL BIOTRANSFORMATION
Academic Session : 2014/2015

I declared that this thesis is classified as:

- | | | |
|--------------------------|---------------------|--|
| <input type="checkbox"/> | CONFIDENTIAL | (Contains confidential information under the Official Secret Act 1977)* |
| <input type="checkbox"/> | RESTRICTED | (Contains restriction information as specified by the organization where research was done)* |
| <input type="checkbox"/> | OPEN ACCESS | I agree that my thesis to be published as online open access (Full text) |

I acknowledge that University Malaysia Pahang reserve the right as follows:

1. The Thesis is the Property of University Malaysia Pahang
2. The Library of University Malaysia Pahang has right to make copies for the purpose of research only.
3. The Library has the right to make copies of the thesis for academic exchange.

Certified by :

(Student's Signature)

(Supervisor's Signature)

New IC/Passport Number

Date :

Name of Supervisor

Date :

NOTES: *if the thesis is CONFIDENTIAL or RESTRICTED, please attach with the letter page 2 from the organization with period and reasons for confidentiality or restriction.



**Thesis submitted in fulfillment of the requirements for the award of the degree of
Master of Engineering.**



Universiti
Malaysia
PAHANG
Engineering • Technology • Creativity

SUPERVISOR'S DECLARATION

We hereby declare that we have checked this thesis and in our opinion, this thesis is adequate in terms of scope and quality for the award of the degree of Master of Engineering (Chemical).

(Supervisor's Signature)

FULL NAME :

POSITION : SENIOR LECTURER

DATE :

(Co-supervisor 's Signature)

FULL NAME :

POSITION : PROFEEESOR

DATE :



STUDENT'S DECLARATION

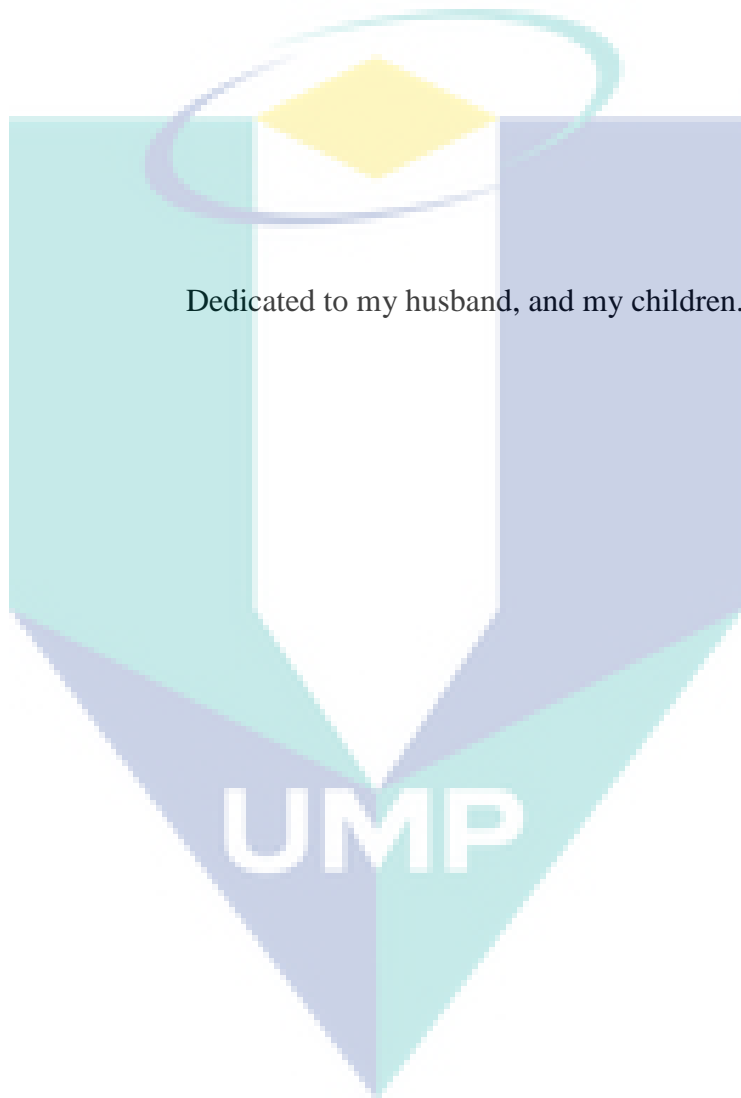
I hereby declare that the work in this thesis is based on m original work except for quotations and citation which have been duly acknowledged. I also declare that it has not been previously or concurrently submitted for any degree at Universiti Malaysia Pahang or any other institutions.

(Author's Signature)

FULL NAME :
POSITION :
DATE :

A large, semi-transparent watermark of the UMP logo is centered on the page. It consists of the teal and blue shield-like emblem with the letters "UMP" in white, bold, sans-serif font across its base.

UMP



ACKNOWLEDGEMENTS

In the Name Of Allah s.w.t, The Most Gracious, The Most Compassionate and The Most Merciful, Thanks to the Al-Mighty for giving me the ability to complete this Master study.

Top in my list, I would like to acknowledge the contributions of my great supervisor, Dr. Hajjah Fatmawati binti Adam for her valuable comments and guidance during the completion of this study. Special thanks to Siti Hana Abu Bakar, now completing her PhD, for all the help that has been given from the starting point to the end. I also would like to express very special thanks to my co-supervisor Professor Dr. Mashitah bt Mohd. Yusoff for her suggestions and co-operation throughout the study. I also sincerely thanks for the time spent proofreading and correcting my many mistakes. Thanks also go to my best friend, Dr. Noormazlinah Ahmad that always there in my hard and critical situation. My sincere thanks also go to the staff of the Faculty of Chemical and Natural Resources Engineering Department and IPS Department who had helped me in many ways to complete my study on the time given.

Special dedication for my beloved husband, Mohd Jazlanuddin bin Azmi, my children, Khairunnisa', Khairunnadia and Aqil, thanks for all the understanding and inspiration that are given to me. Thanks again because always keep me strong to complete this journey. My gratitude also goes to all my family members, my dear parent namely, Haji Kamarudin bin Jaafar and Hajjah Zamnah bt Wan Abdullah, my sibling, Nurul Huda and Norol Farhana, who consistently encouraged me during the difficult time. They made me believe that nothing is impossible in this world can be achieved. My in laws, thanks for all the support and motivation that have made me become stronger. To all my labmates, thanks a lot for the cheering moments that we had together and made my stay at FKKSA unforgettable.

Again, thank you so much, may Allah s.w.t A-Mighty reward them accordingly and be with us all the time.

ABSTRACT

Biotransformation is a branch of biotechnology process that produces the natural compound in the perfume industry naturally. Molecular dynamic simulation is a powerful tool which can be used to understand the molecule interaction at the molecular level through the measurement of the interaction strength between the molecules involved in the biotransformation process. The main objective of this paper is to present the development of a computer-aided simulation model for biotechnology process system. In this study, molecular dynamic (MD) simulation was used to investigate the effect of oxygen from dissolved oxygen gas and water molecule on the structural properties of an important chemical compound in patchouli oil, namely patchoulol, and also the interaction between them. Through the hydroxylation process, the hydroxylase enzyme catalyzes the formation of hydroxyl group on patchoulol by incorporating one atom of oxygen. This process is predicted to produce a new high value compound namely 10-hydroxypatchoulol. It is the intermediate compound for the formation of norpatchoulol, which contributes significantly towards the patchouli oil scent. For better understanding and comparison, the structure of the patchoulol, oxygen and water was simulated in three systems, namely pure, binary and tertiary system. The Condensed-phase Optimized Molecular Potential of Atomic Simulation Studies, (COMPASS) force field was used to run the simulation. Simulations were performed for 1200 ps at 301 K and 1 atm for the liquid-solid state of the mixtures. Radial distribution function was analyzed from the trajectory files to measure the strength of intermolecular interaction between molecules. The result from the modelling simulation system shows the patchoulol is more interested to the dissolved oxygen gas in producing the van der Waals bond. The interaction is presented by sharp peak of RDF with the nearest distance at 3.75Å which it will initiate the formation of hydroxyl group in patchoulol molecule. Meanwhile the experimental work has undergone four stages, microorganism preparation, fermentation medium preparation, fermentation procedure and sample analysis. FTIR analysis covers the analysis from experimental and stimulated from the Gaussian Software analysis. By comparing of the experimental and stimulated data, it shows that there are match peaks at 3200cm⁻¹, showing that the H-bonded in the hydroxyl group and at 1150cm⁻¹, and that the C-O stretch, present as the primary alcohol. The result on both analysis showed the 10-hydroxypatchoulol might be present in the sample of product. GCMS has detected no appearance of 10-hydroxypatchoulol, but it detected 1(2H)-Naphthalenone, octahydro-4,8 a-dimethyl-6-(1-methylethenyl) (4.alpha.,4a.beta., 6.alpha.,8a.beta.)- compound with chemical formula C₁₅H₂₄O. As a conclusion the objective from the modelling aspect was achieved, and produce the new compound instead of the predicted compound, 10hydroxypatchoulol in the experimental work.

ABSTRACT

Biotransformasi adalah satu cabang proses bioteknologi yang menghasilkan sebatian semulajadi dalam industri minyak wangi secara semula jadi. Simulasi dinamik molekul adalah teknologi yang terkini yang boleh digunakan untuk memahami interaksi antara molekul pada peringkat molekul melalui pengukuran kekuatan interaksi antara molekul yang terlibat dalam proses biotransformasi ini. Objektif utama kertas kerja ini adalah untuk membentangkan pembangunan model bantuan komputer simulasi untuk sistem proses bioteknologi. Dalam kajian ini, dinamik molekul (MD) simulasi digunakan untuk mengkaji kesan oksigen daripada gas oksigen terlarut dan molekul air kepada sifat-sifat struktur sebatian kimia penting dalam minyak nilam, iaitu patchoulol, dan juga interaksi antara mereka. Melalui proses hydroxylation itu, enzim hydroxylase memangkinkan pembentukan kumpulan hidroksil, dengan menggabungkan satu atom oksigen pada patchoulol. Proses ini adalah dijangkakan akan menghasilkan sebatian baru yang bernilai tinggi iaitu 10 hydroxypatchoulol. Ia adalah sebatian perantaraan untuk pembentukan norpatchoulenol, yang menyumbang didalam penghasilan bau wangi minyak nilam. Untuk pemahaman yang lebih baik dan perbandingan, struktur patchoulol, oksigen dan air telah disimulasikan dalam tiga sistem, tulen, binari dan tertiar. Force-field Condensed-phase Optimized Molecular Potential of Atomic Simulation Studies,, (COMPASS) telah digunakan untuk menjalankan simulasi. Simulasi dilaksanakan untuk 1200 ps pada 301 K dan 1 atm untuk keadaan cecair-pepejal daripada campuran. Fungsi Taburan Radial (RDF) telah dianalisis dari fail trajektori untuk mengukur kekuatan interaksi antara molekul. Hasil daripada sistem simulasi menunjukkan patchoulol yang lebih berminat untuk gas oksigen terlarut dalam menghasilkan ikatan van der Waals. Interaksi itu dikemukakan oleh puncak RDF dengan jarak yang paling hampir di 3.75Å yang akan memulakan pembentukan kumpulan hidroksil dalam molekul patchoulol. Sementara itu kerja eksperimen telah melalui empat peringkat, penyediaan mikroorganisma, penyediaan media penapaian, prosedur penapaian dan analisis sampel. Analisis FTIR meliputi analisis daripada eksperimen dan simulasi daripada analisis Gaussian Software. Melalui perbandingan data eksperimen dan simulasi, ia menunjukkan bahawa terdapat padanan puncak pada 3200cm⁻¹, menunjukkan H-terikat dalam kumpulan hidroksil dan pada 1150cm⁻¹, regangan CO hadir sebagai alkohol primer. Hasil kedua-dua analisis menunjukkan 10 hydroxypatchoulol mungkin hadir dalam sampel produk. Analisis GCMS telah menunjukkan tiada kesan sebarang kewujudan 10 hydroxypatchoulol, tetapi 1 (2H) - Naphthalenone, octahydro-4.8 a-dimetil-6- (1-methylethenyl) (4.alpha., 4a.beta., 6.alpha., 8a.beta) -. kompaun dengan formula kimia C₁₅H₂₄O, telah dikesan. Kesimpulannya matlamat dari aspek simulasi yang telah dicapai, dan menghasilkan sebatian yang baru dalam ujikaji.

TABLE OF CONTENT

	Page
SUPERVISOR'S DECLARATION	ii
STUDENT'S DECLARATION	iii
ACKNOWLEDGEMENTS	v
ABSTRACT	vi
ABSTRACT	vii
TABLE OF CONTENT	viii
LIST OF FIGURE	xi
LIST OF TABLE	xiii
CHAPTER 1 INTRODUCTION	
1.1 Introduction	1
1.2 Background Of The Study	1
1.3 Motivation	2
1.4 Research Objectives	3
1.5 Research Scope	4
1.6 Thesis Outline	5
CHAPTER 2 LITERATURE REVIEW	
2.1 Introduction	6
2.2 Molecular Interaction	6
2.2.1 Intermolecular Interaction	7
2.2.2 Intramolecular Interaction	13
2.3 Computer Simulation For Microscopic System	14
2.4 Molecular Dynamic Simulation.	14
2.5 Radial Distribution Function	15
2.5.1 Radial Distribution Function in Solid	17
2.5.2 Radial Distribution Function in Liquid	18
2.5.3 Radial Distribution Function in Gas	19
2.6 Molecular Mechanic Force Field	20

2.7	Potential Energy Function	21
2.7.1	Bonded Energy And Non-Bonded Energy	21
2.8	Ensemble In Molecular Dynamic Simulation	25
2.9	Patchoulol As A Substrate In 10-Hydroxypatchoulol Production	27
2.10	10-Hydroxypatchoulol	30
2.11	Hydroxylation	32
2.12	Aspergillus Niger As The Biocatalyst In The Hydroxylation Process	34
2.13	Analytical Equipment For Data Analysis	35
2.14	Significant Of The Molecular Dynamic Simulation Studies In The Biotransformation Work	38
 CHAPTER 3 MATERIALSAND METHODS		
3.1	Introduction	40
3.2	Molecular Dynamic Simulation	40
3.2.1	Geometry Optimization And Energy Minimization	41
3.2.2	Equilibration And Simulation Running Phases	46
3.2.3	Trajectory Analysis	47
3.3	Analysis Of Radial Distribution Function	48
3.3.1	Rdf Analysis In Pure System	48
3.3.2	Rdf Analysis In Binary System	50
3.3.3	Rdf Analysis In Tertiary System	52
3.4	Experimental Work On Biotransformation Process	53
3.4.1	Preparation of Microorganism	54
3.4.2	Preparation of Fermentation Medium	55
3.4.3	Fermentation Procedure	56
3.5	Analysis Of Chemical Compounds Using Gas Chromatography-Mass Spectrometer (GC/MS)	57
3.6	Analysis Of Fourier Transform Infra Red (FTIR)	60
3.6.1	Experimental FTIR Procedure	60
3.6.2	Gaussian FTIR Procedure	61
 CHAPTER 4 RESULT AND DISCUSSION		

4.1	Introduction	64
4.2	Result Of Molecular Dynamic Simulation	64
4.3	Pure Simulation System	65
4.3.1	Pure Patchoulol System	65
4.3.2	Pure Oxygen System	66
4.3.3	Pure Water System	67
4.4	Binary Simulation System	68
4.4.1	Binary Patchoulol/Oxygen System	69
4.4.2	Binary Patchoulol/Water System	70
4.5	Tertiary System	73
4.5.1	Radial Distribution Functions Of H39 With O1, O2 And O3.	73
4.5.2	Radial Distribution Functions Of H41 With O1, O2 And O3.	74
4.5.3	Radial Distribution Functions Of O3---O3 In Three Systems	76
4.6	Experimental Results	77
4.7	FTIR Analysis	78
4.7.1	Experimental FTIR Analysis	78
4.7.2	FTIR Simulated By Gaussian Analysis	79
4.8	GCMS Analysis	82
4.9	Conclusion	92
CHAPTER 5 CONCLUSION AND RECOMMENDATION		
5.1	Introduction	93
5.2	Overall Conclusion	93
5.3	Recommendation For Future Works.	94
REFERENCES		96

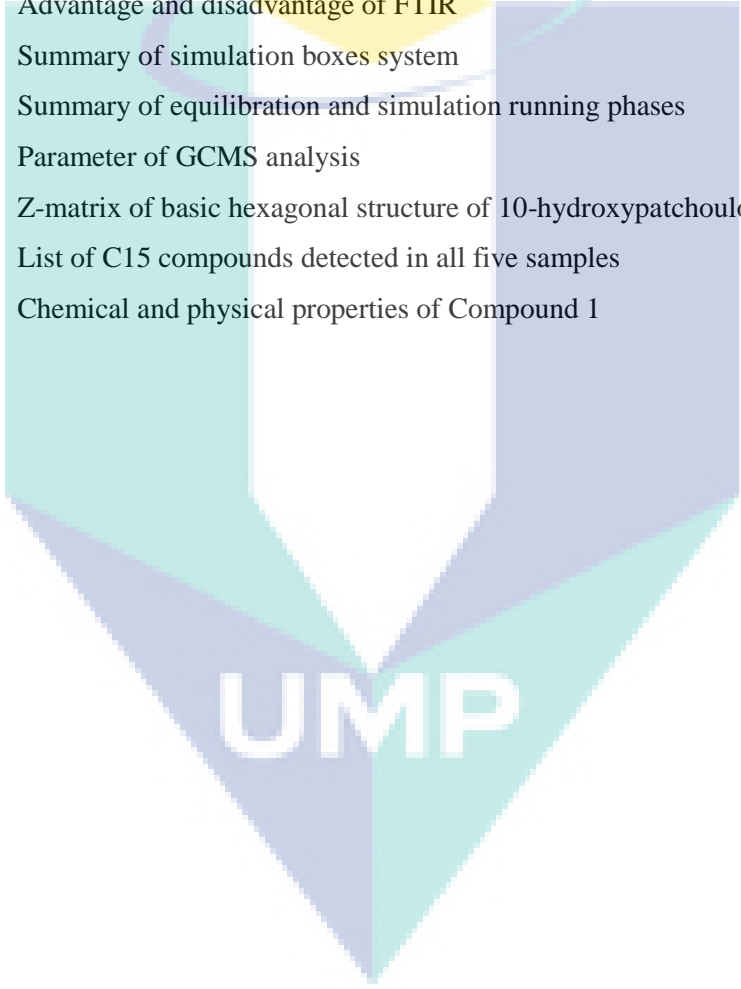
LIST OF FIGURE

Figure	Title	Page
1.1	Overall biotransformation process for norpatchelenol production	3
1.2	Summary of the research scope	4
2.1	The intermolecular and intramolecular interaction of HCl liquid molecules	7
2.2	The classification of intermolecular interaction	8
2.3	Dipole- dipole interaction	9
2.4	Polar-induced polar interaction	9
2.5	Dispersion interaction	10
2.6	Ion-dipole interaction	11
2.7	The hydrogen bond in water molecule	11
2.8	Coulumbic interaction between two atoms	12
2.9	Ionic bonding in NaCl	13
2.10	Covalent Bonding in hydrogen gas	14
2.11	Two dimensional structure of liquid	16
2.12	Typical sketch for radial distribution function	16
2.13	Typical radial distribution function graph of solid	18
2.14	Experimental H-H, O-O, and O-H radial pair distribution functions (RDFs)	18
2.15	Typical radial distribution function graph of liquid	19
2.16	Typical radial distribution function graph of gas	20
2.17	Three movements in bonded energy.	22
2.18	Typical Lennard-Jones potential graph	24
2.19	Structure of (+)-(1S,3S,6R,7R,8R)-Patchoulol and (-)- (1R,3R,6S,7S,8S)-Patchoulol	28
2.20	24 Common compounds in patchouli essential oil	29
2.21	Molecular structure of the 10-hydroxypatchoulol	30
2.22	Production of 10-hydroxypatchoulol	32
2.23	The hydroxylation of patchoulol	33
2.24	An example of <i>Aspergillus niger</i>	35
2.25	Transformation of the Ethylbenzene to Phenylethanol by <i>Aspergillus niger</i>	35
2.26	Diagram of the FTIR	38
3.1	Molecular dynamic simulation step	41
3.2	a) Geometry optimization button and b) Energy minimization button	42
3.3	A supercell containing the 20 molecules of patchoulol in a pure patchoulol system	44
3.4	a) Illustration and b) the concept and working mechanism of periodic boundary conditions	46
3.5	Schematic atomic labelling for a) patchoulol b) oxygen and c) water molecules.	48
3.6	Illustration of hydrogen bond formation between H39 and O1 in pure patchoulol system	49

3.7	Illustration of interaction between O3---O3 in pure oxygen system.	49
3.8	Illustration of interaction between H2---O2 in pure water system	50
3.9	Simple screening simulation	51
3.10	Illustration of van der Waals interaction between a) H41 and O3 and the hydrogen bond interaction between b) H39 and O3	52
3.11	Illustration of hydrogen bonds interaction between a) H41 and O2 b) H39 and O2	52
3.12	Rdf analysis in the tertiary system	53
3.13	Experimental section	53
3.14	Photos of a) magnetic mixer and b) autoclave used in this study	55
3.15	The process of subculture preparation	55
3.16	The transferring hyphae to the fermentation medium process	56
3.17	Summarized step to obtain the 10-hydroxylpatchoulol	58
3.18	Gas chromatography-mass spectrometer (GC/MS) instrument	60
3.19	FTIR instrument	61
3.20	The optimized structure of 10-hydroxypatchoulol	62
4.1	Radial distribution function of H41--- O1 and H39---O1 in pure patchoulol system.	67
4.2	The comparison of radial distribution functions of O3---O3 in pure oxygen system in this work and Thapa and Adhikari, (2013).	68
4.3	Radial distribution function of H2---O2 in pure water liquid system	69
4.4	Radial distribution function of H39---O3 and H41---O3 in binary patchoulol/oxygen system	70
4.5	Radial distribution function of O3---O3 in pure and binary patchoulol/oxygen system showing unchanged structure	71
4.6	Radial distribution function of H39---O2 and H41---O2 in binary patchoulol/water system	72
4.7	Radial distribution function of a) H41 and b) H39 with O2 and O3.	73
4.8	Radial distribution function of H39 with O1, O2 and O3 in tertiary patchoulol/oxygen/water system	75
4.9	Radial distribution function of H41 with O1, O2 and O3 in tertiary patchoulol/oxygen/water system	76
4.10	Radial distribution function of H41 with O3 in binary and tertiary system	77
4.11	Comparison of the radial distribution function of O3---O3 in three systems	78
4.12	The C-O stretch in sample of hydroxylation process	80
4.13	FTIR analysis for both samples	82
4.14	The stimulated IR spectrum	83
4.15	The study of the pathway involved in the process	84
4.16	a) GCMS analysis of Sample 1	85
4.17	C15 compound detected in GCMS	92

LIST OF TABLE

Table no	Title	Page
2.1	The classification of three type of ensemble process	26
2.2	Physical properties of 10-hydroxypatchoulol	30
2.3	Comparison between microbial transformation with animal and plant cell culture	31
2.4	The various hydroxylation yield using patchoulol as substrate	34
2.5	Advantage and disadvantage of GCMS compared to LCMS	36
2.6	Advantage and disadvantage of FTIR	37
3.1	Summary of simulation boxes system	44
3.2	Summary of equilibration and simulation running phases	46
3.3	Parameter of GCMS analysis	58
3.4	Z-matrix of basic hexagonal structure of 10-hydroxypatchoulol	63
4.1	List of C15 compounds detected in all five samples	90
4.2	Chemical and physical properties of Compound 1	91

The logo for UMP (Universitas Muhammadiyah Purwokerto) is a large, downward-pointing arrow shape. It is composed of several overlapping geometric shapes in shades of teal, light blue, and purple. The letters 'UMIP' are written in a bold, white, sans-serif font across the center of the arrow.

UMIP

CHAPTER 1

INTRODUCTION

1.1 Introduction

The purpose of this chapter is to discuss the research background, motivations, objectives and detail structure of the thesis. This chapter also explains the importance of the investigation of the conversion of patchoulol to 10-hydroxypatchoulol at molecular level.

1.2 Background of the Study

Essential oil is an aromatic liquid that is extracted from various parts of the plants (Buchbauer and Baser, 2010). It contains the true essence of the plant and has many therapeutic benefits. Patchouli essential oil extracted from dried Patchouli (*Pogostemon cablin*) leaves is an important ingredient in many fragrant products such as perfumes and is also used widely in medicine. In general, patchouli oil consists of over 24 different organic compounds that contribute to their fragrance. Its marker compound, patchouli alcohol ($C_{15}H_{26}O$) or patchoulol is a terpene. According to Suhara et al. (1981), patchoulol can be converted to 10-hydroxypatchoulol through biotransformation with a *Pithomyces species*, a fungi. 10-Hydroxypatchoulol is the starting compound for

the production of various flavour compounds such as nor-patchoulenol. Biotransformation has become an important approach or technique to produce a natural fragrance substance instead of direct extraction and chemical synthesis. The biotransformation process originally started with vinegar production around 2000 years BC and remains the best example for the microbial oxidation process (Vasic-Racki, 2006). This process uses the microbe as the modifying agent to transform one compound to another, which is catalyzed by specific enzymes.

Over the last two decades, the application of molecular mechanic methods had increased in many areas of biochemical research. Molecular dynamics simulation is one of the methods that can be used to understand the physical movements of atoms and molecule and also the interaction between them (Allen, 2004). Through molecular dynamic simulation, the transformation of patchoulol ($C_{15}H_{26}O$) to 10-hydroxypatchoulol ($C_{15}H_{26}O_2$) through biotransformation with *Aspergillus sp*, can be explored at the molecular level. In this study, the simulation is carried out in the solution phase. The entire compound in this simulation represents the liquid phase, where oxygen will be simulated as dissolved oxygen. The strength of intermolecular interaction which exists amongst the molecules will be calculated by the radial distribution function (RDF) which describes the probability of finding the nearest neighbour atom at a given distance from a reference atom.

1.3 Motivation

The quality of the essential oil is considered through the strength of the scent. Patchoulol is one of the highest contributors for the patchouli essential oil scent. A study conducted by Tesseire, (1973) discovered a compound namely, norpatchoulenol is capable to increase the strength of the fragrance. Norpatchoulenol is an expensive fragrance that can be obtained by the chemical reaction method from the 10-hydroxypatchoulol compound. However, 10-hydroxypatchoulol only can be attained by microbial process that used patchoulol as the substrate. 10-hydroxypatchoulol is an important compound that has to be produced in a huge quantity in order to produce more norpatchoulenol. Because of the economical reason, this study was designed to understand the interaction between patchoulol with the two variables, water and oxygen

at molecular level by molecular dynamic simulation method, which is, the interaction to produce the 10-hydroxypatchoulol in the actual experiment. The result from the simulation was expected to give an overview which variable can give the higher impact in 10-hydroxypatchoulol production, either water or dissolved oxygen gas. It will also provide the future researchers with crucial points of what parameters should be controlled in the actual experiment thereby reducing the cost and the steps in the biotransformation process. Next, the production of the 10-hydroxypatchoulol can be increased. **Figure .1.1** summarizes the process of the conversion of patchoulol to nor-patchelenol.

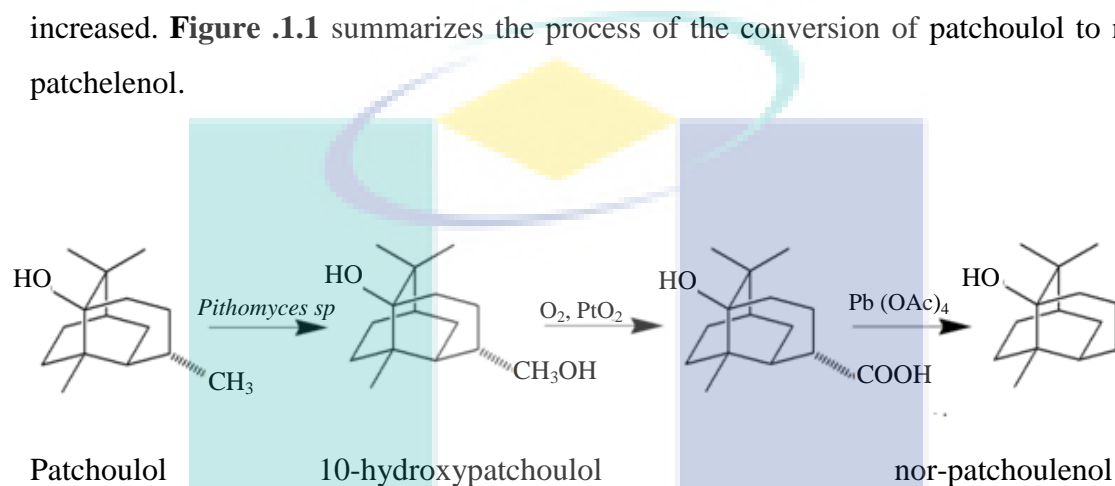


Figure .1.1. Overall biotransformation process for norpatchelenol production

Source Suhara et al, 1981

1.4 Research Objectives

The objectives of studying the computer simulation and experimental approaches are:

- (i) To determine the interaction between patchoulol as the substrate with two different phases of matter, oxygen gas and water through molecular dynamic simulation. The radial distribution function graph will describe the strength of the interaction between patchoulol with water and oxygen gas. The result can explain the mechanism of biotransformation of patchoulol compound into 10-hydroxypatchoulol.

- (ii) To compare and confirm that biotransformation activity will convert the active patchoulol compound to the 10-hydroxypatchoulol through biotransformation experimental work.

1.5 Research Scope

In order to achieve the objective of this study, the research scopes are as follows, and continued by a flow chart (Figure 1.2) :

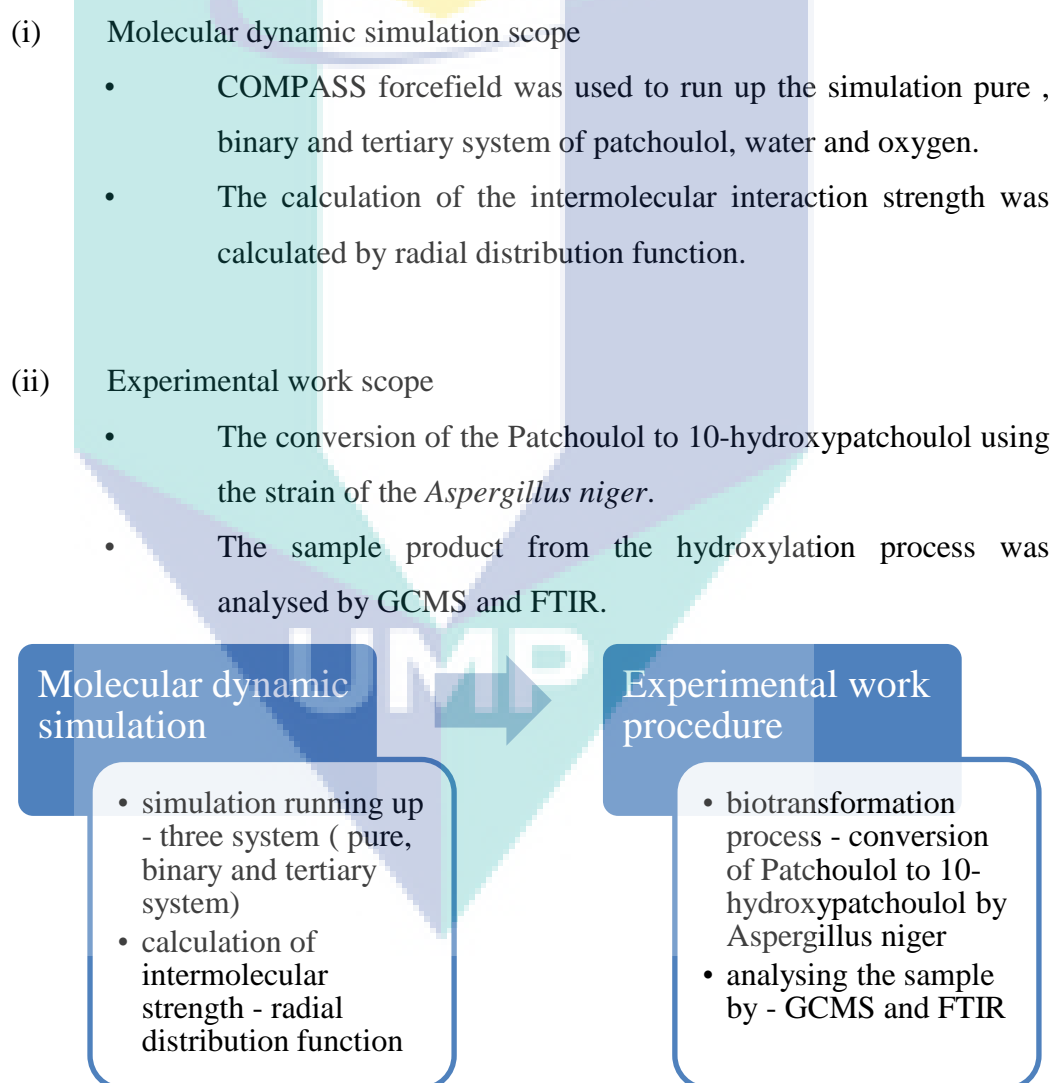


Figure 1.2. Summary of the research scope

1.6 Thesis Outline

This thesis contains five chapters and summarized as follows:

- (i) Chapter 1 describes the research background, motivation, objectives and layout of thesis
- (ii) Chapter 2 review principle, theoretical and conceptual background behind the molecular dynamic simulation and biotransformation process through the literature.
- (iii) Chapter 3 explains the materials that used in the process of biotransformation and the molecule structure of the patchoulol, water and oxygen gas that used in the computer simulation. This chapter also details out the steps and technique used in molecular dynamic simulation and biotransformation experiment.
- (iv) Chapter 4 discusses the intermolecular interaction between molecules which is presented through the radial distribution function graph of three systems: pure, binary and tertiary. This chapter also discusses the results from GCMS and FTIR analysis and confirms the simulation and biotransformation work
- (v) Chapter 5 summarizes the conclusion of the study finding and provides some suggestions for recommendation for future works.

CHAPTER 2

LITERATURE REVIEW

2.1 Introduction

This chapter is divided into three parts. The first part discusses the molecular dynamic simulation principles. It describes the background of the molecular dynamic simulation as well as theories behind the technique. The second part discusses a detailed biotransformation process. It covers the background theories of biotransformation and all relevant processes. It also discusses the theories of GCMS and FTIR as the analysis and characterisation instrument in this study.

2.2 Molecular Interaction

In order to understand the basic activity in the biological system, it is important to know how the interaction between molecules and its site of action. Molecular interaction in biological system is important where it holds the molecule together either by repulsive or attractive force. The interaction among molecules consists of two types of interactions, namely intramolecular and intermolecular interaction. Atoms in a molecule will hold each other by intramolecular interaction. Intramolecular interaction includes (i) chemical bond-stretching, (ii) bond-bending, and (iii) bond torsion around a dihedral angle. This interaction is a strong bond compared to intermolecular interaction

and needs more energy in breaking up. On the other hand, intermolecular interaction is the interaction that holds molecules together to form any matter either gas, solid or liquid. This interaction is not quite strong and can easily be broken up by increasing or decreasing the energy. This study focuses more on intermolecular interaction and will be discussed more in next subtitle. **Figure 2.1** shows the two interactions which made up the HCl liquid.

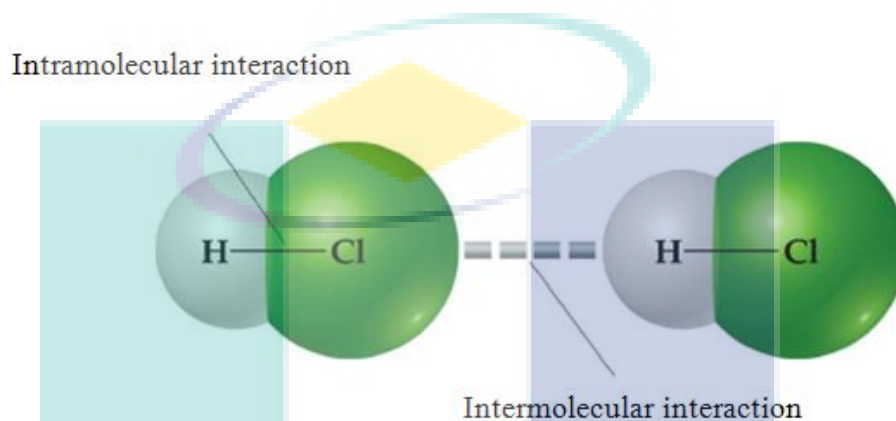


Figure 2.1. The intermolecular and intramolecular interaction of HCl liquid molecules

Source <http://wps.prenhall.com/wps/media/objects/3311/3391416/blb1102.html>

2.2.1 Intermolecular Interaction

As discussed in Section 2.2, this interaction is a weak type of interaction compared to intramolecular interaction. Nevertheless, this interaction is strong enough to control the physical properties such as boiling and melting points, vapor pressures, and viscosities.

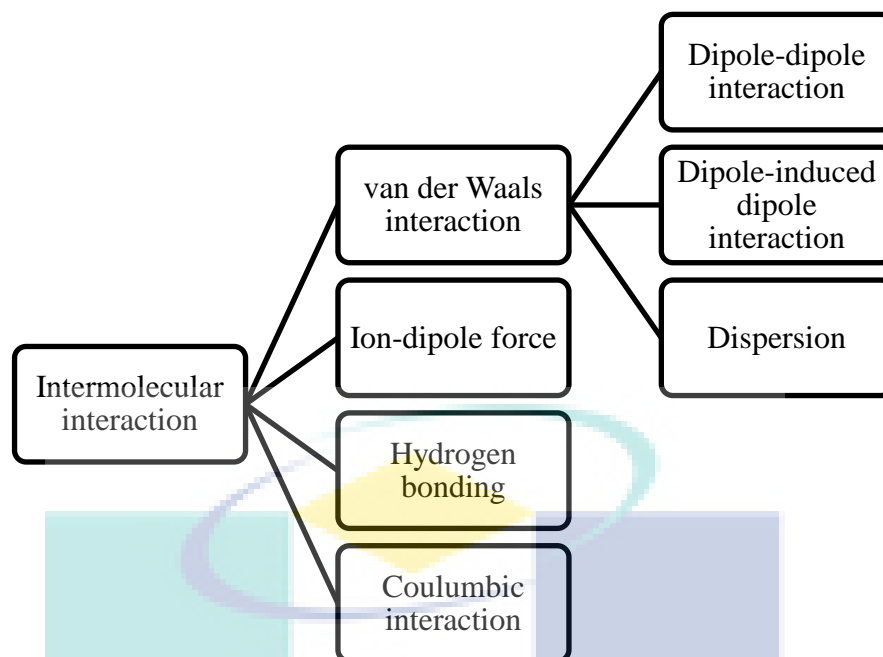


Figure 2.2. The classification of intermolecular interaction

(i) Van der waals interaction

This interaction is an attractive and repulsive force between the molecules and groups of some molecular groups (Grimme et al., 2006). This force is important in fluid systems and for adhesion between microscopic bodies. It can be divided into three groups, dipole-dipole interaction, dipole-induced dipole interaction and dispersion interaction.

Dipole-dipole interaction is one type of intermolecular force that occurs between the molecules that have permanent dipoles (Chang and Overby, 2011). “Dipoles” is represented the polar covalent molecules that having two “poles”. The pole means that the molecule has a partial positive charge in one end and a partial negative charge at the opposite end. Then, the molecules will orientate themselves so that the opposite charges attract principle operates effectively (Ophardt, 2003). Figure 2.3 shows the orientation of polar molecules in a solid. An example of a dipole-dipole interaction can be seen in chloroform (CH_3Cl), where the positive end will attract negative end.

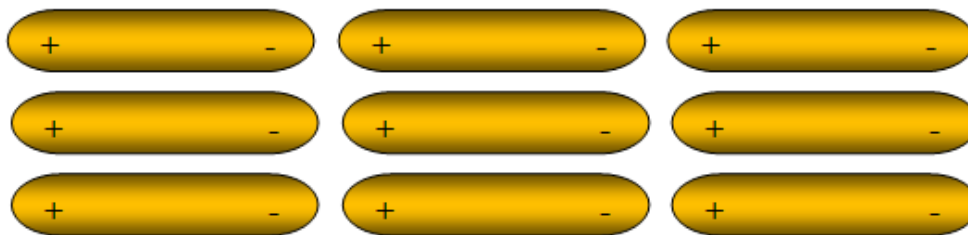


Figure 2.3. Dipole- dipole interaction

Source Chang and Overby (2011)

According to Chang and Overby, 2011, dipole-induced dipole interaction is a type of attractive interaction that occurs in nonpolar substance (Figure 2.4a). Due Figure 2.4 b) and c), the force from the ion and the polar molecule will cause the electron distribution in the nonpolar molecule. As a result, the nonpolar molecule will have of partial positive and negative charge and it is said to be an induced dipole.

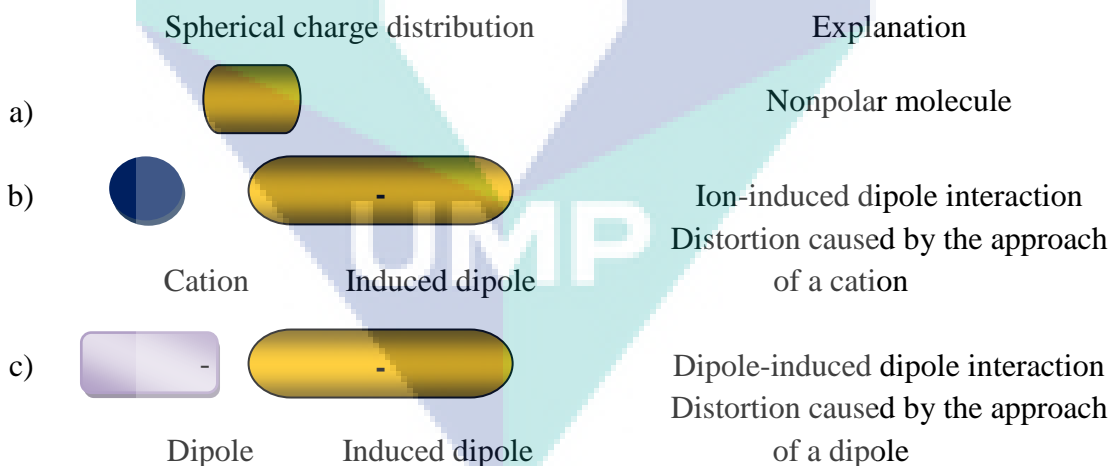


Figure 2.4. Polar-induced polar interaction

Source Chang and Overby (2011)

Dispersion interaction is an attraction which presents between an instantaneous dipole and induced dipole due to the charged fluctuations. This interaction usually operates between non-polar like between hydrogen (H_2) molecules, chlorine (Cl_2)

molecules and methane (CH_4) molecules. Figure 2.5 shows the average electron clouds of two nonpolar molecules. However, sometimes, the dipole moment can be produced due to the electron distribution in one molecule. Although the dipole moment is just temporary, it is still capable to attract and induce other molecules. The strength of this interaction is increasing as the number of the electrons increased.

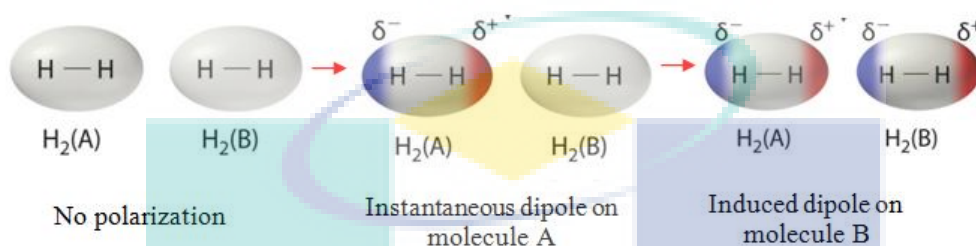


Figure 2.5 . Dispersion interaction

Source : http://images.flatworldknowledge.com/averillfwk/averillfwk-fig11_005.jpg

(ii) Ion-dipole force

This type of interaction is also important in the solutions of ions. The strength of this interaction makes the ionic substance much more possible to dissolve in polar substance. An ion-dipole force is an attractive force that results from the electrostatic attraction between an ion and a neutral polar molecule that has a dipole (Chang and Overby, 2011). Figure 2.6 shows the interaction between ion and dipole molecule. A positive ion will attract the negative end of neutral polar molecule. A negative ion will attract the positive end of neutral polar molecule. Ion-dipole attractions can become stronger as the charge and the size on the ion increases, or as the magnitude of the dipole of the polar molecule increases.

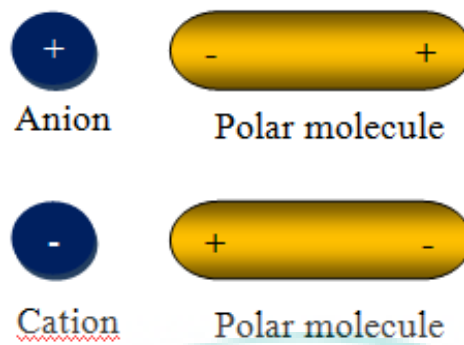


Figure 2.6. Ion-dipole interaction

Source Chang and Overby (2011)

(iii) Hydrogen Bond

Chang and Overby, 2011, mentioned that hydrogen bond is a strong, special dipole-dipole interaction, where the attractive force between the hydrogen atoms in a polar bond, with an electronegative atom of a different molecule. Usually the hydrogen has the partial positive charge, and the electronegative atom is oxygen, nitrogen, or fluorine, which has a partial negative charge. Water is a special strong type of polar molecule and connects each other by strong hydrogen bond. It is different from other polar molecule because of the structure itself as presented in Figure 2.7.

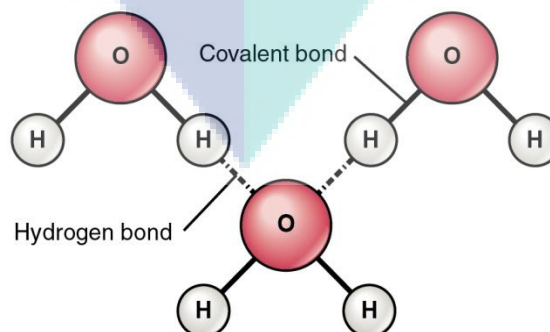


Figure 2.7. The hydrogen bond in water molecule

Source Chang and Overby (2011)

(iv) Coulombic Interaction

All molecular interactions are fundamentally electrostatic in nature. The interaction that creates the bonds between atoms in a molecule can be explained by Coulombic interaction and described by Coulomb's Law. It explained the physical basis behind the bonding of two atoms. Based on Coulomb's Law of electric charge, there are two main causes of the energy release that can be associated with the bonding. It indicated that charges repel each other due to the spreading of the electron in space and opposite charges attract one another due to the attraction between electrons and protons from different atom (Vollhardt and Schore, 2007). **Figure 2.8** illustrates the attraction that creates between proton and electron from two different atoms in one molecule. The centre of each atom is made up of a nucleus which consists of a number of protons and neutrons. Electrons that float around the nucleus are called electron clouds.

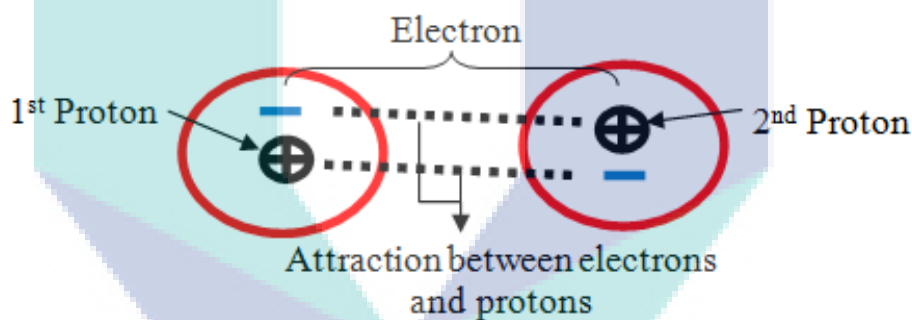


Figure 2.8. Coulombic interaction between two atoms

Source Gabler 1978

The protons of the first atom will attract the electrons of the second atom as two atoms approach one another. At the same time, the protons of the second atom attract the electrons of the first atom. As a result, a bond is created when the simultaneous attraction is formed between two atoms (Gabler, 1978). This interaction can be summarized mathematically and is known as Coulomb's Law:

$$F \propto \frac{q_1 q_2}{r^2} \quad (2.1)$$

Where

F = electrical force acting between two atoms

q_1 = magnitude of the charges of first atom

q_2 = magnitude of the charges of second atom

r = distance between the two atoms.

2.2.2 Intramolecular Interaction

Compared to intermolecular interaction, intramolecular interaction is a strong type of interaction that occurred in a molecule. The force that acts at each interaction holds the atoms together to form a molecule (Zumdahl et al., 2007). There are two main types of forces that occurred in intramolecular interaction, ionic and covalent bonding. Ionic bonding involves the transferred process of electron valence from one atom to the other atom. The atoms that have lost electron are called cations whereas the atoms that gain electron are called anions. The example of the ionic bonding can be found in NaCl where sodium attracts to chlorine by transferring an electron to chlorine as shown in Figure 2.9.



Figure 2.9. Ionic bonding in NaCl

Source Shipman et al., 1993

In contrast to ionic bond, covalent bond involves the sharing of a pair of valence electrons by two atoms. This sharing of electron can form stable molecule and always occurs between same elements as in the periodic table. The simple phenomena of covalent bond can be seen in hydrogen molecule as illustrated in **Figure 2.10**.

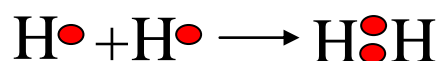


Figure 2.10. Covalent Bonding in hydrogen gas

Source

<http://www.mikeblaber.org/oldwine/chm1045/notes/Bonding/Covalent/Bond04.htm>

2.3 Computer Simulation For Microscopic System

The molecular interaction can be investigated by experimental and computer simulation methodology. In this research, the molecular interaction is studied by computer simulation where it can compute the microscopic behaviour by implementing the microscopic system (Tuckerman and Martyna, 2000). Microscopic system refers to molecular structure and intermolecular interaction between systems. By definition, computer simulation is a computer program that was developed to simulate a model of particular system (McHaney, 1991). The contribution of computer simulation is the accuracy and the properties of materials which can be tested and predicted. The two main families of the computer simulation technique are Molecular Dynamic and Monte Carlo. Monte Carlo methods are used for simulating systems with many coupled degrees of freedom, such as fluids, disordered materials, strongly coupled solids, and cellular structures (Baeurle and Stephan, 2009).

2.4 Molecular Dynamic Simulation.

Molecular dynamic (MD) is a computer simulation technique that is used to solve the problem of structural and dynamical features of complex liquids (Moura and Fereitas, 2003). The molecular dynamic method was first introduced by Alder and Wainwright in the late 1950's (Tuckerman, 2010). The movement and properties of a molecular system can be observed after they were allowed to be interacted in a specified time. The trajectory of atoms and molecules are solved numerically by Newton's equation of motion, and the force and the potential energy are defined by molecular force field. The advantage of Molecular dynamic rather than Monte Carlo is that it gives

more information in term of transport coefficient, time-dependent responses to perturbation, rheological properties and spectra. (Allen, 2004).

The molecular dynamics simulation method is support by Newton's second law or the equation of motion

$$F = ma \quad (2.1)$$

where

F = force exerted on the particle (N)

m = mass (kg)

a = acceleration (m/s^2)

The numerical solving of the equations of motion will produce a trajectory that will describe the positions, velocities and accelerations of the particles as they change with time. From this trajectory, the average values of properties can be determined. The molecular dynamic simulation method is deterministic by which the positions and velocities of each atom can be recognized as the state of the system which can be predicted at any time, whether in the past or the future. Therefore, it is possible to determine the acceleration of the system.

2.5 Radial Distribution Function

The molecular structure and the interaction between molecules can be computed from radial distribution function (RDF). According to Podesta, (2002), the radial distribution function describes the average distribution of molecules around any particular molecule. Figure 2.11 shows the radial distribution function of two dimensional structures of solids. The ring structure explains how many atom lie within the particular annular area. For example, there are no atoms found in the first and second section from the reference atom. But, there are six atoms that appear in the third section.

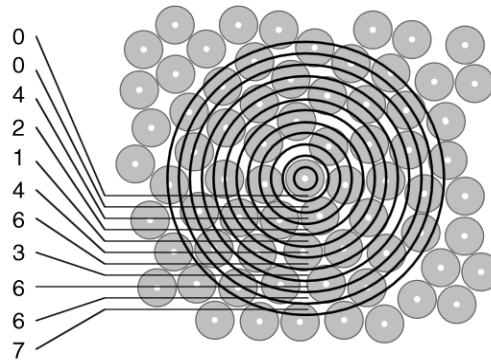


Figure 2.11. Two dimensional structure of liquid

Source Podesta, (2002)

Figure 2.12 is the radial distribution function graph of molecular dynamic simulation of liquid argon at temperature of 100K and at density of 1.48 g/cm³ (Li, 2007). The graph illustrate the first peak is at $r \approx 3.7 \text{ \AA}$ with $g(r)$ value at about 3. (DeKock and Gray, 1989) has mention that, most molecules have size in range 1 \AA to 3 \AA . This means, according to Figure 2.12 two molecules would be found at about three times, at distance 3.7 \AA .

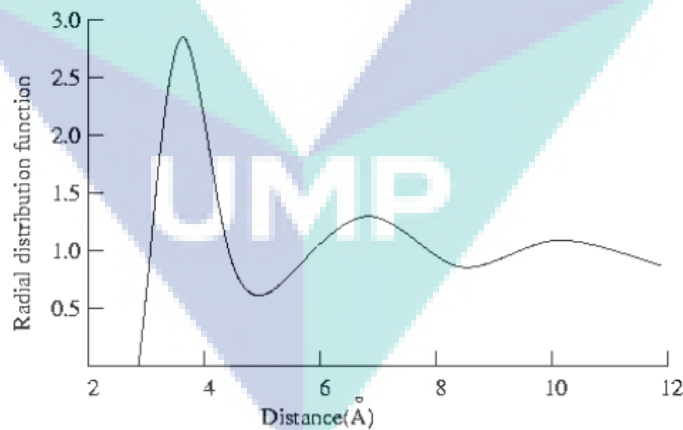


Figure 2.12. Typical sketch for radial distribution function

Source Li (2007)

Basically, RDF can be computed experimentally through radiation scattering technique, x-ray diffraction, and direct visualization via confocal microscopy (Brunk and Ashari, 2012). It is also can be determined by computer simulation methods like

Monte Carlo method and Molecular Dynamic simulation (Chandler, 1987). The structure and the nature of the solid, liquid or gas phase will reflect the pattern of the radial distribution function. Generally, there is a significant difference in pattern of radial distribution function for three phases.

Mathematically, the formula of finding RDF is

$$g(r) = \frac{n(r)}{\rho 4\pi r^2 dr} \quad (2.2)$$

Where

$g(r)$ = radial distribution function

$n(r)$ = number of atom in a shell of width dr at distance r

$4\pi r^2 dr$ = volume of the dr area

ρ = bulk density of the whole system

2.5.1 Radial Distribution Function in Solid

In a solid, the radial distribution function has an infinite number of sharp peaks where the separations and height are the characteristic of the lattice structure. **Figure 2.13** show the typical radial distribution function for solid. The RDF for solid also shows the probability to find the higher number of neighbored atom compared to liquid because of the atoms are arranged closer in the solid lattice system. Therefore, there are more peaks appear in solid phase than in liquid phase.

A study by Matsumoto et al., (2002) simulated the freezing water that can be classified as solid. This was the first study which simulated freezing water and it has successfully done so by using the superpower computer. The study involved the periodic box of 512 water molecules. The step size was 1 fs and the simulation was performed using TIP4P forcefield of water. Figure 2.14 shows the radial distribution function of the freezing water at 220 K. In this study, three possible pairs of distribution functions were investigated. The first one measures the probability of two O atoms (gOO), then two H atoms (gHH), and the last is of one O atom and one H atom (gOH).

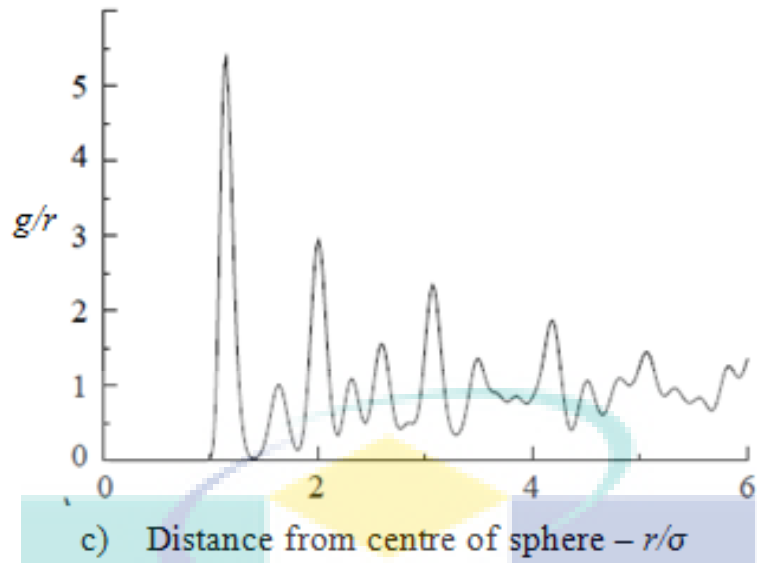


Figure 2.13. Typical radial distribution function graph of solid
 Source Barrat and Hansen, (2003)

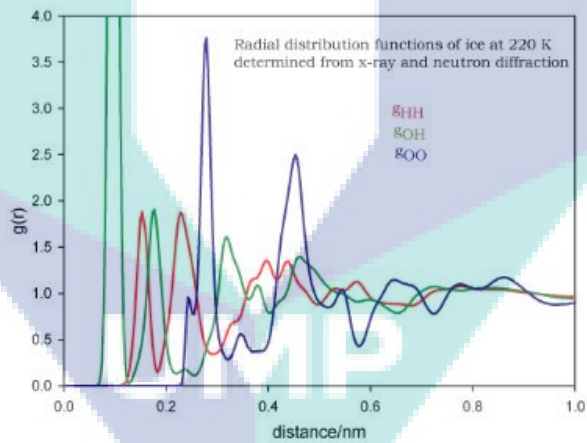


Figure 2.14. Experimental H-H, O-O, and O-H radial pair distribution functions (RDFs)
 Source : Matsumoto et al., (2002)

2.5.2 Radial Distribution Function in Liquid

Radial distribution function of liquid is does not have much difference compared to solid. It is intermediate between the solid and the gas, with small number of peaks as short distance. Figure 2.15 shows the typical radial distribution function for liquid. The

RDF of the liquid is not much structured than in solid. This is because, even though the packing is similar to solid, the molecule can still move freely.

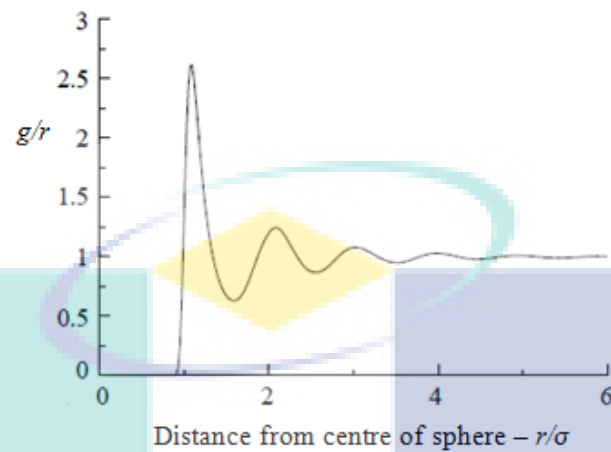


Figure 2.15. Typical radial distribution function graph of liquid

Source Barrat and Hansen, (2003)

2.5.3 Radial Distribution Function in Gas

The radial distribution function of gas is different with the liquid and solid. This is due to the distribution of the molecule itself. Figure 2.16 illustrates the typical radial distribution function of gas. The graph shows after the first peak, the graph have become less structured and the RDF will approach 1. According to Thapa (2013), it is due to the low of gas phase density and there is less number of atoms around the central reference atom.

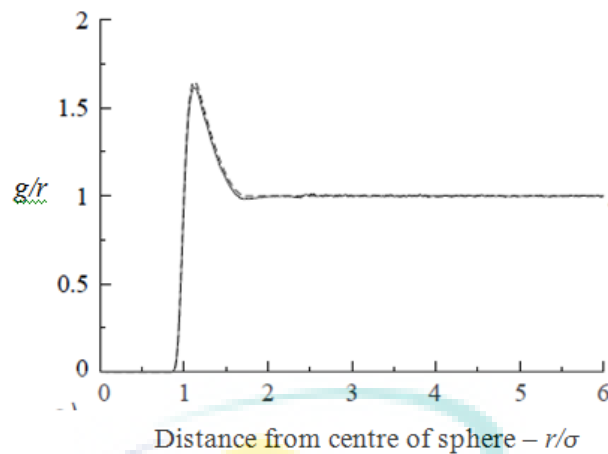


Figure 2.16. Typical radial distribution function graph of gas

Source Barrat and Hansen, (2003)

2.6 Molecular Mechanic Force Field

In a molecular system, force field is an empirical potential energy function that use the mathematical functions and parameters to models the main interaction in the system (Guevara Carrión, et al., 2012). The growth of force field development had been summarized comprehensively by Sun, (1998). He explained that, force field goes through three stages of development. At the early stage, the general force fields were made and it achieved the great coverage. At the second stage of development, the UFF6 force field was designed for combination molecules of elements on the periodic table. Due to the generality of parametrization, these force fields are predicted to produce the reasonable predictions of molecular structures only. Subsequently, emphasis was made to improve the quality of prediction in a focused area of applications in order to be more precise, especially in biochemistry. Recently, there were numerous numbers of force-field developed but it is important to choose the best force-field to get the most accurate result in simulation works. In this work, COMPASS force field was chosen as it is parameterized accurately to predict intermolecular properties of molecules in condensed phases. COMPASS stands for Condensed-phase Optimized Molecular Potentials for Atomistic Simulation Studies. According to Gabbar and Suzuki, (2004), force field is used to calculate the geometry and energy in a molecular system. It is included in the atom type which defines the atoms in a molecule, parameters such as bond and angle,

and equation that calculate the energy of a molecule. An element may have several atoms types that are represented as an element. For example, ethylbenzene contains both sp^3 -hybridized carbons and aromatic carbons. Force field contains parameters for all different types of bonds and the total energy of the molecule is divided into several parts called potential energy function.

2.7 Potential Energy Function

Potential energy function is a collection that is calculated by force field system. It is the total energy in the molecular system. The molecular system consists of main interactions such as non-bonded and bonded interaction. The summation of nonbonded and bonded interaction energies will yield the total energy of the system. Bonded energy describes the energy of the bonds, angles and rotation in a molecule, whereas nonbonded energy describes two components, the Van der Waals interaction energy and electrostatic interaction energy.

$$E_{total} = E_{bonded} + E_{non-bonded} \quad (2.3)$$

$$E_{total} = (E_{bond-stretch} + E_{angle-bend} + E_{rotate-bond}) + (E_{van-der-Waals} + E_{electrostatic}) \quad (2.4)$$

2.7.1 Bonded Energy and Non-Bonded Energy

The value of the energy is calculated as a sum of internal, or bonded, terms E_{bonded} , which describe the bonds, angles and bond rotations in a molecule. **Figure 2.17** shows the three movements that occurred in bonded energy.

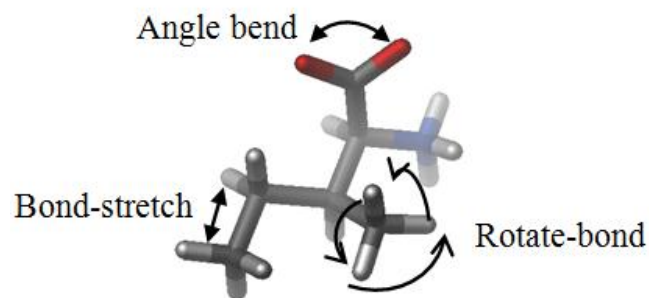


Figure 2.17. Three movements in bonded energy.

Source http://www.ch.embnet.org/MD_tutorial/pages/MD.Part2.html

The first term in the bonded energy equation is representing the bond stretching. It is referring to the interaction between atomic pairs where atom is separated by one covalent bond (MacKerell, 1998). The energy of the molecule will go up whenever the bond is compressed or stretched. The energy potential is described as follows:

$$E_{bonding} = \sum k_b (b - b_0)^2 \quad (2.5)$$

Where

k_b = force constant

b_0 = ideal bond length

b = actual bond length

The second term in the bonded energy equation is related with the alteration of bond angle from the ideal value of q_0 . Values of q_0 and k_i are depending of the chemical type of atom constituting the angle. The energy potential is described as follows:

$$E_{angle-bend} = \sum k_i (q - q_0)^2 \quad (2.6)$$

Where

k_i = force constant

q_0 = ideal bond length

q = actual bond length

The third term represents the torsion angle potential function which separated by 3 covalent bonds (1,4 pairs). The motion that represent this term is a rotation, described by a dihedral angle and coefficient of symmetry ($n=1,2,3$), around the middle bond. This potential is assumed to be periodic and is often expressed as a cosine function. The energy potential is described as follow:

$$E_{rotate-bond} = \Sigma V_i [(1 - \cos (n\theta))] \quad (2.7)$$

Where

V_i = torsion force constant

θ = torsion angle in degree

n = symmetry of the bond

In this work, only nonbonded energy is taken into account for the analysis of intermolecular interaction. It is focussed specifically on interaction between neighboured molecules. The energy term representing the contribution of non-bonded interactions has two components, the Van der Waals interaction energy and the electrostatic interaction energy. Recall the non-bonded energy as follows:

$$E_{non-bonded} = (E_{Van\ der\ Waals} + E_{electrostatic}) \quad (2.8)$$

The van der Waals interaction comes from repulsive and attractive forces between two atoms and it is most important for the stability of the biological macromolecules (Lipkowitz, 1983). The van der Waals interaction is most often modelled using the Lennard-Jones 6-12 potential., as the formula is shown below,

$$V(r) = 4\epsilon \left\{ \left[\frac{\sigma}{r} \right]^{12} - \left[\frac{\sigma}{r} \right]^6 \right\} \quad (2.9)$$

Where

V = intermolecular potential between two atom or molecule

ϵ = well depth or measurement of the attraction strength of two particles

σ = distance at which the intermolecular potential is zero

r = distance of separation between both particles (from the center of one particle to the center of the other particle)

Figure 2.18 shows the typical Lennard-Jones potential graph. It indicates that the deeper the well depth (ϵ), the interaction between two molecules will become stronger. When the bonding potential energy is equal to zero, the distance of separation, r , will be equal to σ .

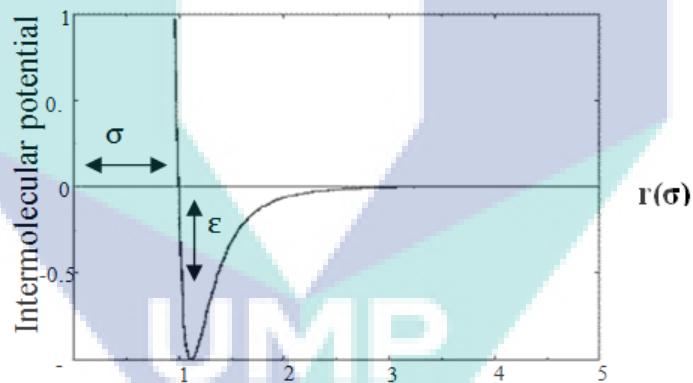


Figure 2.18. Typical Lennard-Jones potential graph

Source : Côté et al., (2001)

The electrostatic interaction can be described as the electric force between a pair of atoms and it is represented by Coulomb potential. D is the effective dielectric function for the medium and r is the distance between two atoms having charges qi and qk .

$$E_{electrostatic} = \sum_{\text{nonbonded pairs}} \frac{q_i q_k}{r_{ik}} \quad (2.10)$$

Basically, the electrostatic energy has to evaluate in each pair of atom. But, it becomes a problem when it comes to long range electrostatic. It is due to the range that exceeds the length of the simulation cell. In easier way, it can be solve by increasing the simulation cell dimension. But, this method will increase the computational cost. The other technique that can be applied in dealing with the long range electrostatic is the Ewald Summation. Abdalnour et al., 1995 had mentioned that, it is the best technique to calculate the electrostatic interaction in the periodic system. Allen and Tildesley 1989 explained the modification in Ewald Summation that involves two mechanisms.

- (i) Positioning one type of Gaussian clouds that having the opposite charge on the ions. The combination of ions and the Gaussian clouds will be treated as the short range interaction. The calculation will be operated at the Real space. Then, second set of the Gaussian clouds that having the same charges as the original point will be position on the ions in order to obviate the first Gaussian effect. The Gaussian potential is obtained by Poisson's equation.
- (ii) Self-energy correction. It is arises from a Gaussian acting on its own site and it is introduced to complete the Ewald Summation.

2.8 Ensemble In Molecular Dynamic Simulation

In molecular dynamics simulation, the macroscopic properties of a system will be explored through microscopic simulations. The connection between microscopic simulations and macroscopic properties is examined via statistical mechanics. It will study a macroscopic system from a molecular point of view by distribution of the system within the ensemble. An ensemble is a collection of all possible systems which has different microscopic states but compatible with macroscopic state (Dill et al., 2003). The macroscopic state of a system is usually defined by a small set of parameters, for example, the temperature, T, the pressure, P, and the number of particles, N. The microscopic state of a system is defined by the atomic positions, q, and momenta, p. Table 2.5 shows the three different ensembles with different characteristics

according to the simulation system; NVT (Canonical ensemble), NPT (Isothermal-isobaric ensemble) and NVE (Microcanonical ensemble).

As explained by Dill et al., (2003), the isothermal–isobaric ensemble is a type of statistical mechanical ensemble where the number of particle (N) temperature (T) and pressure (P) are maintained and conserved. In this ensemble, the barostat and thermostat are needed as the real chemical reaction that will be conducted with the constant pressure condition. The microcanonical ensemble is a type of statistical mechanical ensemble where the number of particle (N), volume (V) and energy (E) are maintained and conserved. According to Gibbs and Willard (1902), this ensemble corresponds to state in a mechanical system that has specific total energy. The energy in this system is constantly remaining as no exchanges occur with the environment. Meanwhile, the canonical ensemble is an ensemble that maintains the number of particle (N), volume (V) and temperature (T). In this ensemble, the energy can be exchange with the heat bath. Because of that, there will be differ in total energy at every possible stage in the system (Gibbs, and Willard, 1902).

Table 2.1

The classification of three type of ensemble process.

NVT	NPT	NVE
<ul style="list-style-type: none"> • Canonical ensemble • Conserved number of particle (N), volume (V) and temperature (T). • Energy process is exchanges with a thermostat 	<ul style="list-style-type: none"> • Isothermal - isobaric ensemble • Conserved number of particles (N), pressure (P) and temperature (T) • Need barostat and thermostat 	<ul style="list-style-type: none"> • Microcanonical ensemble • Conserved number of particles (N), volume (V) and energy (E) • No energy exchanged

2.9 Patchoulol As A Substrate In 10-Hydroxypatchoulol Production

Aroma compound is the key or marker compound in the fragrance study. The rate of the aroma compound percentage will affect the quality of the essential oil (Mahanta et al., 2007). In the patchouli essential production, patchoulol is the marker compound where, approximately, 30% - 40% of the main constituent of patchouli oil is the patchoulol compound. The structure of patchoulol was first found in 1963 by x-ray crystallography (Jensen, 2011). Patchoulol exists in two configurations (Naf et al., 1981). (-)- (1R,3R,6S,7S,8S)-Patchoulol is a strong, typical patchouli scent with an earthy, slightly camphoraceous, powdery cellular note which was indistinguishable from natural patchoulol and deep woody like patchouli oil. Meanwhile, (+)- (1S,3S,6R,7R,8R)-Patchoulol, is much weaker, less characteristics, nearly indefinable and is not the reminiscence of patchouli. **Figure 2.19** shows the structure comparison of positive and negative patchoulol.

Patchoulol is a terpene extracted from the patchouli leaves and is one of 24 compounds in patchouli oil that contributes to the wish scent of this essential oil. Figure 2.20 shows the common 24 compounds found in patchouli oil. In medical application, the patchoulol compound can be used for treatment of diseases caused by infection of *Helicobacter pylori*, such as gastritis, peptic ulcer and early gastric cancer (Lai et al., 2014). Yu et al., (2014) have suggested that, a quite narrow antimicrobial spectrum possessed by patchoulol can inhibit the *Helicobacter pylori* without influencing growth and propagation of other bacterial populations (including other gram negative bacteria). In addition, the patchouli alcohol may kill *Helicobacter pylori* without damaging probiotics, therefore, it can keep the ecological balance of bacterial populations in the intestinal tract of a human body. In the cosmetic industry, patchoulol is an excellent choice for skin treatment, fragrant addition in facial bends treatment and bath oils. This is due to its characteristic of pleasant and long lasting woody, earthy, camphoraceous odour (Ramya et al., 2013).

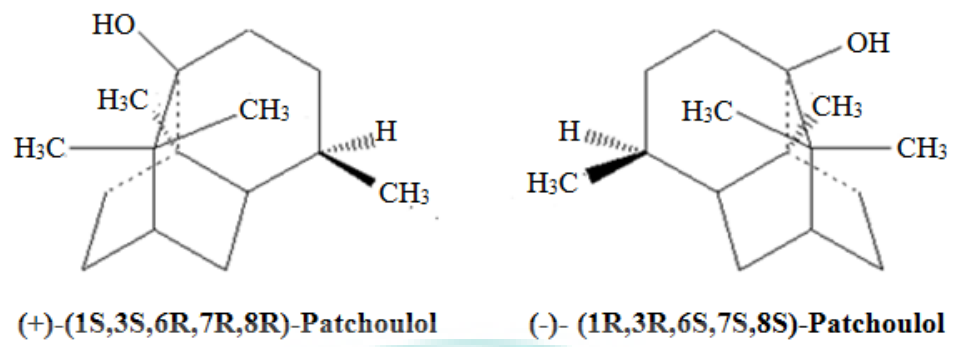
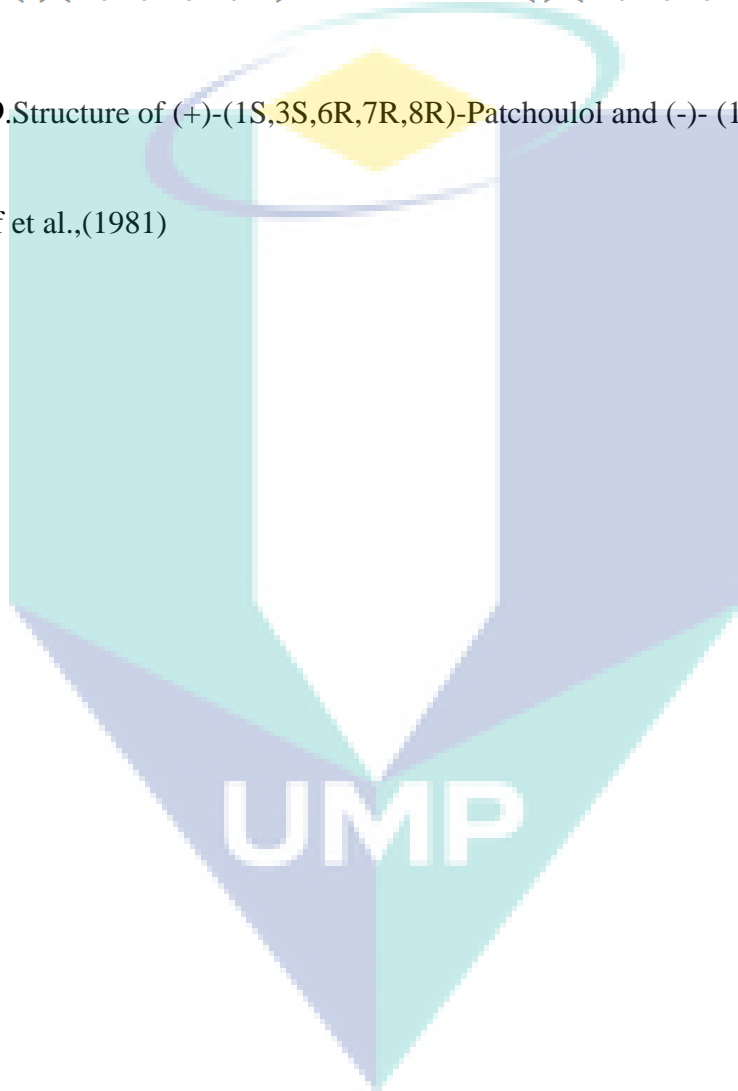


Figure 2.19. Structure of (+)-(1S,3S,6R,7R,8R)-Patchoulol and (-)-(1R,3R,6S,7S,8S)-Patchoulol

Source: Naf et al.,(1981)



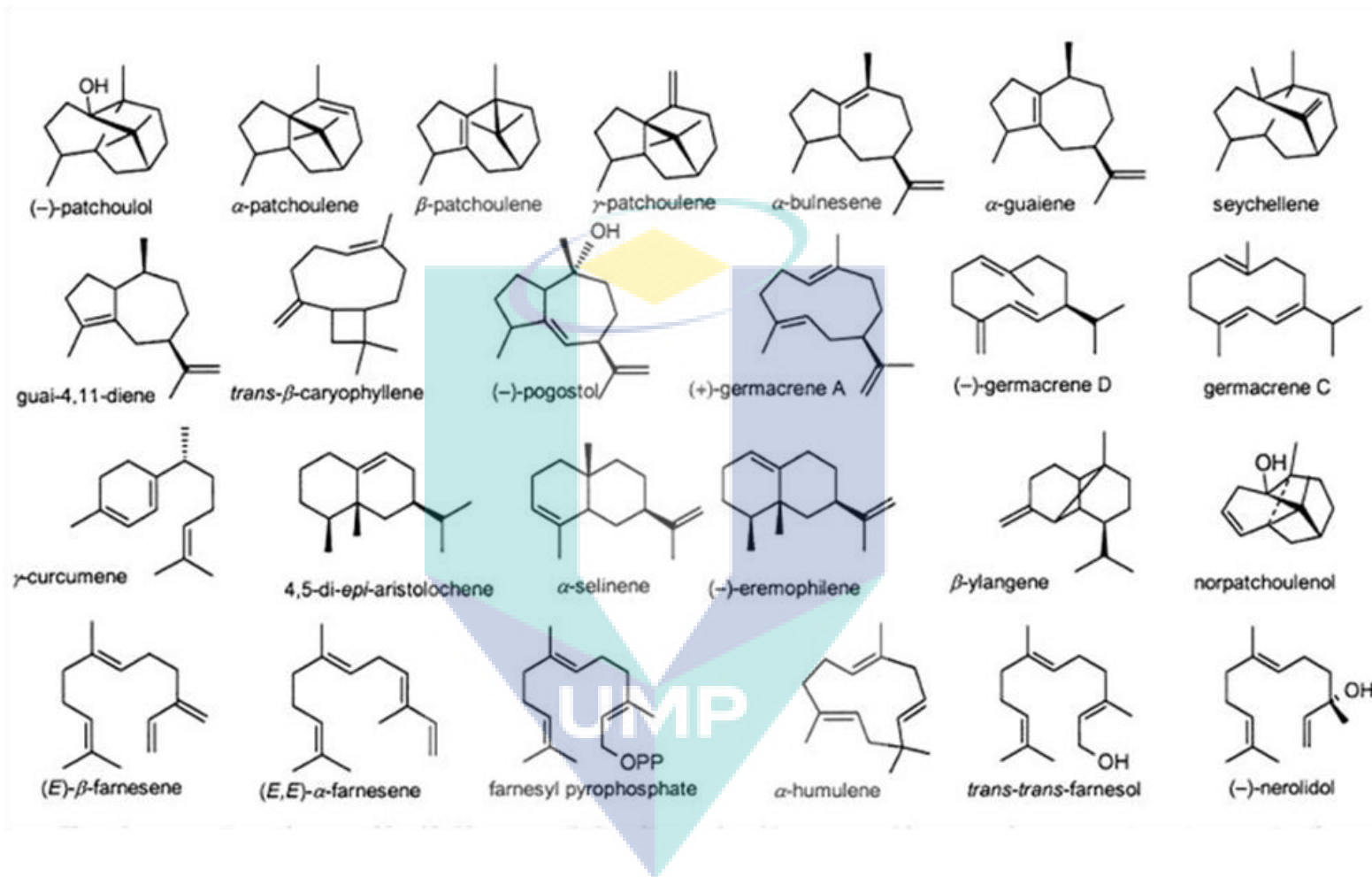


Figure 2.20. 24 Common compounds in patchouli essential oil

Source : Buré and Sellier, (2004); Dung et al., (1990)

2.10 10-Hydroxypatchoulol

As explain in Section 2.9, patchoulol is the aromatic and marker compound in the essential oil. Beside of that, patchoulol also can act as the substrate in the production of the 10-hydroxypatchoulol. At present, there is limited information about 10-hydroxypatchoulol (**Figure 2.21**). But, the production of 10-hydroxypatchoulol ($C_{15}H_{26}O_2$) has been studied by Suhara et al., (1981). This compound was discovered by hydroxylation of the patchoulol, one of the chemical compounds in the patchouli oil. According to Teisseire (1973), this reaction then will lead to the production of the nor-patchoulenol, an expensive compound in the patchouli oil. Table 2.2 shows the characteristic of the 10-hydroxypatchoulol.

Table 2.2

Physical properties of 10-hydroxypatchoulol

Characteristic	Identify
Molecular Formula	$C_{15}H_{26}O_2$
Physical states	Colorless crystal
Melting point	104 °C

Source : Suhara et al, (1981)

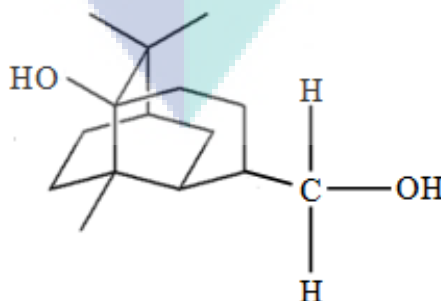


Figure 2.21 Molecular structure of the 10-hydroxypatchoulol

Source : Suhara et al, (1981)

The transformation of the patchoulol to the 10-hydroxypatchoulol can be done by the biotransformation process. Biotransformation is the biological process where an organic compound is converted to the interested compound. Basically, biotransformation can be done by three methods, microbial transformation, plant cell culture transformation and animal cell culture transformation. Mostly, the microbial transformation is selected as the method in the study due to four factors that has be listed by Shishirkawde, (2011). Compared to the plant and animal cell culture, microbes have the higher metabolic rate and surface-volume rate that lead to the more efficient transformation. Next, microbes also have the higher growth rate compared to plant and animal cell that decrease the time of the transformation process. Besides, by using plant and animal cell culture, it is difficult to maintain the sterility in the process, where the sterility is the major factor that have be considered in the biotransformation process. The summary of the four factors has been tabulated in the Table 2.3.

Table 2.3

Comparison between microbial transformation with animal and plant cell culture

Properties	Microorganism	Plant and animal cell culture
Surface-volume ratio	High	Low
Growth rate	High – less time consuming	Low – more time consuming
Metabolic rate	High – efficient transformation	Low – not efficient transformation
Sterility	Easy to maintain	Difficult to maintain

There are several different types of reactions in the biotransformation process. Each has different mechanisms producing different products. The reactions are glucosylation, oxido reaction, hydrolysis, epoxidation, reductions of carbonyl groups, reduction of C-C double bonds, nitroreduction and hydroxylation. This study concentrate on the hydroxylation in converting the patchoulol to the 10-hydroxypatchoulol.

2.11 Hydroxylation

At present, hydroxylation is the most important biotransformation approach in producing natural products in perfumery industry. Kim (2005) state that, the hydroxylation process becomes one of the recent developments of the commercialized process in transform the natural precursor into valuable fragrance compound via microbial metabolic pathway. According to Dorland, (2007), hydroxylation is an oxidative process where the CH group is converted to the COH group. This can be happen when an oxygen atom from molecule oxygen is introduced into the aromatic organic compound and formed the hydroxyl group. The conversion process was catalysed by an enzyme called hydroxylase. The remaining oxygen atom will be reduced to water (Held et al., 2000). The biotransformation of patchoulol had yield various organic compound by using various fungi as the catalyst as shown in Table 2.4.

A research that is conducted by Suhara et al., (1981) used the microbial transformation in the experiment and stated that the 10-hydroxypatchoulol was easily obtained by this process reactions compared by chemical methods. In this study, 10-hydroxypatchoulol was obtained in 25% yields in 1 litre fermentation jars at 2 gram of patchoulol by the *Pithomyces sp.* **Figure 2.22** shows that the CH₃ group from the patchoulol molecule transformed to the CH₂OH and formed the 10-hydroxypatchoulol.

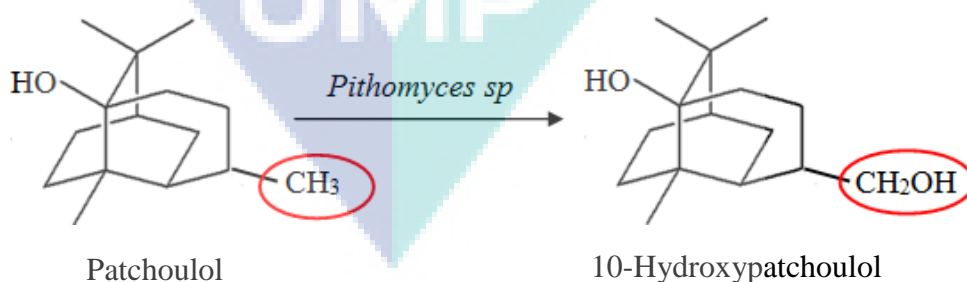


Figure 2.22. Production of 10-hydroxypatchoulol

Source Suhara et al., (1981)

Hanson et al., (1999) had reported the hydroxylation of patchoulol by two types of fungus namely *Mucor plumbeus* and *Cephalosporium aphidicola*. The hydroxylation

of the patchoulol with *Mucor plumbeus* for five days gave two hydroxylation products that detected by the NMR spectrum. The first metabolite that is detected by the spectrum is 5 α -hydroxypatchoulol. The formation of the metabolite was showed by the formation the OH group in C4 compared to the starting compound. The second metabolite that detected by the spectrum is 9 α -hydroxypatchoulol. The location of the formation of the OH is at C9. This study shows two atoms hydrogen receive atom oxygen and become the OH group (**Figure 2.23**) and form the hydroxyl derivatives. On the other hand, the incubation of the patchoulol for ten days with *Cephalosporium aphidicola* only gave the 5 α -hydroxypatchoulol metabolite that is identical with the compound that obtained from *Mucor plumbeus*

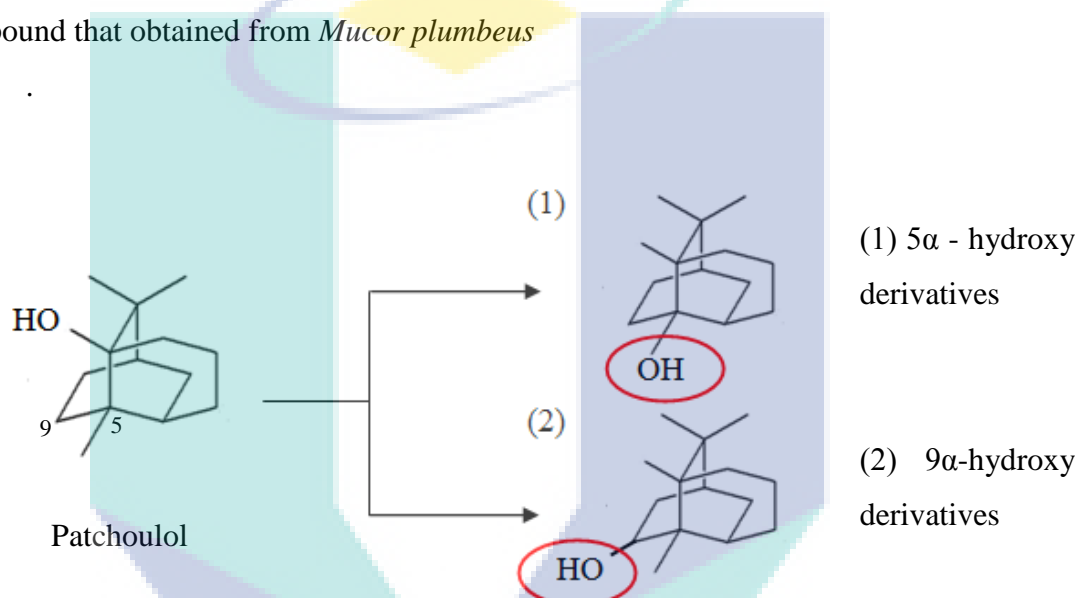


Figure 2.23. The hydroxylation of patchoulol

Source Hanson et al., (1999)

A research that has been done by Aleu et al, (2001) also uses patchoulol as the substrate to demonstrate the antifungal activities on a *Botrytis* species, a type of pathogen fungus that implicated disease in flowers, fruits and vegetables. After the fermentation of the patchoulol over three days, eight compound was isolated from the neutral fraction patchoulol, 1) 5-hydroxypatchoulol, 2) 7- hydroxypatchoulol, 3) 8-hydroxypatchoulol, 4) 8-Acetoxypatchoulol, 5) 9- hydroxypatchoulol, 6) 9-acetoxypatchoulol, 7) 3- hydroxypatchoulol and 8) 2,14-dihydroxypatchoulol. A summary of the work that have been done by three researchers were tabulated in Table 2.4.

Table 2.4

The various hydroxylation yield using patchoulol as substrate

Microorganism	Yield	Analysis	References
<i>Pithomyces sp.</i>	10-hydroxypatchoulol	Gas chromatography	Suhara et al., 1981
<i>Mucor plumbeus</i>	1) 5 α -hydroxypatchoulol 2) 9 α -hydroxypatchoulol	x-ray crystallography	Hanson et al., 1999
<i>Boytrytis cinera</i>	1) 5-hydroxypatchoulol 2) 7- hydroxypatchoulol 3) 8- hydroxypatchoulol 4) 8-Acetoxypatchoulol 5) 9- hydroxypatchoulol 6) 9- acetoxypatchoulol 7) 3- hydroxypatchoulol 8) 2,14-dihydroxypatchoulol	NMR	Aleu et al., 1999

2.12 Aspergillus Niger As The Biocatalyst In The Hydroxylation Process

Aspergillus niger shown in **Figure 2.24** is an aerobic haploid filamentous fungi which is a very important microorganism in the field of biology. *Aspergillus niger* was selected due to their capability to grow within a short period (Dalli et al., 2006). In addition, Machida and Gomi, (2010) had mentioned that, *Aspergillus niger* is one type of fungi that produce hydroxylase enzyme that is important in this transformation. In addition, *Aspergillus niger* is one type of major producer for hydrolytic enzyme amongst fungi (Godfrey and West, 1996). The fungi can be found in mesophilic environments such as decaying vegetation or soil and plants (Schuster et al., 2002). This type of fungi also has the capability to produce extracellular enzymes and citric acid. Due to that capability, *Aspergillus niger* became the industrially used organism after it is introduced in fermentation industry in 1919 (Schuster et al., 2002). *Aspergillus niger* is useful in waste management and can be an important resource in the biotransformation process.

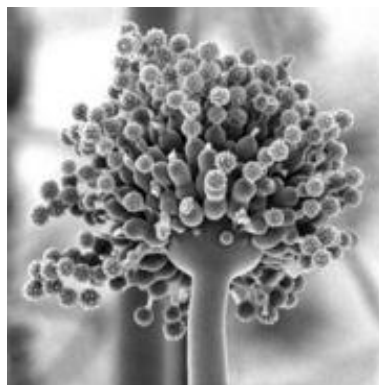


Figure 2.24: An example of *Aspergillus niger*

Aspergillus niger also be selected in this study because of the capabilities of this fungi to act as the catalyst in introducing hydroxyl group in hydroxylation process. A study was conducted on *Aspergillus niger* by Yadav et al, (2011) found that this fungus can act as the biocatalyst excellently in the process of hydroxylation. In that study, *Aspergillus niger* was capable to transform the ethylbenzene, an organic compound to the useful compound, namely phenylethanol. This compound is said to be interested because of their antimicrobial properties. In the **Figure 2.25**, it can be seen that, the addition of the oxygen and form the OH group in the red circle.

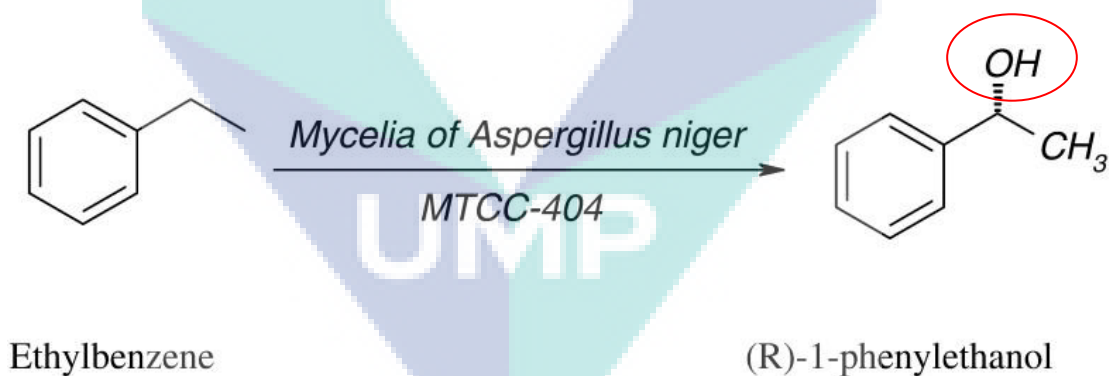


Figure 2.25 :Transformation of the Ethylbenzene to Phenylethanol by *Aspergillus niger*
Source Yadav et al, (2011)

2.13 Analytical Equipment For Data Analysis

The aim of this study is to identify the 10-hydroxypatchoulol, interested compound that have been transformed from patchoulol through GCMS and FTIR

analysis. GCMS had been used for identification of the component of the organic compound mixture (Hajšlová and Cajka, 2007). On the other hand, FTIR can identify the unknown materials by obtain an infrared spectrum of absorption of a solid, liquid or gas (Griffiths and de Hasseth, 2007). Due to Colthup et al, (1975) the characteristic of the infrared absorption bands is correspond to the fundamental vibrations of the functional group.

Basically, the GCMS is combination of two parts, one is gas chromatography (GC) and the other is mass spectrometer (MS). Gas Chromatography (GC) is a separating technique of the chemical mixture by evaporating into gas phase (Simonich, 2015). Then, Mass Spectrometer (MS) will identify the chemical based on their structure. The identification of phytochemical compounds is based on the peak area, molecular weight and molecular formula (Arunkumar and Muthuselvam, 2009). Table 2.5 had tabulated the advantage and disadvantage of GCMS techniques that have been listed by Lynch (2013).

Table 2.5

Advantage and disadvantage of GCMS

GC/MS	
Advantage	<ul style="list-style-type: none"> • Increased in sensitivity • High-reproducibility in generating mass spectra • Large transferable mass spectral library is available • Ideal for volatile analysis
Disadvantage	<ul style="list-style-type: none"> • Incapable to detect non-volatile, polar and thermally labile compounds. • Prolonged sample preparation needed.

Source : Lynch (2013).

Some researcher have use GCMS in detecting their extraction compound in their studies. Arunkumar and Muthuselvam (2009) have reported about 26 bioactive phytochemical compounds were identified in the ethanolic extract of Aloe Vera by GCMS analysis. J. Sitosterol (C₂₉H₅₀O) with retention time 38.78 had peak area 13.19%, Oleic acid (C₁₈H₃₄O₂) with retention time (21.85) and 9,12,15-Octadecatrienoic

acid, methyl ester (Z,Z,Z) (C₁₉H₃₃O₂) with retention time 22.6 ranks net having peak area 11.74% and 11.36% respectively. Whereas, Ivanka Kostova et al.(2002) had studied about acidic fraction obtained from *Paronia peregrine* and *Paeonia tenuifolia* roots. The research discovered about fourteen aromatic and 24 aliphatic acids were determined by GC-MS analysis, where benzoic acid and its monohydroxy-dihydroxy- and tri-hydroxy derivatives are the main acid compounds of both *Paronia* species. Ahmed Al-harrasi and Salim Al-Saidi, (2008) revealed the presence of 34 monoterpenes and 16 sesquiterpenes in phytochemically centrifuged oleogum resin of *Boswellia acra* essential oil also by GCMS.

Fourier Transform InfraRed is used to identify the unknown organic either in solid, gas or liquid. In addition, FTIR also can be used to determine the amount and the quality of an individual compound in a given substance (Vasava, 2012). Basically, due to , FTIR has three main components, namely, radiation source, interferometer and detector (Hsu, 1997). The characteristics of the infrared absorption bands can be associated with the functional group that has the wavelength in range 1200-3600 cm⁻¹. On the other hand, the characteristics of the infrared transmission bands can be associated with the fingerprint group that has the wavelength in range 600-1200 cm⁻¹ (Colthup et al., 1975 ; Griffith and de Haseth, 1986). Vasava, (2012) had listed the advantage and disadvantage of the FTIR as in Table 2.6.

Table 2.6

Advantage and disadvantage of FTIR

Advantage	Disadvantage
Highly sensitive, high resolution and can identify the small concentrations of contaminants	Having only single beam
The result of the spectrum can be obtained in the short time	
The result can be accurately obtained within 1 to 2 seconds	

Source : Vasava, (2012)

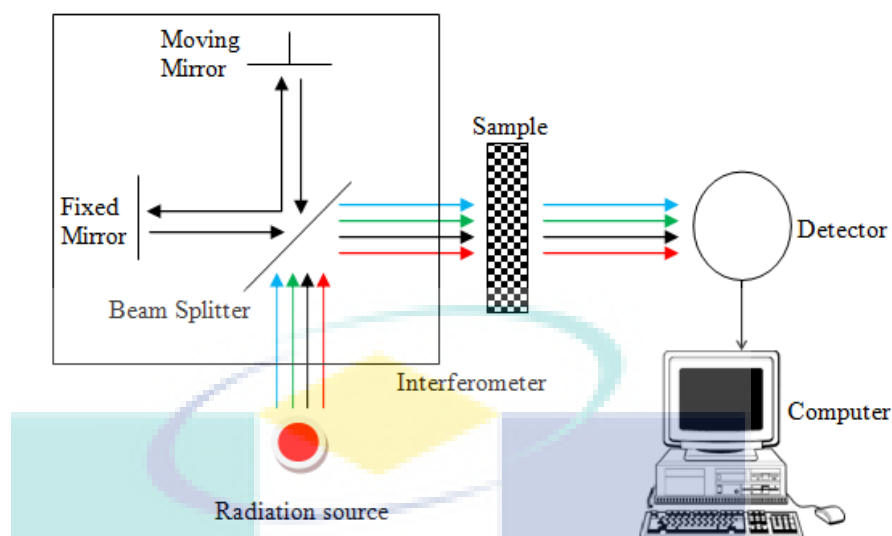


Figure 2.26. Diagram of the FTIR
Source Hsu 1997

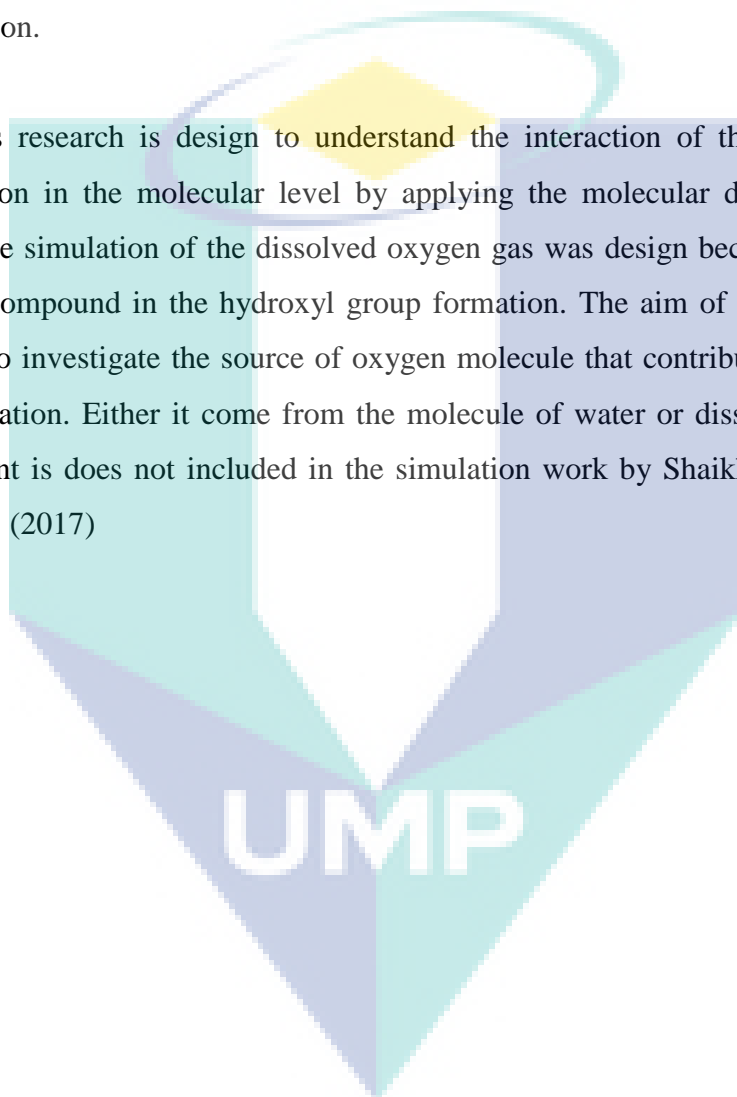
2.14 Significant Of The Molecular Dynamic Simulation Studies In The Biotransformation Work

In general, molecular dynamic simulation had become a powerful tool in understanding the physical basis of the structure and function of biological macromolecules. Adam et al, (2014) had come out with a simulation work on the extraction of the patchoulol by different solvents, namely acetone, ethanol, and hexane. Besides that, molecular dynamic simulation also were used widely in the crystallization process as in paper by Abdul et al, (2013).

To date, there are several researchers that are applying the molecular dynamic simulation in the hydroxylation process but in different objective. Early 2000's, Shaikh et al, (2001) had come out with the simulation on the Cytochrome P450 enzyme. This enzyme is a heme-containing monooxygenase from the soil bacterium *Pseudomonas putida* that catalyzes the 5-exohydroxylation of camphor. Shaikh et al, (2001) discovered the formation of O-H bond and breaking of C-H bonds, then the formation of the C-O bond. This paper is presented clearly with all step required, but it lack of

formation on where the oxygen is come from in order to form the hydroxyl group in the camphor compound. In 2015, the advanced paper by Sigdal et al, (2015) had investigated the computational approach that can predict the formation of the regioselective products catalyzed by sMMO wild-type (WT) and L110Y/G mutants using toluene and ethylbenzene as substrates. They use the experimental results by Borodina et al., (2007) as the starting point to develop the computational approach for the simulation system. This paper also clearly explains the steps that are go through in the simulation.

This research is design to understand the interaction of the molecule in the hydroxylation in the molecular level by applying the molecular dynamic simulation method. The simulation of the dissolved oxygen gas was design because oxygen is the important compound in the hydroxyl group formation. The aim of this study is to the oxygen is to investigate the source of oxygen molecule that contribute to the hydroxyl group formation. Either it come from the molecule of water or dissolved oxygen gas. This element is does not included in the simulation work by Shaikh et al, (2001) and Sigdal et al, (2017)



CHAPTER 3

MATERIAL AND METHOD

3.1 Introduction

This chapter detail out of materials and methodologies applied in this research. The methodology part involved the experiments and molecular simulation technique. The molecular dynamics simulation method was applied to study the intermolecular interaction between patchoulol as compound of and interest oxygen atom from water and dissolved oxygen gas. The experimental work was designed to study the biotransformation of patchoulol to 10-hydroxypatchoulol for further verification and confirmation.

3.2 Molecular Dynamic Simulation

Molecular dynamic simulation was carried out to understand the structure and microscopic interaction between compounds simulated in the bulk system. **Figure 3.1** summarizes the steps applied in the simulation process.

Forcite module in the Material Studio 5.5 software package was applied to run the dynamic simulation. The procedure began with the sketching of a single molecule of

patchoulol, water, and oxygen separately. Instead of sketching, the molecular structure also can be obtained from <http://www.chemspider.com> database. After the molecules have been prepared, the cleaning process was carried out to obtain the right structure in terms of bonded properties such as, torsion and their angles in the molecule.

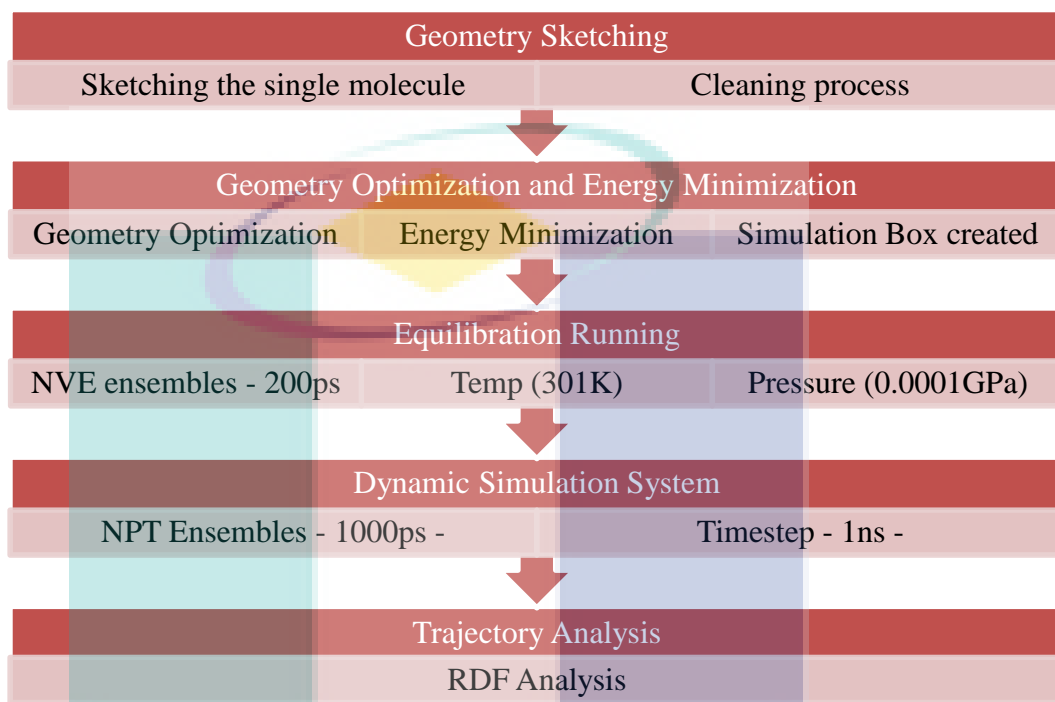


Figure 3.1. Molecular dynamic simulation step

3.2.1 Geometry Optimization and Energy Minimization

Geometry optimization is a crucial step in computer-aided simulation. The method was used to compute the stable configuration of the molecule of study. The stable-state of the molecular system depends on the global and the local minima of their potential energy surface. The process started with the structure of a non-equilibrated molecule which was optimized to get the most stable geometry structure condition. Then, the system underwent an energy minimization process in order to obtain the lower energy value. The purpose of this step was to adjust the structure to the force field, particularly distribution of solvent molecules and also to relax possible steric clashes created by guessing coordinates of atoms. The method used in this study was the Smart

Minimizer, with the maximum iteration of 5000. **Figure 3.2** shows the geometry optimization and energy minimization button in Material Studio Package software.

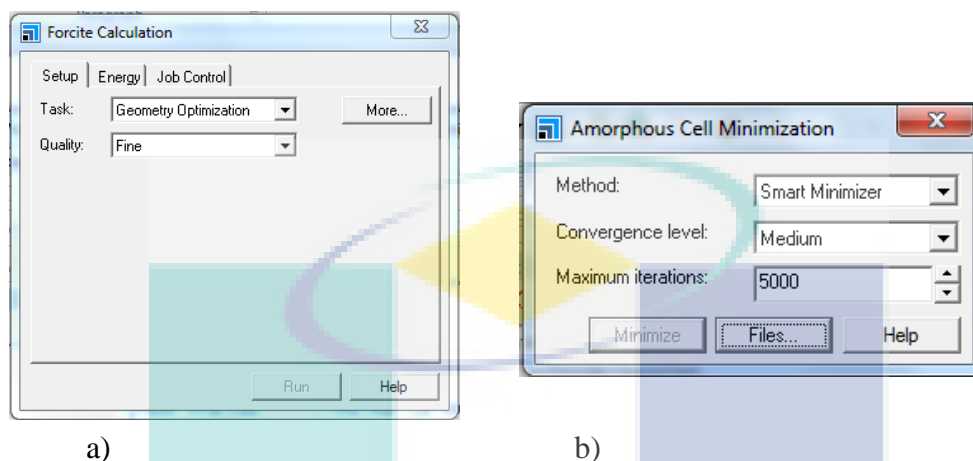


Figure 3.2. a) Geometry optimization button and b) Energy minimization button

The COMPASS forcefield was selected as a potential energy prediction for the molecular system. The density of the mixture was calculated using the density mixture formula (equation 3.1).

$$\rho_{\text{mix}} = \frac{Wt_{\text{solute}} + Wt_{\text{solvent}}}{\left[\frac{Wt_{\text{solute}}}{\rho_{\text{solute}}} \right] + \left[\frac{Wt_{\text{solvent}}}{\rho_{\text{solvent}}} \right]} \quad (3.1)$$

Next, a simulation box was created according to the three systems. Table 3.1 shows the classification of the three systems that were done in this work. **Figure 3.3** is an example of the box created for pure patchoulol system. The number of the molecule in the simulation was decided due to the capability of the computer in simulating the molecule. In the beginning, the number of the molecule was calculated based on the calculation below. The calculation is the example for the binary patchoulol/water system. After some simulation that have been done using the number of molecule based on the calculation, the simulation was failed to run due to the huge number of atom that have to be calculate. Later, the number was decided after some simulation due to the cpu capabilities.

Patchoulol

Water

Mass : 0.225mg / 0.00023 g

Density of water

JMR : 222.36

$$= \frac{\text{mass in gram}}{\text{volume in mL}}$$

$$= 1 \text{ g/mL}$$

No of molecule of patchoulol

For 1 liter of water , there is 1000 mass in gram

=No of mole x Avogadro Number

No of molecule of water

$$= \left(\frac{\text{mass in gram}}{\text{JMR}} \right) \times \text{Avo. Number}$$

=No of mole x Avogadro Number

$$= \frac{0.00023}{222.36} \times (6 \times 10^{23})$$

$$= \left(\frac{\text{mass in gram}}{\text{JMR}} \right) \times \text{Avo. Number}$$

$$= 0.00000103 \times (6 \times 10^{23})$$

$$= \frac{1000}{18} \times (6 \times 10^{23})$$

$$= 55.56 \times (6 \times 10^{23})$$

The ratio of the molecule

$$= \frac{55.56 \times (6 \times 10^{23})}{0.00000103 \times (6 \times 10^{23})}$$

$$= 53,941,747.6$$

Ratio water to patchoulol = 53,941,747 : 1

∴ impossible to simulate in computer

Table 3.1

Summary of simulation boxes system

System	Number of molecule	Density (g/mL)	Box size
Pure system			
• Patchoulol	20	1	20 x 20 x 20
• Oxygen	500	0.0001	265 x 265 x 265
• Water	500	1	108 x 108 x 108
Binary system			
• Patchoulol + oxygen	10 + 200	1	108 x 108 x 108
• Patchoulol + water	10 + 200	1	125 x 125 x 125
Tertiary system			
• Patchoulol + water + oxygen	10 + 500 + 200	1	125 x 125 x 125

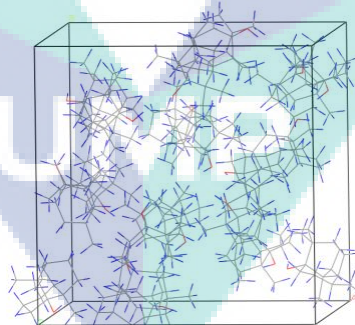


Figure 3.3. A supercell containing the 20 molecules of patchoulol in a pure patchoulol system

3.4.2.1 Boundary Condition

Computer-aided simulation is always applied to small numbers ($10 < N < 10\ 000$). It is easier to prevent the molecule from drifting apart by holding the system through

cohesive force between molecules and confining the molecule in the container. However when it is performed with a few hundred molecules to thousand atoms or molecules, a large fraction of molecule will appear on the cube surface with difference force. This is called the surface effect problem. This problem usually will be removed by boundary conditions. There are two types of boundary conditions which are different depending on their functions (Li, 2005). The first type is the isolated boundary condition. This type of boundary can be used to study cluster and molecules surrounded by vacuum. The particles will then interact among themselves. The second type is the periodic boundary condition. In this work, the periodic boundary was used due to the suitability of the boundary to study the particle in bulk liquid and solids. In this boundary, the molecules are located in a box called supercell. Next, the supercell replicated the periodic images of it and surrounded the original supercell (**Figure 3.4a**). The molecules interacted with the molecules in the same supercell and also with the molecules in adjacent image supercell. In addition, the periodic images will be reacting the same way with the original molecule. As in **Figure 3.4b**), if one molecule is missed out of the box, one of the periodic images will enter the original box from the opposite face (Côté et al., 2001). Therefore the density and number of molecules will be maintained. With this modification, the large system can be replaced and simulated with a small number of molecules and surface effect problems can be removed. Once again, after the box has been created, the simulation box can be minimized to have the lowest and stable energy configuration.

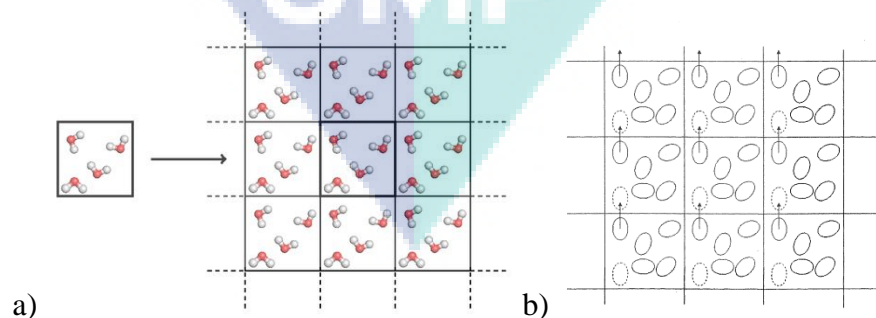


Figure 3.4. a) Illustration and b) the concept and working mechanism of periodic boundary conditions

3.2.2 Equilibration and Simulation Running Phases

After the system has reached stable energy by energy minimization steps, an equilibration phase will be needed. This step is required to ensure that the desired temperature was achieved. In this process, the system was equilibrated by NVE ensemble for 200ps to the desired temperature of 301 K and at the pressure of 0.0001 GPa. In NVE ensembles, the number of particles, volume and the energy are constant. Within these dynamic run, the temperature and pressure will be controlled by the Nose-Hoover Thermostat with a decay constant of 0.1 ps, and the Berendsen barostat also with a decay constant of 0.1 ps. Molecular dynamic simulation was carried out in densities and temperature in the range of $1 \leq \rho \leq 0.001$ g/mL and $299 \leq T \leq 302$ K, respectively, and the pressure was set about 0.0001 GPa in every simulation. After finishing an equilibration period, the system was resumed with the simulation running phase. In this process, the NPT ensemble was chosen due to the suitability in studying the intermolecular interaction at constant temperature and pressure. The total simulation time carried out was at 1000 ps with a 1 ns timestep. All the parameters were tabulated in Table 3.2.

Table 3.2

Summary of equilibration and simulation running phases

Equilibration Phase				
NVE ensemble	Total simulation time	200 ps		
	Density	$1 \leq \rho \leq 0.001$ g/mL		
	Pressure	0.0001 GPa	Berendsen barostat	Decay constant :0.1 ps
	Temperature	$299 \leq T \leq 302$ K	Nose-Hoover Thermostat	Decay constant :0.1 ps

Table 3.2 continued

Simulation Running Phase		
NPT ensemble	Total simulation time	1000 ps
	Time step	1 ns

3.2.3 Trajectory Analysis

The last step in molecular dynamic simulation is the analysis of radial distribution function (rdf) from the trajectory output files. The rdf measured the intermolecular interaction between molecules. In this work, the calculation of rdf is based on two types of intermolecular interactions, hydrogen bonding and the van der Waals interaction which exists in the study system. Both interactions play important roles in biotransformation activities. The initial step in trajectory analysis was the atomic labelling. The purpose of the labelling was to give a command to the computer to count the atom of interest in the rdf calculation to describe the hydrogen bond and van der Waals interactions. Labelling process required only a single molecule from the bulk of system. For example, in one periodic boundary box for pure water system, one molecule of water over 100 molecules of water was chosen in the labelling process. The basic schematic atomic labelling for three molecules is presented in **Figure 3.5**.

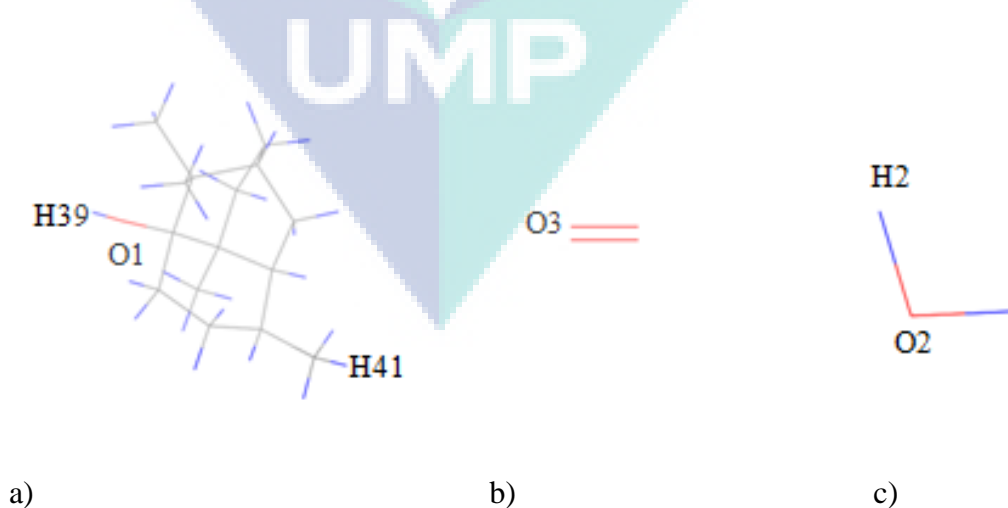


Figure 3.5. Schematic atomic labelling for a) patchouliol b) oxygen and c) water molecules.

Next procedure was the atom selection process. Atom selection process is the selection of the atom from the older labelling molecule and to synchronize it with all atoms from the same molecule in a system. Once the process is completed, the rdf calculation can be measured from the trajectory. The rdf calculation was computed from the Forcite module in the Material Studio Package.

3.3 Analysis Of Radial Distribution Function

In this work, the analysis of rdf was calculated on the two types of the important interactions, hydrogen bonding and van der Waals interaction. These two interactions will represent the structure and the interaction in pure and binary system. All the analysis was run at 20.0 cut off and 0.5 intervals.

3.3.1 RDF Analysis in Pure System

The purpose of the analysis on pure system was to investigate the interaction that contributes to self-assembly between molecules. For patchoulol and pure water systems, the simulation was run at liquid phase while the oxygen pure system was run at gas phase. Hydrogen bond is a strong interaction between an electronegative atom and a hydrogen atom bonded to another electronegative atom (Section 2.9.1). In pure patchoulol system, O1 plays the role as an electronegative atom attracted to H39. H39 is the hydrogen atom from the neighbouring patchoulol molecule bonded to oxygen. The interaction is illustrated in **Figure 3.6** as the hydrogen bond was form between H39---O1 where the patchoulol molecule form the self-assembly in the liquid phase at 301 K.

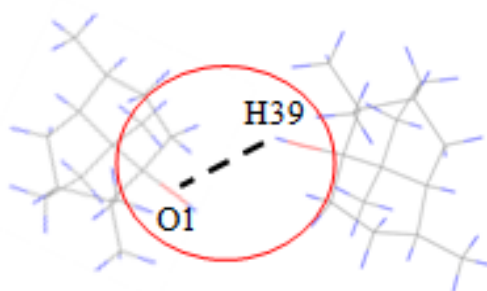


Figure 3.6. Illustration of hydrogen bond formation between H39 and O1 in pure patchoulol system

Dissolved oxygen gas plays an important role to act as a hydrogen bond donor to the patchoulol molecule in the biotransformation process. At present, there are a few papers reporting the simulation of oxygen in the gas phase. Most of the papers have reported the study in liquid oxygen. In this work, the capability of COMPASS force field to simulate the oxygen in the gas phase was investigated. Besides that, the result of the rdf analysis was also compared with the interaction in binary system to investigate the effect of oxygen on patchoulol system. **Figure 3.7** illustrates the rdf calculated between O3---O3 between the oxygen molecules.

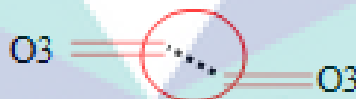


Figure 3.7. Illustration of interaction between O3---O3 in pure oxygen system.

In addition, the interaction in pure water system also was conducted in order to investigate the hydrogen bond interaction which occurs between the oxygen and the hydrogen atom amongst water molecules in the system. The illustration of interaction between H2 and O2 investigated is presented in **Figure 3.8**.

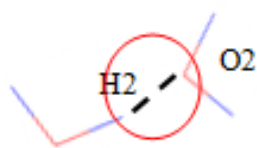


Figure 3.8. Illustration of interaction between H2---O2 in pure water system

3.3.2 Rdf Analysis in Binary System

The purpose of the analysis on binary system is to investigate the interaction which initiated the formation of hydroxyl group in the biotransformation process, either from dissolved oxygen gas or water molecule. All simulations in this system were run in liquid phase including the oxygen as it dissolves in water. The key step in this simulation is the interaction between patchoulol and oxygen. From theory, the biotransformation of patchoulol to 10-hydroxypatchoulol occurred when one atom oxygen was incorporated into hydrogen (labelled as H41) as shown in **Figure 3.5**.

A simple screening simulation has been done between two molecules patchoulol with twenty molecules of dissolved oxygen gas, in order to calculate which hydrogen was strongly attracted with the O3 (**Figure 3.9**). As a result, the oxygen was attracted more to H41 compared to other hydrogen. Because of that, H41 had been selected to be the reference atom in this simulation.

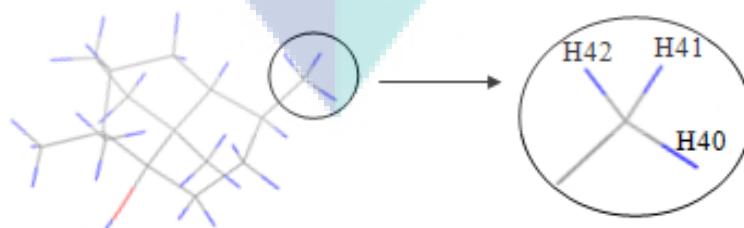


Figure 3.9. Simple screening simulation

The first system investigated in binary system was the patchoulol/oxygen system. In this system, there are two interactions of interest which have to be investigated. Two interactions which calculated were:

- (i) Hydrogen from patchoulol molecule (H41) with oxygen from dissolved oxygen gas (O3). The purpose of this analysis was to investigate the van der Waals interaction that led to the formation of hydroxyl group formation (Figure 3.10a).
- (ii) Hydrogen from patchoulol molecule (H39) and oxygen from dissolved oxygen gas (O3). The purpose of this study was to investigate the hydrogen bond that might be form as the H39 is attached with oxygen in the patchoulol molecules. It is predicted that, the higher electronegativity of the hydrogen (H39) will attract the oxygen from the dissolved oxygen molecules. This analysis also will be compared with the H41---O3 interaction (Figure 3.10a) in order to compare the strength of the interaction.

Meanwhile, in binary patchoulol/water simulation system, the calculation of rdf was to investigate two types of hydrogen bonds which might occur in this system (**Figure 3.11**). The three types of hydrogen bonds which will be calculated were:

- (i) Hydrogen from patchoulol (H41) and oxygen from water (O2). The purpose of this analysis was to calculate the probability of an interaction between patchoulol and water molecules, which can initiate the hydroxyl group formation.
- (ii) Hydrogen from patchoulol (H39) and oxygen from water (O2). The purpose of this analysis was to investigate any interaction between these two atoms which have the probability to affect the interaction among patchoulol molecules.



Figure 3.10. Illustration of van der Waals interaction between a) H41 and O3 and the hydrogen bond interaction between b) H39 and O3

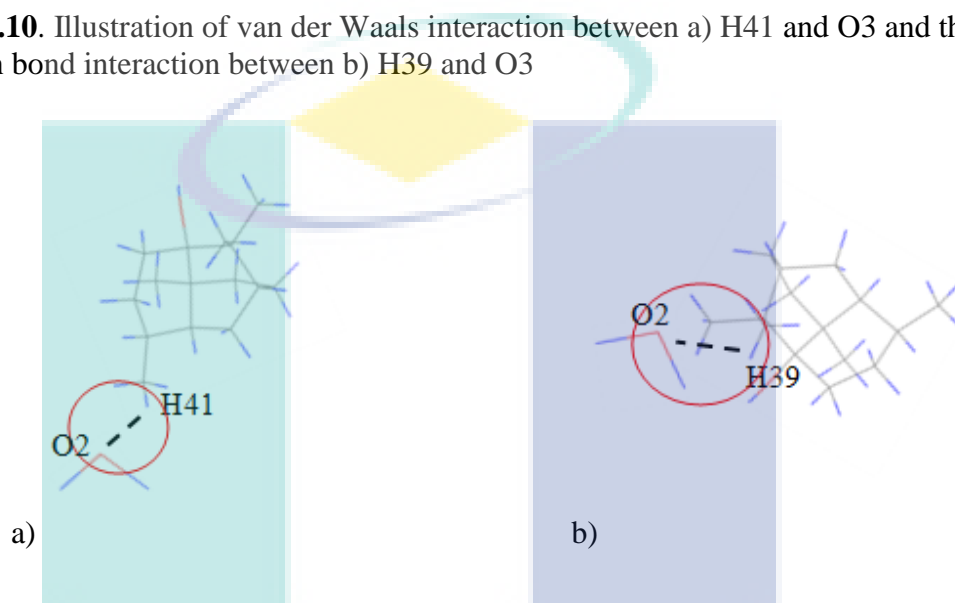


Figure 3.11. Illustration of hydrogen bonds interaction between a) H41 and O2 b) H39 and O2

3.3.3 Rdf Analysis in Tertiary System

Biotransformation activity involves three elements simultaneously, namely patchoulol, water and oxygen. Due to that, a tertiary system was conducted to mimic the real experiment. In tertiary system, the patchoulol, water and oxygen molecules were combined together and allowed to interact. The number of each molecule was described earlier in Table 3.1. Four analyses were carried out and **Figure 3.12** tabulated the rdf analysis in the tertiary system.

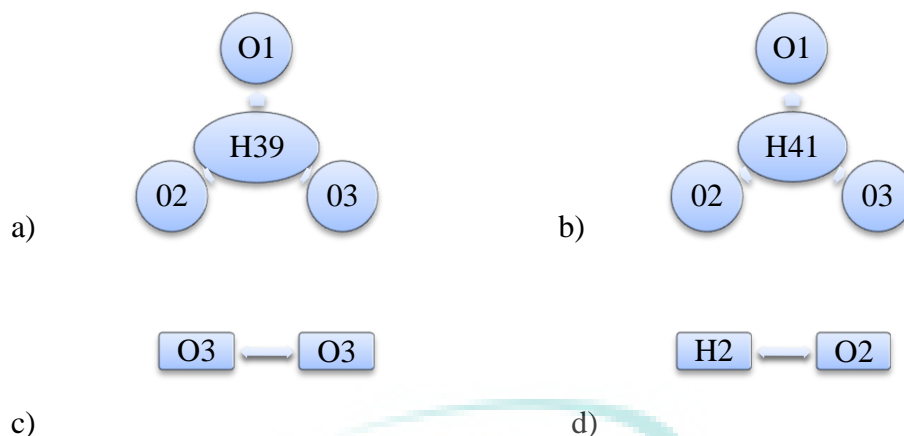


Figure 3.12. Rdf analysis in the tertiary system

In **Figure 3.12(a)** the rdf analysis determined the strongest hydrogen bond. The rdf calculation in **Figure 3.20(b)** determined which of the two elements, either water or oxygen, as a key factor initiating the formation of the hydroxyl group. Whereas rdf data of **Figure 3.20(c)** and **(d)** were calculated and compared with the data from pure and binary system.

3.4 Experimental Work On Biotransformation Process

In this work, the biotransformation process was carried out to verify the molecular dynamic simulation process between the interaction of patchoulol and oxygen. In addition, it is designed in order to study the biotransformation process of patchoulol. Basically, the experimental section is divided into four activities as shown in **Figure 3.13**

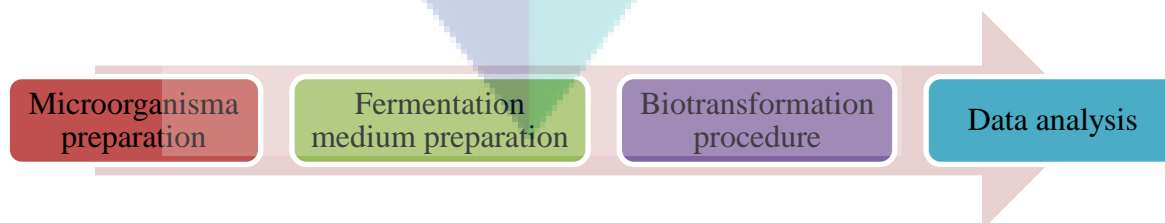


Figure 3.13: Experimental section

3.4.1 Preparation of Microorganism

Aspergillus niger was obtained from Permulab Sdn.Bhd, Petaling Jaya, Selangor. To avoid any contamination from other microbes, all the processes involving fungi were carried out in a laminar flow chamber. In the preparation of the agar plate, dehydrated potato dextrose agar (39 g) was mixed with distilled water in a (1 L) clean beaker. The mixture was heated and mixed using a magnetic mixer (**Figure 3.14a**) for two minutes to ensure complete dissolution of agar. The medium was then sterilized in an autoclave for 15 minutes at 121°C, 15 psi (**Figure 3.14b**). The sterilization process is important as to prevent contamination of other microbes in the medium. Then, the medium was cooled down to 45 °C prior to allowing it to set in sterile petri plates. If the plates were going to be refrigerated for future use, the petri plates will have to be stored upside down with the agar on the upper half of the dish to prevent condensation from dripping down and contaminating the growing surface.

Next, the process was continued with the subculture process. In this process, the culture of *Aspergillus niger* was inoculated onto the agar by removing out some hyphae by inoculating loop and was placed in the centre of the plate. The hypha was chosen because it is the most active structure and it has the capability to spread out from this region in a very short time. The details of the subculture process are as presented in Figure 3.15. Firstly, to avoid any possible contamination, the loop used must be sterilised using a flame until it glows. Then, the heating process was repeated each time before the transfer of hyphae process to ensure that no contamination occurs. The loop was ensured to be cold before it can be inserted in the fungus culture or otherwise the *Aspergillus niger* might die. Again, the inoculated petri plate has to be stored upside down at 29-30°C with the agar on the upper surface in the incubator. A colony of fungus was left to grow within 5 to 7 days.

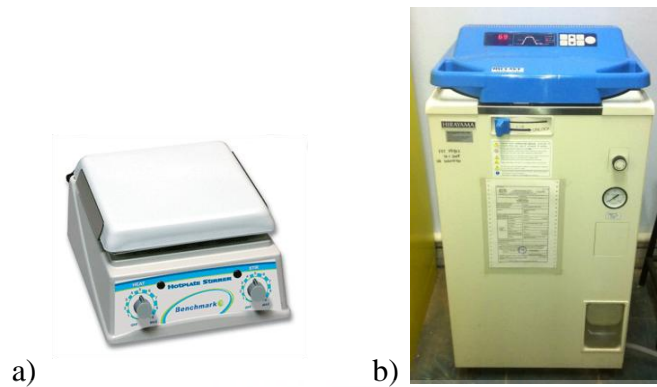


Figure 3.14. Photos of a) magnetic mixer and b) autoclave used in this study

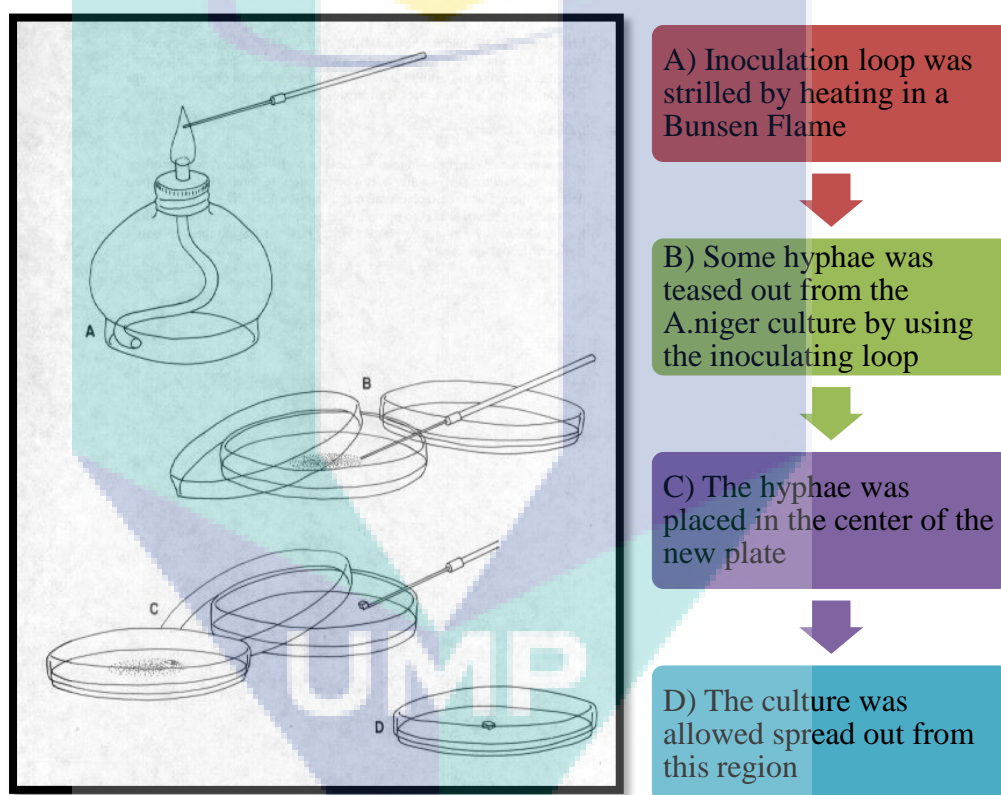


Figure 3.15: The process of subculture preparation

3.4.2 Preparation of Fermentation Medium

Medium was made up of glucose (40 g), yeast extract (1 g), potassium dihydrogen phosphate (5 g), sodium nitrate (2 g), magnesium sulphate (0.5 g), ferrous sulphate (10 mg) and zinc sulphate (5 mg). The medium was mixed with 1 litre of

distilled water. The medium (1 L) was divided into six conical flask with each conical flask contains 150 ml of medium. Media were autoclaved at 121°C for 5 min.

3.4.3 Fermentation Procedure

The procedure for biotransformation began with the inoculated process of *Aspergillus niger* into the fermentation medium. About 2 cm² of the hyphae was removed from *Aspergillus niger* culture (5 days old) and transferred to the fermentation (Figure 3.16). The medium was then placed on the rotary shaker at 200 rpm (30°C) for three days.

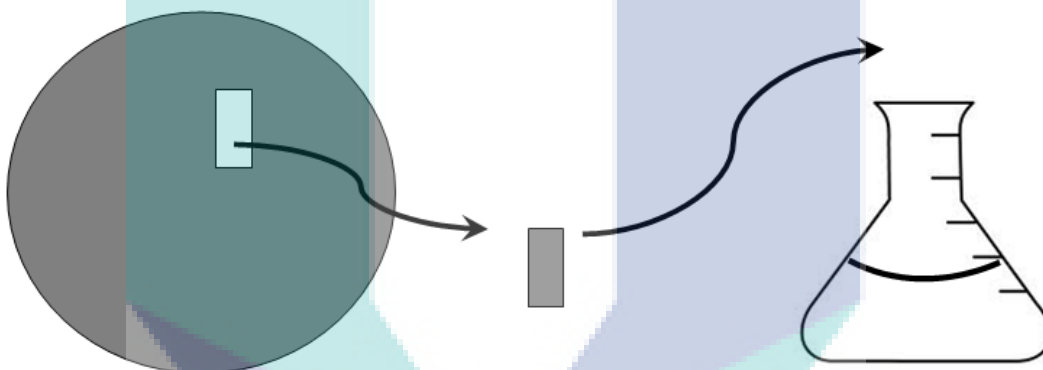


Figure 3.16. The transferring hyphae to the fermentation medium process

Next, 0.225 mg patchoulol mixed with 1.5 mL ethanol that give 150ppm, was evenly distributed between six fermentation media. Patchoulol (C₁₅H₂₆O) used was the hexagonal-tropezohedral crystal with molecular weight of 222.36 g/mol and 1.0284 mL and 99% purity which was purchased from Carbosynth, UK. It is soluble in ethanol, but practically soluble in water. The calculation that gives 150 ppm is stated as below:

$$\frac{0.225 \text{ mg (patchoulol)}}{0.0015 \text{ liter (ethanol)}} = 150 \text{ ppm} \quad (3.2)$$

Again, the fermentation process was carried out through incubation in the rotary shaker at 200 rpm (30°C) for 5 days. According to Suhara et al, (1981), the best phase of the 10-hydroxylation production is between fourth day and seventh day. Next, the

fermentation medium was separated with hexane using rotary evaporator (Figure 3.17). About 100 mL of hexane was added to the fermentation medium forming two layers (Figure 3.17a). The upper layer was the hexane layer, and the bottom layer was the culture medium layer. It was placed on a rotary shaker and allowed to rotate at a speed of 200 rpm (30 °C). While the shaker was operated, the hexane solvent extracted the 10-hydroxypatchoulol compound. A study by Foong, (2008), utilized hexane as an extraction solvent in order to extract the patchoulol compound from the patchouli oil. Similarly, it was predicted that, hexane will extract out the 10-hydroxypatchoulol. Then, the fermentation medium was separated from the solvent by using a separating funnel. The lower layer will be removed and the upper layer (hexane solvent layer + 10-hydroxypatchoulol compound) was evaporated in vacuum (Figure 3.17b). The temperature of the rotary evaporator was set at 68°C which is the boiling point of hexane. The flask containing the hexane layer was subjected to the water bath. The hexane boiled, evaporated and formed hexane vapour. When the hexane vapour flowed through the water-cooler condenser, it condensed and formed the liquid hexane which accumulated in the receiving flask. Then hexane solvent in the receiving flask was removed and the residue in the sample flask will be taken and analyzed by GC-MS.

3.5 Analysis Of Chemical Compounds Using Gas Chromatography-Mass Spectrometer (Gc/Ms)

A gas chromatography-mass spectrometer (GC/MS) was used to analyse the chemical content of the sample of the biotransformation process. In this study, the compound predicted to be present in the sample was 10-hydroxypatchoulol. In this part, the GC being used was the Agilent 7890A type model G3440A, with the GC system of Agilent Technologies. The GCMS condition for capillary column was tabulated in Table 3.3. About 10% of sample in hexane will be analysed by GCMS and the calculation is showed below:

$$\frac{1 \text{ ml sample}}{10 \text{ ml hexane}} \times 100 = 10\% \quad (3.3)$$

Table 3.3

Parameter of GCMS analysis

Parameter	GCMS (Agilent 7890A)
Injector temperature	300 °C in pulsed splitless inlet (10:1)
Injection volume	1 μL via auto sampler
GC Condition	80°C and hold at 0.5 minutes before it was increased to 245°C and hold at 20 minutes
Carrier gas	Helium at 1mL/min
Column	Type DB-WAX 25 m x 250 μm x 0.2 μm
Heating rate	5°C as the run time 38.5 minutes

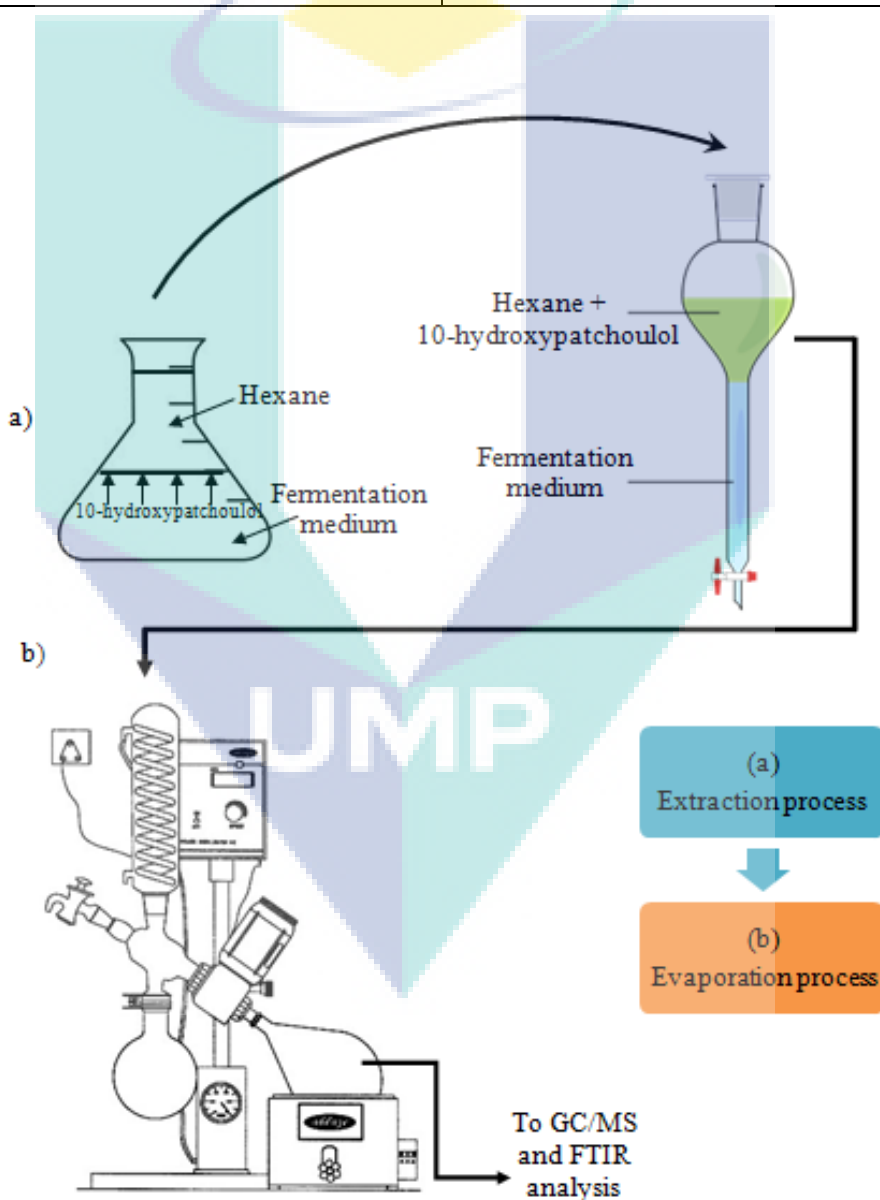


Figure 3.17. Summarized step to obtain the 10-hydroxy patchouliol

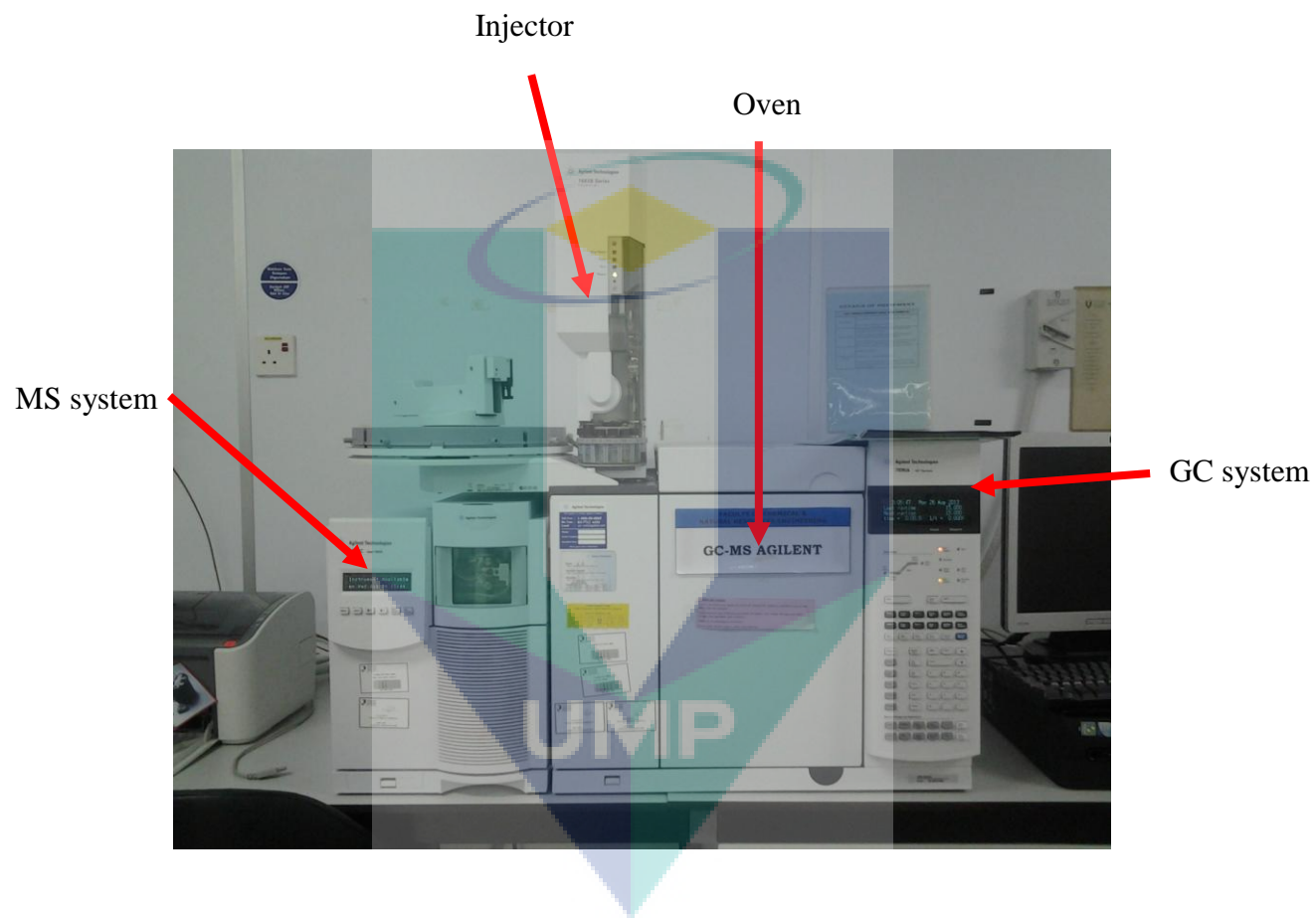


Figure 3.18. Gas chromatography-mass spectrometer (GC/MS) instrument

3.6 Analysis Of Fourier Transform Infra Red (FTIR)

The characteristics of the certain molecule will be representing by the vibrational spectrum of the molecule. This unique physical property can be detected by the analysis of the Fourier Transform Infra Red (FTIR). In this study, the FTIR will be conducted by experimental and simulation.

3.6.1 Experimental FTIR Procedure

There are two samples were analysed by experimental procedure, pure patchoulol and sample of biotransformation. The FTIR spectra of the samples were scanned by the Perkin Elmer ATR-FTIR with spectra range of 700-4000 cm^{-1} (**Figure 3.19**).



Figure 3.19. FTIR instrument

3.6.2 Gaussian FTIR Procedure

The simulation of the quantum mechanics on the molecule of the 10-hydroxypatchoulol was conducted because there is a limited information on this molecule. Through this simulation, the surface information related with the functional group and the frequency can be gathered. For the first step, the structure of 10-hydroxypatchoulol was first constructed using Material Studio software and saved as mol.file that can be used in Gaussian software. Then the structure will be transferred to Gaussian software and was run in the quantum mechanics discipline. The internal coordinate like bond length, bond angle and dihedral angle of the basic structure will be presented in **Error! Reference source not found.** in a form of z-matrix. The second step in the Gaussian simulation is the energy optimization. This step is crucial in order to get the right structure and in the optimum energy level. The failure in this step will cause the simulation cannot be run perfectly. **Figure 3.20** shows the optimized structure of the 10-hydroxypatchoulol. Then, the structure was left to be vibrated and was produced the IR spectrum data.

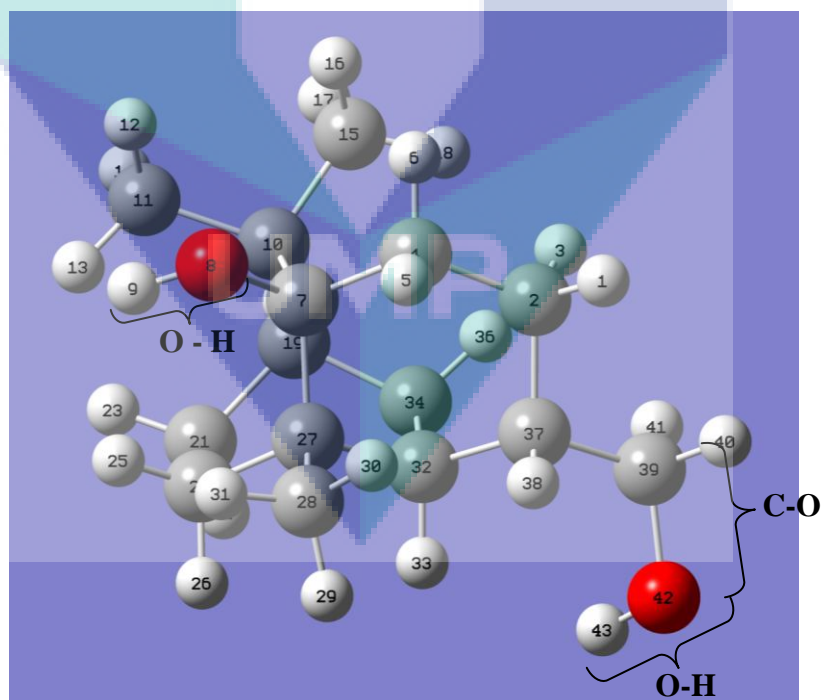


Figure 3.20. The optimized structure of 10-hydroxypatchoulol

Table 3.4:

Z-matrix of basic hexagonal structure of 10-hydroxypatchoulol

Atom no	Atom	References atom	Bond Length (Å)	Reference atom	Bond Angle (°)	Reference atom	Dihedral Angle (°)
1	H	NIL	NIL	NIL	NIL	NIL	NIL
2	C	1	1.099607	NIL	NIL	NIL	NIL
3	H	2	1.09846	1	105.6458	NIL	NIL
4	C	2	1.548513	1	108.4677	3	-118.4190865
5	H	4	1.095999	2	108.935	1	-44.3702542
6	H	4	1.095146	2	109.8298	1	70.8216089
7	C	4	1.554792	2	117.1251	1	-164.0736954
8	O	7	1.48046	4	100.573	2	165.3706442
9	H	8	0.978852	7	110.7569	4	-179.9260806
10	C	7	1.614323	4	116.0775	2	-75.2196354
11	C	10	1.557819	7	111.4158	4	-130.0577739
12	H	11	1.095197	10	110.6697	7	67.2562736
13	H	11	1.096701	10	114.0669	7	-54.628973
14	H	11	1.098392	10	109.3237	7	-173.9380683
15	C	10	1.55252	7	113.467	4	-11.9246675
16	H	15	1.096677	10	111.0985	7	-60.4158094
17	H	15	1.098952	10	109.4087	7	-178.8489865
18	H	15	1.093043	10	113.4332	7	61.3037143
19	C	10	1.57226	7	107.7843	4	110.0029138
20	H	19	1.100297	10	108.3211	7	-170.8489669
21	C	19	1.547008	10	111.037	7	68.4328767
22	H	21	1.098732	19	108.7789	10	-173.6622045
23	H	21	1.095593	19	111.5661	10	69.4091776
24	C	21	1.554552	19	108.2516	10	-53.3643743
25	H	24	1.100448	21	110.9155	19	110.8029393

Table 3.4 continued

Z-matrix of basic hexagonal structure of 10-hydroxypatchoulol

Atom no	Atom	References atom	Bond Length (Å)	Reference atom	Bond Angle (°)	Reference atom	Dihedral Angle (°)
26	H	24	1.09872	21	110.6013	19	-132.5068416
27	C	24	1.558839	21	111.7755	19	-11.6170585
28	C	27	1.54697	24	107.289	21	-172.7276341
29	H	28	1.099298	27	109.8578	24	67.7903809
30	H	28	1.093102	27	113.6623	24	-171.4352086
31	H	28	1.096129	27	110.5336	24	-51.2880718
32	C	27	1.571687	24	108.1007	21	-51.6616297
33	H	32	1.102634	27	106.0806	24	-56.6041275
34	C	19	1.547636	10	111.1858	7	-50.3559169
35	H	34	1.098756	19	108.7647	10	-175.567209
36	H	34	1.095628	19	110.1156	10	-59.7888381
37	C	2	1.549038	1	109.3724	4	-124.0345136
38	H	37	1.097986	2	108.7706	1	49.2819071
39	C	37	1.541141	2	110.4297	1	-66.5161169
40	H	39	1.095244	37	109.8695	2	54.3972861
41	H	39	1.101791	37	111.203	2	-65.1312189
42	O	39	1.466606	37	113.1167	2	170.1478768
43	H	42	0.979748	39	110.2343	37	64.59383

CHAPTER 4

RESULTS AND DISCUSSION

4.1 Introduction

This chapter discusses two main parts, the experimental and the modelling simulation analysis. Section 4.1 will discuss the result of the experimental work to verify the biotransformation process. It will cover the analysis from the FTIR and GCMS analysis. Section 4.2 will cover the molecular dynamic simulation, particularly the radial distribution function of pure, binary and tertiary system to describe the structure change.

4.2 Result Of Molecular Dynamic Simulation

The simulation work focused on two important intermolecular interactions which exist in the study system, namely, hydrogen bond and Van Der Waals interaction. Hydrogen bonding formation is important in the water and organic compound structure such as patchoulol. The intermolecular interaction between the molecules was calculated using radial distribution function.

4.3 Pure Simulation System

The main purpose of the investigation of the pure system is to get the preliminary information of the interaction and distribution of the molecule in their self-environment at a molecular level. Then, this information is compared with the result obtained in binary and tertiary system.

4.3.1 Pure Patchoulol System

In pure patchoulol system, as in **Figure 3.6** O1 is referred to the oxygen from the hydroxyl functional group from the molecules of the patchoulol. O1 plays a role as an electronegative atom to attract the H39 which is the hydrogen atom from the neighbouring patchoulol molecule bonded to the oxygen. Figure 3.14 illustrates the hydrogen bond formed between H39---O1. Figure 4.6 represents the radial distribution function of H39 with O1 from the neighbouring molecule with a sharp peak, in red line at the distance of 2.25 Å. It reflects that there is a strong intermolecular interaction formed between these two atoms. It suggests an agreement with the experimental work **Figure 4.13a)** when a peak appeared at 3500 cm⁻¹ showing the presence of the -OH group and H-bonding. Similar to hydrogen bond, van der Waals bond is also important in biological activity which in this case, might initiate the formation of any group with another group or oxygen to form hydroxyl group. This work also calculates the rdf between H41---O1 to investigate whether the van der Waals interaction might be present. Figure 4.6 also shows the radial distribution function of H41---O1, in green line, which the distance between the first nearest neighbour atom of H41 and O1 can be obtained at distance of 8.75 Å. As a result, the broad peak rdf pattern appeared and the distance reflected weak van der Waals interaction between H41 and O1 as compared to hydrogen bonding of H39---O1.

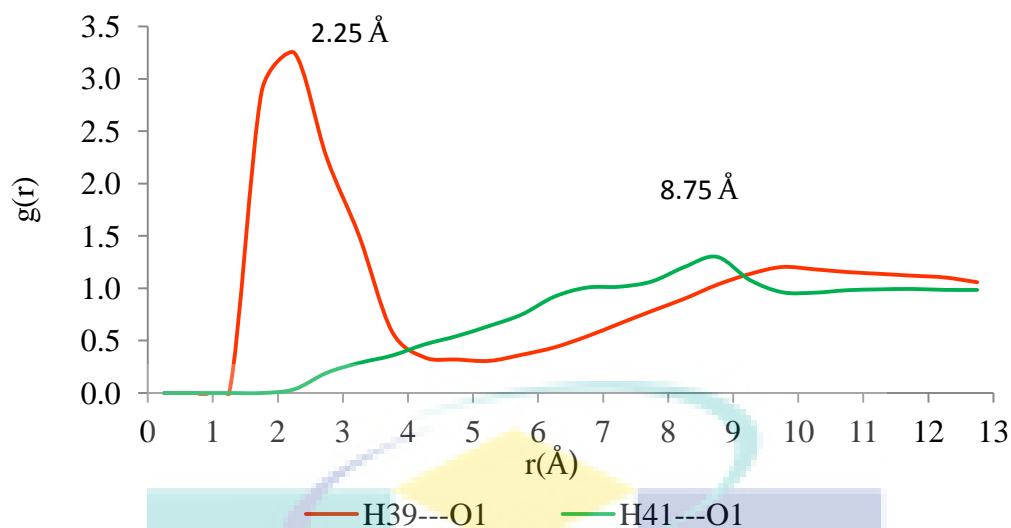


Figure 4.1. Radial distribution function of H41--- O1 and H39---O1 in pure patchouliol system.

4.3.2 Pure Oxygen System

As discussed in Section 2.4, dissolved oxygen gas plays an important role in a biotransformation process, act as a hydrogen bond donor to the patchouliol molecule. The objective of this section is to investigate the interaction of molecule oxygen in gas phase. In addition, this work is also conducted to investigate the capability of COMPASS force field to simulate oxygen in the gas phase. A simulation comprising 500 pure oxygen molecules was set up to observe the interaction between the molecules at a temperature of 301K. Barrat and Hansen (2003), described the typical pair distribution function for gas using Lennard-Jones potential and showed that the oxygen has spread out after the first peak and became less structured. **Figure 4.2** shows the comparison of radial distribution function between oxygen gas in pure system and the work was done by Thapa and Adhikari (2013). GROMACS 4.0.5 (GRONingen MACHine for Chemical Simulations) has been used in their simulations with the in-built force field ffG43a1 for modeling the oxygen molecules. The analysis of O3---O3 interaction showed the first peak in both systems was at 4.25Å. It was found that, it is in good agreement with the work done by Thapa and Adhikari (2013). These authors had also simulated oxygen gas with the final temperature and pressure at 302 K and 1 bar and obtained the first peak at 4.26Å. The RDF pattern also is in good agreement with the typical pair distribution of Barrat and Hansen, (2003). Based on this result, it shows

that, the COMPASS force field was capable to simulate the oxygen in the gas phase successfully.

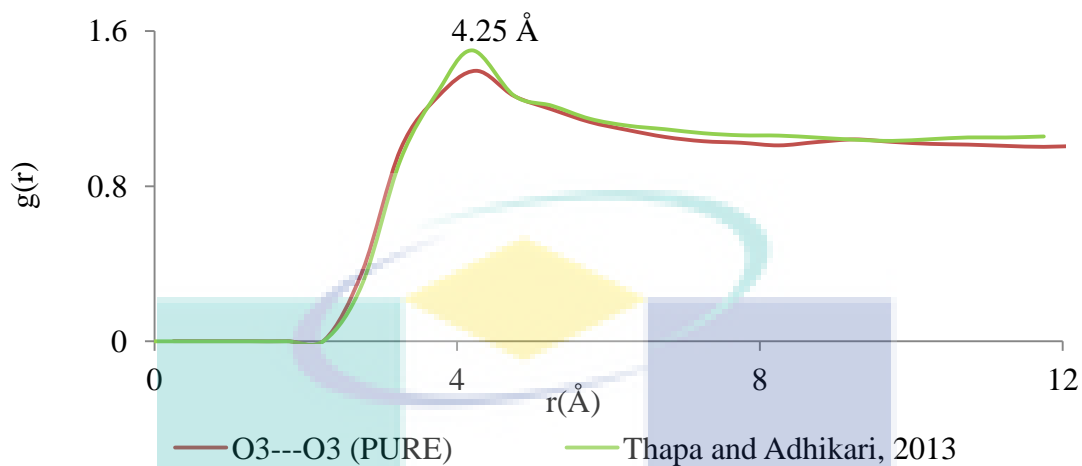


Figure 4.2. The comparison of radial distribution functions of O3---O3 in pure oxygen system in this work and Thapa and Adhikari, (2013).

4.3.3 Pure Water System

Although water is not the most important element in the process of biotransformation, it is needed in the media preparation and incubation processes. To some extent, it will affect the reaction that occurs in the process. Due to this reason, a simulation which consists of a pure water system was conducted to compare the change of their interaction in pure and mixture system. **Figure 4.3** shows the radial distribution function of pure water molecule between H2 and O2 atoms. The graph shows that there are two sharp peaks appears. The water molecule is one of the examples of molecule which has a strong hydrogen bond interacting between them. It is due to the high electronegativity possessed by the oxygen in water molecule and also the hydrogen, which has excessive positive charges that is strongly attracting other oxygen from neighbouring water molecule. The graph shows the nearest neighbouring hydrogen from the referent oxygen as 1.75Å. It indicated that there was a strong hydrogen bond between oxygen with hydrogen from the neighbouring molecule. In the liquid phase, the graph is in a good agreement with the work been done by Rahman and Stillinger (1971). They have simulated 216 molecules of water at 307K at mass densities 1 g/mL by

molecular dynamic simulation techniques. They stated that the two peaks rise from hydrogen bond interaction between the neighbouring molecules.

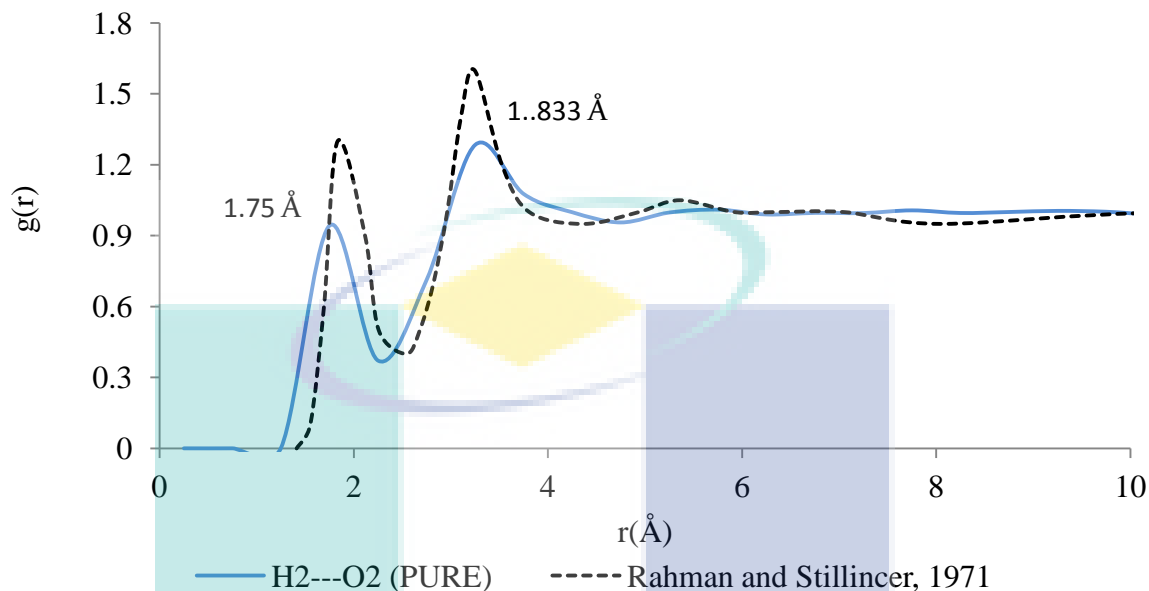


Figure 4.3. Radial distribution function of H2---O2 in pure water liquid system

The simulation of the pure system follows the typical pair distribution function pattern and exhibits good agreement with the literature. Therefore, the pure system simulation results can be used as a reference for other simulation works of binary water system.

4.4 Binary Simulation System

The important key in this simulation work is to understand the interaction between oxygen, either from water or dissolved oxygen gas with H41, hydrogen from patchoulol molecule, as explained in the hydroxylation process in Section 2.4. It is crucial because it reflects the van der Waals interaction that initiates the formation of hydroxyl group in the biotransformation process. Two simulation types of binary system was conducted, a) patchoulol with oxygen and b) patchoulol with water.

4.4.1 Binary Patchoulol/Oxygen System

In order to demonstrate the strength of interaction between dissolved oxygen and patchoulol molecule, a simulation comprising ten patchoulol molecules and two hundred dissolved oxygen gas molecules were constructed. The radial distribution function analysis was calculated between O3 with H41 to analyse the van der Waals interaction. Van der Waals interaction that exists between H41---O3 might have initiated the formation of the hydroxyl group at H41. In addition, the radial distribution function analysis of the interaction between O3 and H39 were also carried out to determine either such interactions will affect the interaction between O3 and H41.

Figure 4.4 shows the location of the first neighbouring atom from radial distribution function graph between a) H41 and O3 is at 5.25Å, b) H39 and O3 is at 7.25Å. The difference between rdf readings of about 2Å suggested that the interaction between H41---O3 is stronger than H39---O3 even though a hydrogen bond had formed between H39---O3. This reflects that the hydrogen bonding interaction between H39 and O3 does not interrupt the interaction between H41 with O3.

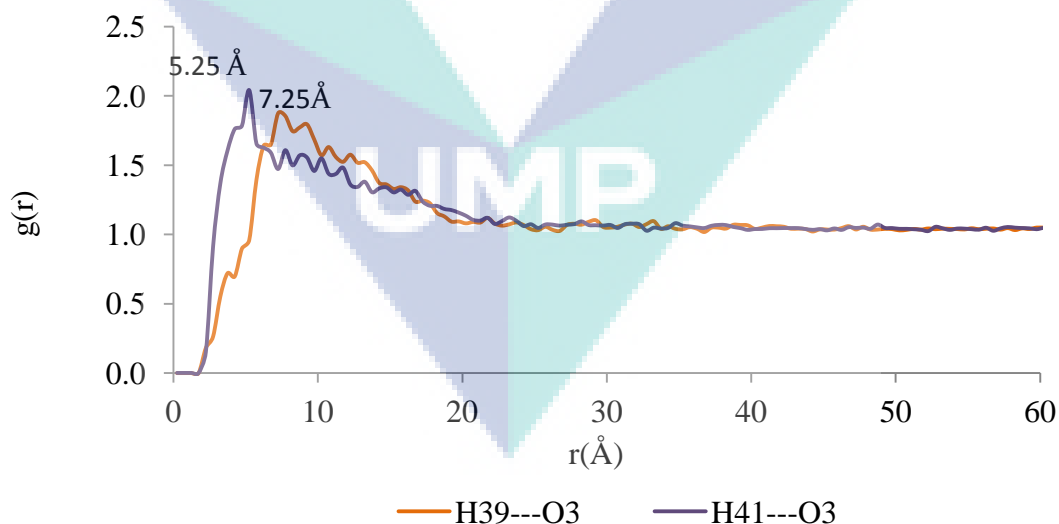


Figure 4.4. Radial distribution function of H39---O3 and H41---O3 in binary patchoulol/oxygen system

The comparison between the simulations of O3---O3 in pure and binary systems was made to show whether there was perturbation in the interaction or structured

change. **Figure 4.5** shows the interaction of the molecule of dissolved oxygen in the pure and binary systems. The radial distribution function of oxygen in the binary system shows the first neighbouring atom peaked at a distance of 4.25\AA , which was similar to the pure oxygen system. There was no change on the structure which would reflect the repulsive force of oxygen in the binary system that have the same repulsive strength as in the pure system. It also showed that the presence of patchoulol molecule is not significantly interrupted by the interaction of the molecule of dissolved oxygen gas in the binary system in the presence of 10-hydroxypatchoulol molecules. Therefore further investigation should be conducted to understand more on this repulsive interaction in a simulation system.

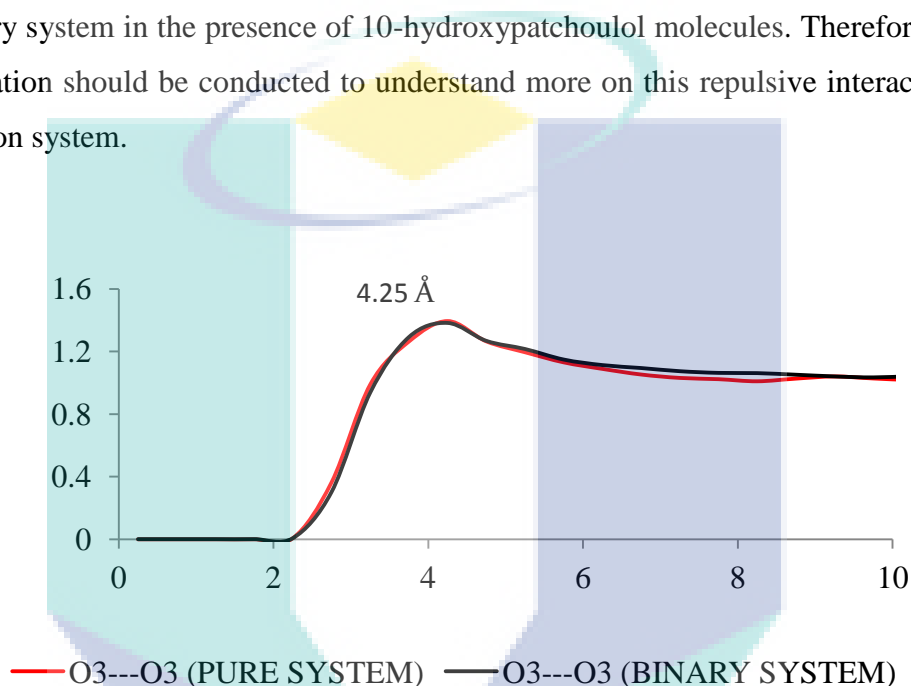


Figure 4.5. Radial distribution function of O3---O3 in pure and binary patchoulol/oxygen system showing unchanged structure

4.4.2 Binary Patchoulol/Water System

A simulation of two hundred molecules of water and ten molecules of patchoulol were conducted to investigate the effects of interaction between water and patchoulol molecules. This simulation will determine the radial distribution function between O2 from water molecule with H39 and H41 from patchoulol molecule as explained in Section 3.6.2. **Figure 4.6** shows the radial distribution function of O2 with H39 and H41. The graph explains that oxygen from water (O2) is strongly attracted to H39 evidence by the sharp peak at 1.75\AA but there is a huge peak at 19.75\AA was observed

for H41---O2. This could arise from the less interaction between H41 and O2. According to the explanation on the hydrogen bonds in Section 2.9.1, O2 is the oxygen atom from water molecule which has high electronegativity charges. Besides that, H39 also attached with the oxygen atom in the patchoulol molecules. Because of two reasons, the interaction between H39---O2 is more strongly than H41---O2.

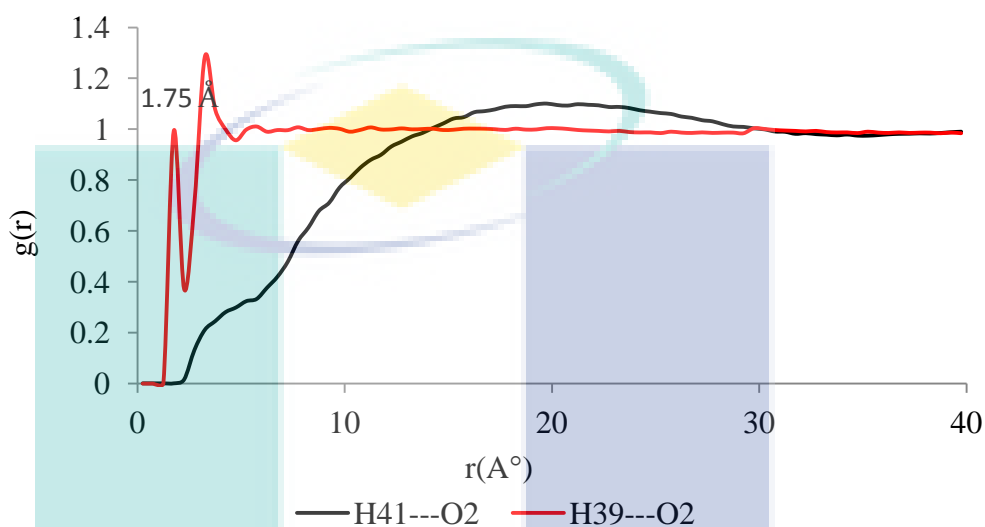


Figure 4.6. Radial distribution function of H39---O2 and H41---O2 in binary patchoulol/water system

Two major conclusions can be drawn from the simulation of the binary systems. This simulation suggests that the H41 is more attracted to form van der Waals interaction with dissolved oxygen gas compared to oxygen from water to form the hydroxyl group in H41. It is also suggest that, H39 is strongly attracted to water molecule to form hydrogen bond.

The two conclusions are reinforced by a description of two graphs from **Figure 4.7** (a) and (b). **Figure 4.7** (a) which shows the radial distribution function between H41 --- O3 and H41 --- O2. Implicitly, it is an attraction comparison between H41 with water and dissolved oxygen gas. From the results, it shows that H41 is more attracted to oxygen gas from water. This suggests the occurrence of the formation of the hydroxyl group is between H41 and oxygen gas instead of water. It shows that oxygen might be the oxygen donor to the patchoulol in order to convert to 10-hydroxypatchoulol through the hydroxylation process. Meanwhile **Figure 4.7** (b) shows the radial distribution

function between H39 --- O3 and H39 --- O2. It is the comparison of attraction between H39 with water and oxygen gas. From the result, it indicates that H39 is more attracted to water than oxygen. This occurs when there is a formation of hydrogen bond between water and H39. Hydrogen bond is much stronger attraction than the van der Waals interaction. Water is one type of molecule which possesses strong electronegativity than oxygen gas. Therefore, water will cause the H39 to be more attracted towards it thus producing hydrogen bond.

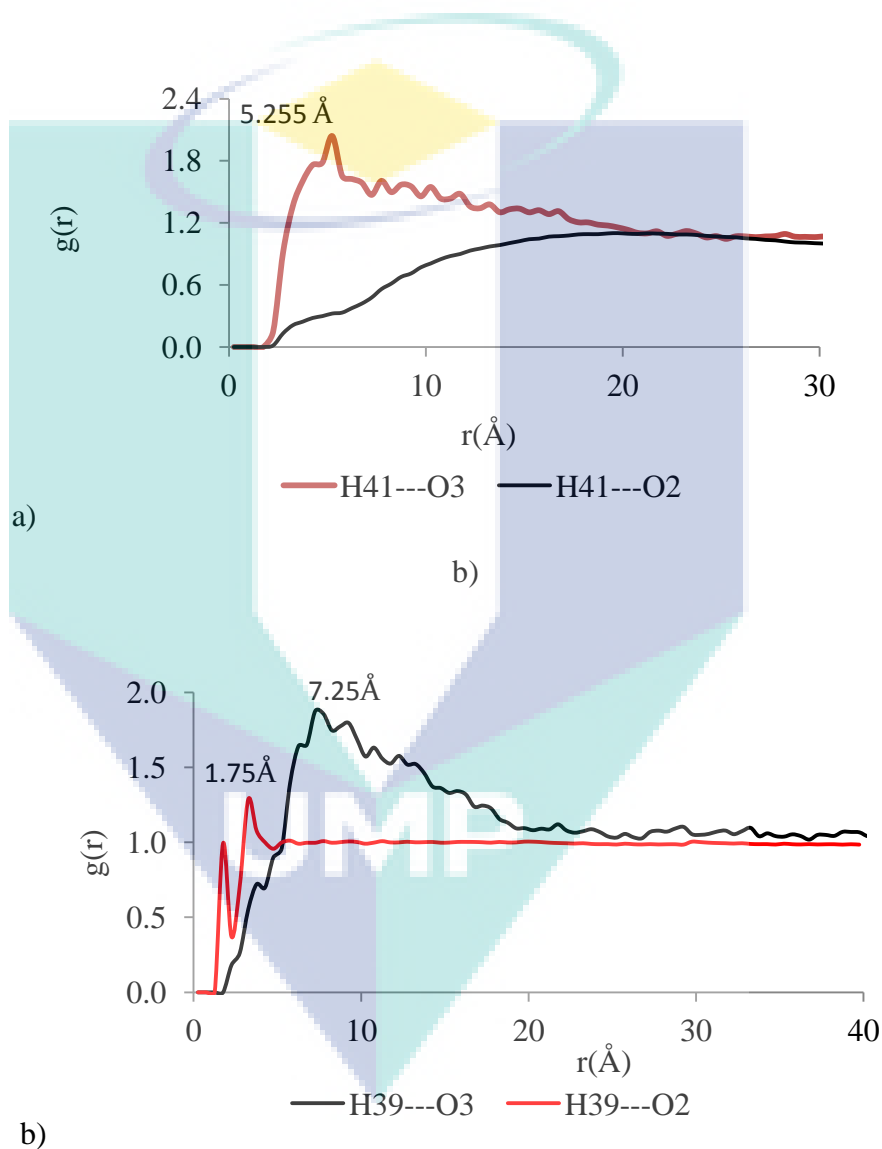


Figure 4.7. Radial distribution function of a) H41 and b) H39 with O2 and O3.

4.5 Tertiary System

Previously, the study has gone through the simulation in pure and binary systems. The investigation thus continued with simulation on the tertiary system. The interaction might occur between three important molecules, namely, patchoulol, oxygen and water. This simulation is not without challenges as a longer time needed due to a larger number of atoms. Three sections of radial distribution functions are discussed. The first section will discuss radial distribution function between H39 with O1, O2 and O3 to determine the hydrogen bond formation between H39 with the oxygen atom from patchoulol, water and oxygen gas respectively, as well as the interaction amongst them. The second section will discuss the radial distribution function between H41 with O1, O2, and O3 to determine van der Waals interaction which might occur and which initiates the hydroxyl group formation in H41. O3 --- O3 is the radial distribution function between oxygen atoms in the oxygen gas investigated in the third section. At this stage, the radial distribution function will be compared by pure, binary and tertiary systems. It reveals the distribution and the interaction of oxygen atom in the three systems. In this part also, the comparison of the radial distribution function between the interactions of H2 --- O2 in three systems were also be investigated.

4.5.1 Radial Distribution Functions of H39 With O1, O2 And O3.

The radial distribution function calculation analysis was carried out between H39 and O1, O2 and O3 to determine where hydrogen bond will be formed. **Figure 4.8** illustrates the radial distribution function between H39 with the oxygen from patchoulol, water and oxygen gas. The graph showed the interaction of H39 --- O1 at 2.25Å, H39 --- O2 at 1.75Å and H39 --- O3 at 7.25Å. It explains on the stronger hydrogen bonding forming between H39 and the water molecule. This is due to the stronger electronegativity effect on O2 in the water molecule. Indirectly, it reflects that at a certain temperature and pressure, water can contribute to the dissolving process of patchoulol in the solution during the biotransformation process.

On the other hand, the interaction between H39---O1 is still strong by having the highest number of $g(r)$ that explains the H39 and O1 still approach each other with higher numbers and contributed to the strong bond between them. These are the conditions which exhibited the self-assembly of patchoulol molecule. The interaction between H39-O3 shows a broad peak that suggests a weak interaction between them. It explains the absence of hydrogen bond between them. Based on the graph, it can be concluded that, the hydrogen bonds were formed in H39 and O2, the oxygen from the water molecules.

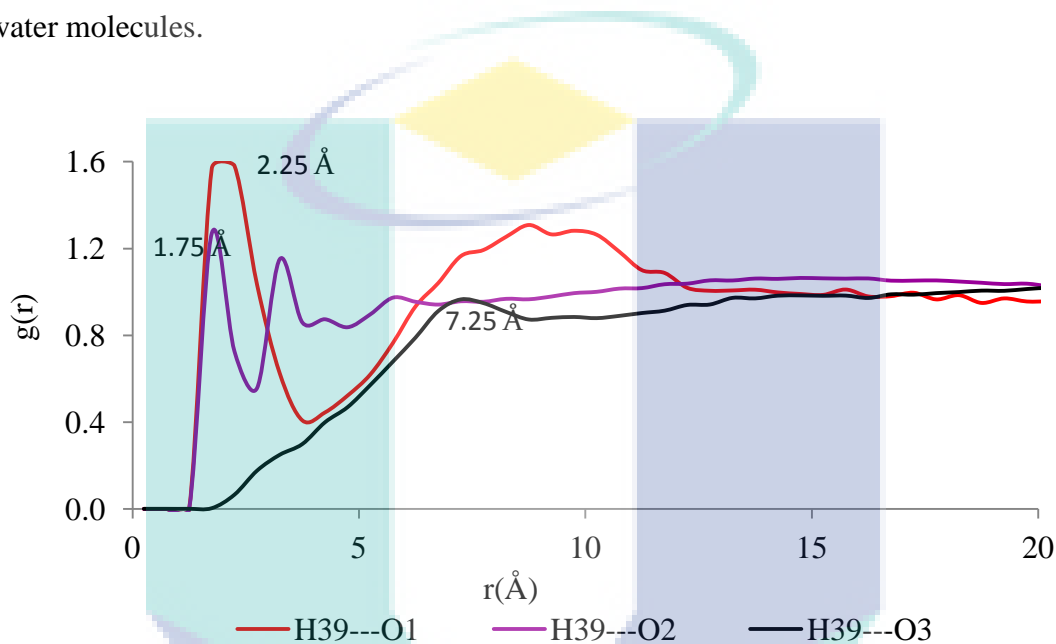


Figure 4.8. Radial distribution function of H39 with O1, O2 and O3 in tertiary patchoulol/oxygen/water system

4.5.2 Radial Distribution Functions of H41 With O1, O2 And O3.

The interaction of H41 with the oxygen is important because it reflects the important step in the biotransformation process. Due to that interest, the analysis of radial distribution function between H41 and O1, O2 and O3 are conducted to determine which interaction more likely represented by the van der Waals attraction. The radial distribution function between H41 with O1, O2 and O3 are presented in **Figure 4.9**. Only two peaks arise from the three radial distribution functions. It shows that, H41 --- O3 have a slightly sharp peak with the nearest distance at 3.75 \AA , and the first slightly broad peak for H41---O1 is at 6.75 \AA . The sharp peak explains that there is strong

interaction between H41 and O3, oxygen from dissolved oxygen gas. This clearly explains that the van der Waals interaction might occur at H41---O3 that initiate the formation of the hydroxyl group at H41. This also may suggest that, with the assistance of an enzyme as catalyst in the real experiment, the oxygen from dissolved oxygen probably participated in forming the hydroxyl group at H41 and continue with the formation of 10-hydroxypatchoulol . In addition, it could be said that there is less interaction developed between H41 and O1 oxygen from the patchoulol molecules. As in the binary system, there is no peak appearing in H41---O2 and this also suggests that there is no interaction occurring between them. So, this concludes that, water is not the contributor for the oxygen donor to H41.

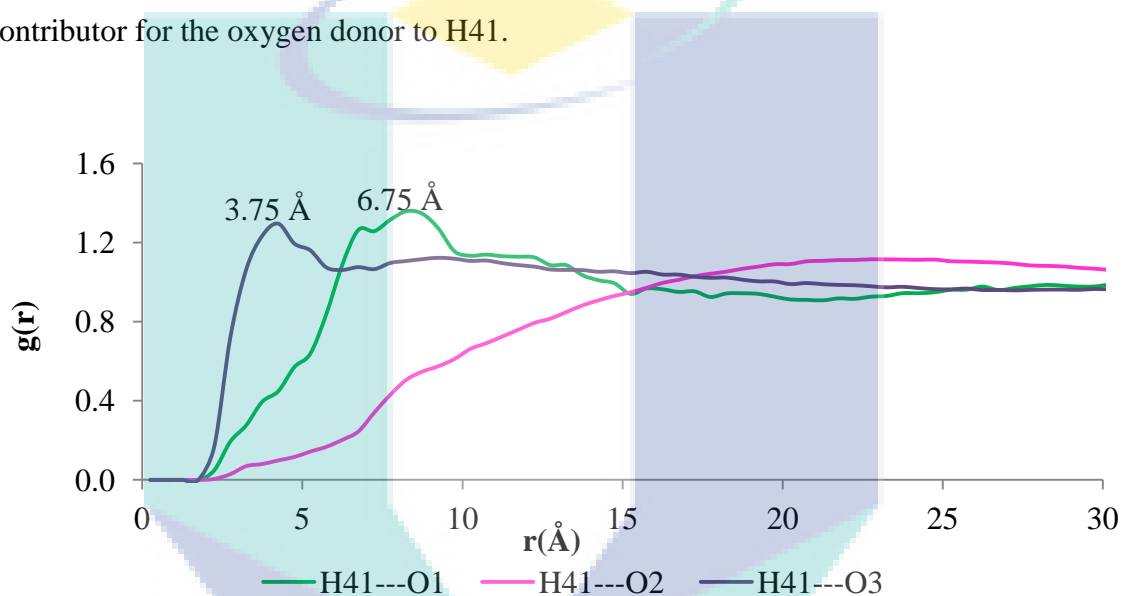


Figure 4.9. Radial distribution function of H41 with O1, O2 and O3 in tertiary patchoulol/oxygen/water system

Meanwhile, **Figure 4.10** shows the comparison of radial distribution function of H41---O3 in binary (patchoulol/oxygen) and tertiary system (patchoulol/oxygen/water) system. According to the graph, the presence of water in the tertiary system had decreased the value of $g(r)$ compared to the binary system. It suggests the probability of neighbouring oxygen can be found 1 time more in binary system compared in tertiary system. It suggest the presence of more water molecules in the solution will decreased the number of colliding process between H41 and O3 in the tertiary system. On the other hand, the first oxygen can be found nearly at 3.75\AA in the tertiary system compared to 5.25\AA in the binary system. This suggests that the interaction of H41 with

the oxygen is stronger in tertiary system compared to the patchoulol/oxygen binary system.

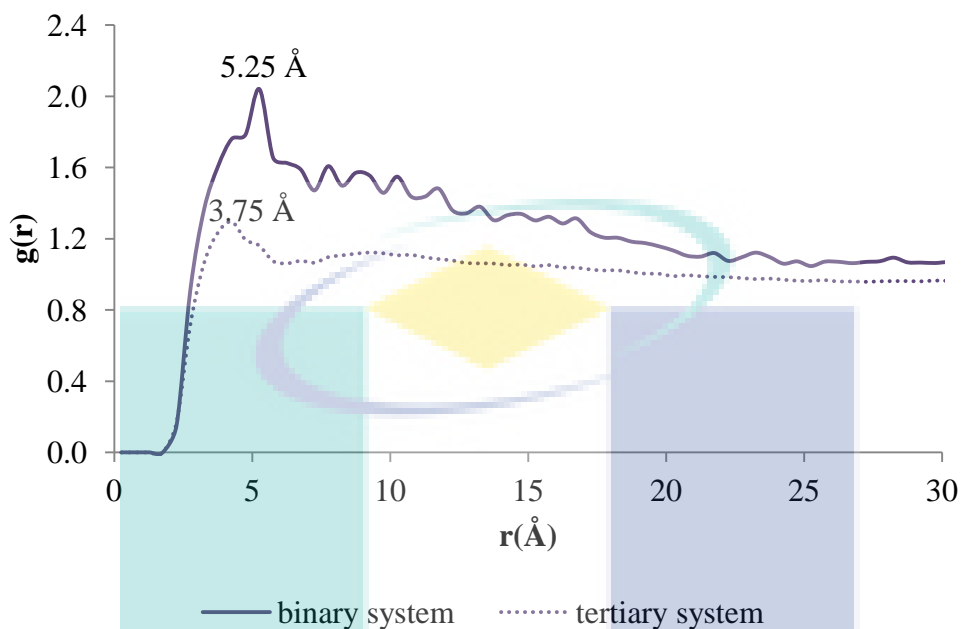


Figure 4.10. Radial distribution function of H41 with O3 in binary and tertiary system

4.5.3 Radial Distribution Functions of O3---O3 in Three Systems

The simulation between O3---O3 and H2---O2 were conducted in every simulation. The interaction between O3---O3 is important because it will reflect the level of interaction with patchoulol as oxygen plays a role in the formation of van der Waals bonding. Based on the simulation of binary and tertiary system, the O3 was shown to form a strong bond with H41 as compared to H2. These may indicate that there is the change in the interaction of oxygen in the binary and tertiary system. The changes will be determined by comparing the interaction of O3---O3 in binary and tertiary system with the interaction of O3---O3 in pure simulation system. According to Campbell et al., (2006) the structure of water molecules benefit them to attract other atom. Due to these, the comparison of radial distribution function between pure, binary and tertiary system simulation were carried out to investigate the changes that can be occurred in the interaction.

Figure 4.11 shows the radial distribution function of the O3---O3 in three systems. It was found that, the value of the radial distribution function of binary and tertiary were at 4.25Å, the same position with pure simulation system. It shows that there is no change in the interaction between the molecules of oxygen in any system. According to Thapa and Adhikari (2013), the height of the peaks will decrease in small amount respectively with the rise of in the simulation temperature. But, by referring to **Figure 4.11**, the unchanged in the size of the peaks in the pure and binary system might be due to the unchanged in the temperature and the pressure on the simulation system. On the other hand, **Figure 4.11** also indicates the increasing pattern in the value of $g(r)$. It shows the $g(r)$ value increase 1 time in tertiary system compared to binary and pure system. The increasing of the $g(r)$ value suggests the possibility to find the nearest molecules is 1 times more than in the binary and pure system.

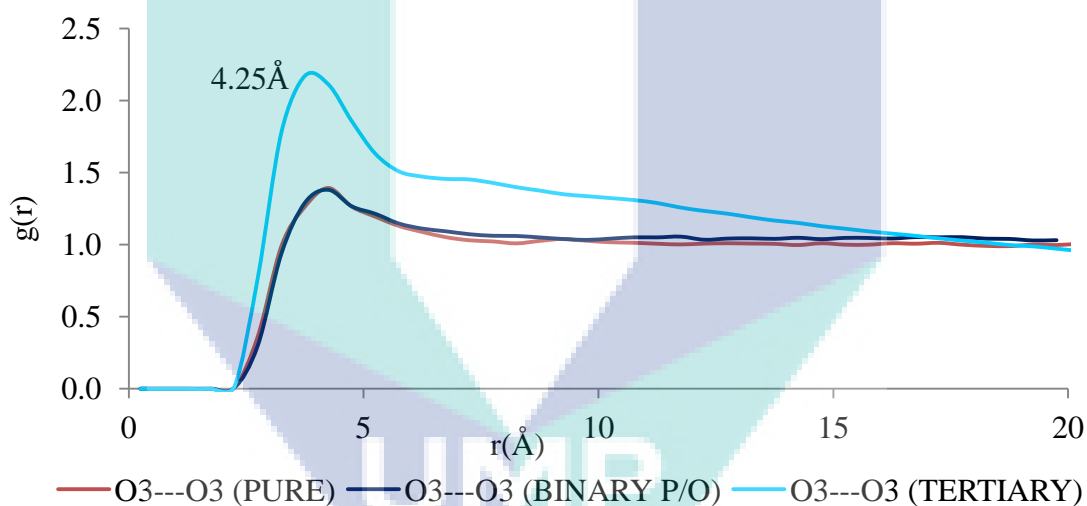


Figure 4.11. Comparison of the radial distribution function of O3---O3 in three systems

4.6 Experimental Results

This section will report on the biotransformation process results based on GCMS and FTIR analyses. FTIR analysis in the first section of the experimental work investigated the functional group which appears in the compound. Section 4.2 displays the comparison of two results from the FTIR analysis. The first is the experimental analysis of the patchoulol and the product of biotransformation. Secondly is the FTIR

result of the 10-hydroxypatchoulol simulated data from the Gaussian Software. Next is the result of GCMS, which was described in much more detail. This section will reveal the chemical compounds detected via GCMS, where the 10-Hydroxypatchoulol probably exists. The GCMS results will illustrate the identity of the compound, percentages and the other parameters. Subsequently, the search continues by comparing the results with the data in the NIST data bank.

4.7 FTIR Analysis

In this study, the surface analysis on the raw material of patchoulol and the sample of the biotransformation were tested with FTIR. The analysis can be considered as a preliminary result and can also provide an initial overview on the structural and functional information of the compound found in the product sample.

4.7.1 Experimental FTIR Analysis

Figure 4.13 shows the two FTIR graphs, where a) the red line represents the patchoulol and b) the blue line represents the product of the biotransformation process. Generally, both graphs recorded four major peaks. Referring to the graphs, it indicated the occurrence of the chemical reaction on the raw material which is patchoulol. It can be seen in **Figure 4.13a**), shows the presence of sharp peak at 3500cm^{-1} indicating the –OH group with the H-bonded in the molecule. The H-bonded group represented the –OH that attached as hydrogen bonding with any molecule. Meanwhile, **Figure 4.13b**) shows the presence of the watery element appear around $3100\text{-}3600\text{cm}^{-1}$ represented by a broad peak. Berthomieu and Hienerwadel, (2009) stated that, this area is responsive to hydrogen- bonding properties of water molecules.

Both graphs illustrated a slightly broad peak which appeared around $2900\text{ - }3000\text{cm}^{-1}$ that represent the C-H stretch, that are belong to all organic compound. According to Coates (2000), the presence of the aromatic rings in a structure is determined from C-H ring that occurs around 3000cm^{-1} and demonstrated as multiplicity of weak-to-moderate bands and can be seen in both graphs. Then, there is

slightly a broad peak appeared around $1400 - 1600\text{cm}^{-1}$ in both graphs. These peaks demonstrated the C-C stretch in a ring form, appearing from the molecule. Additionally, there is also an increase on peak depth in **Figure 4.13b**) in range 1150 cm^{-1} compared to **Figure 4.13a**), which may be caused by the existence of C-O stretch. However, there was an increment in the size of the peak area in the product compared to raw. **Figure 4.12** suggesting an increasing C-O stretch in the product sample after hydroxylation process indicated that the biotransformation process of patchoulol has occurred.

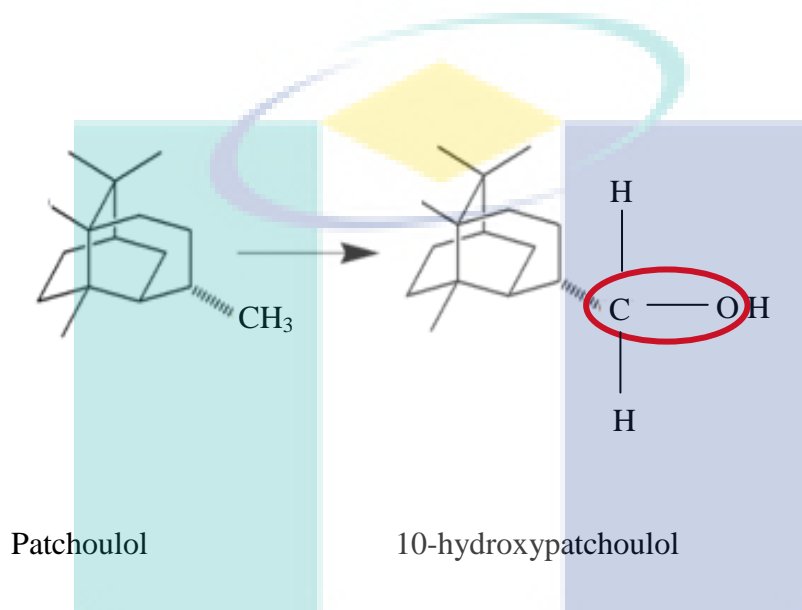


Figure 4.12. The C-O stretch in sample of hydroxylation process

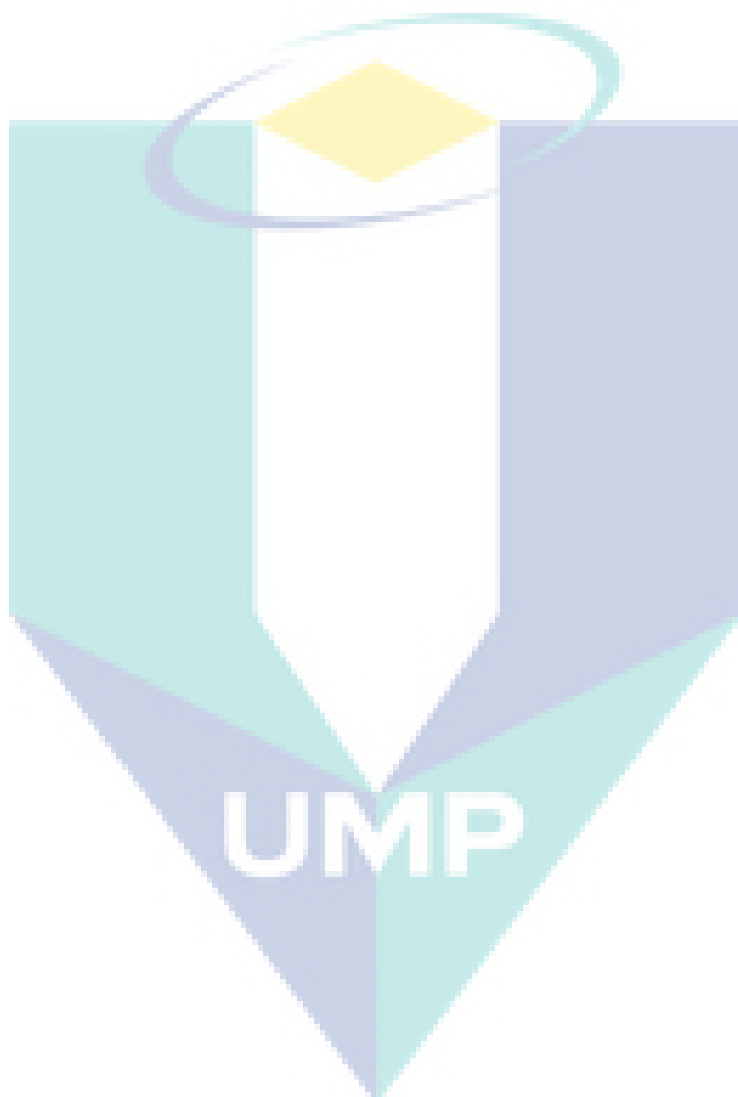
4.7.2 FTIR Simulated By Gaussian Analysis

The analysis of the stimulated IR spectra was measured from $700\text{ cm}^{-1} - 4000\text{cm}^{-1}$ range, following the experimental FTIR data. Based on the IR simulated graph, it demonstrate two main peaks at, (i) $2900\text{cm}^{-1} - 3200\text{cm}^{-1}$, and (ii) $900\text{cm}^{-1} - 1500\text{cm}^{-1}$. **Figure 4.14** shows the optimized structure of 10-hydroxypatchoulol which contain ($n=41$) atoms which represented by the blue lines. The fundamental vibration of the 10-hydroxypatchoulol molecules in the simulated spectra was estimated by the following equation

$$\text{Vibration} = (3n-6) \tag{4.1}$$

By comparing with the experimental data (**Figure 4.13b**), it shows that there is a match peak at 3200cm^{-1} that shows the H-bonded in the hydroxyl group. A peak at

range 1150cm^{-1} also appeared on the simulated data showed the C-O stretch was present as the primary alcohol. It can be concluded that the 10-hydroxypatchoulol might be present in the sample because of two peaks C-O and O-H appearance in **Figure 4.13b**.



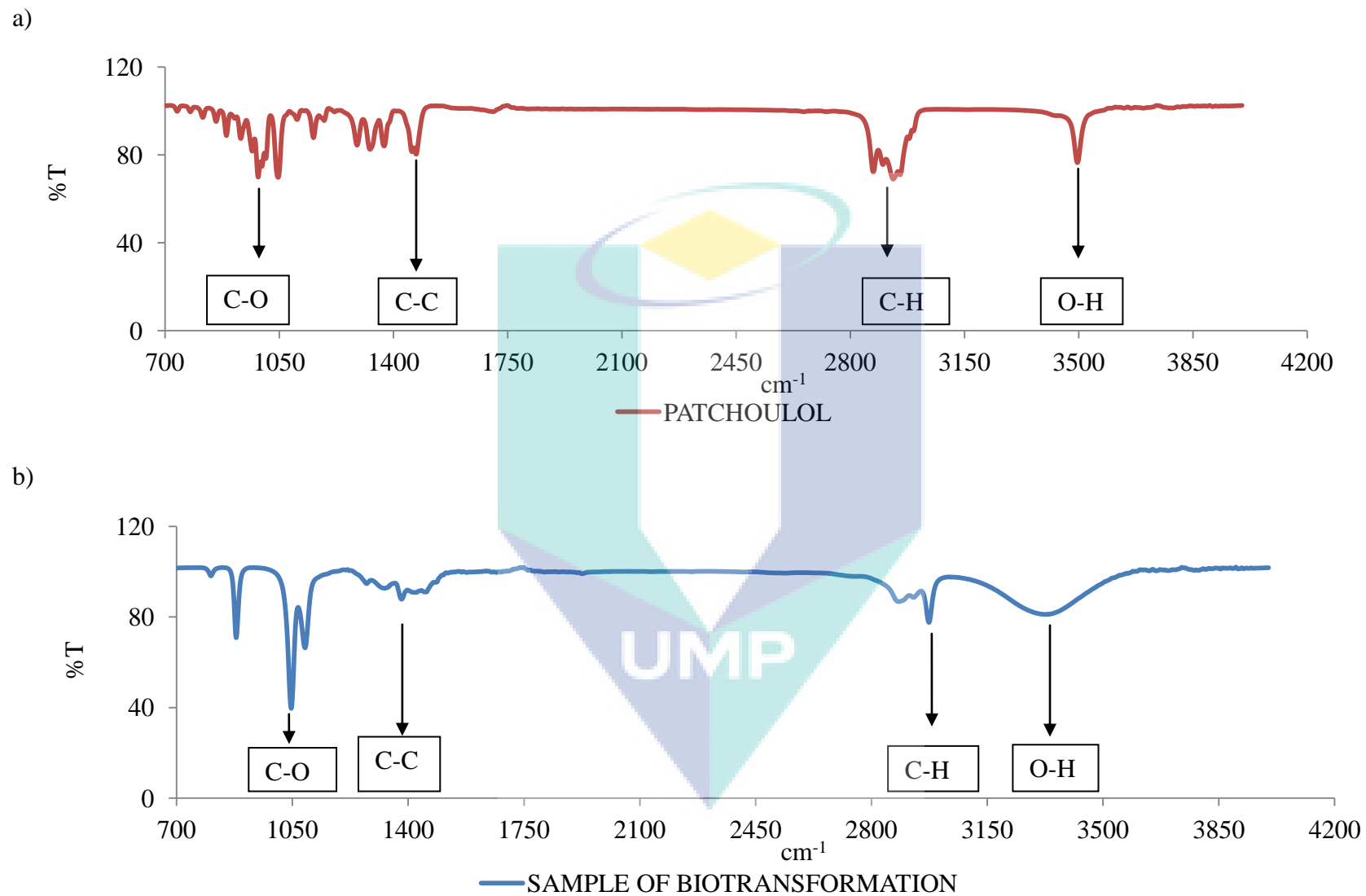


Figure 4.13. FTIR analysis for both samples

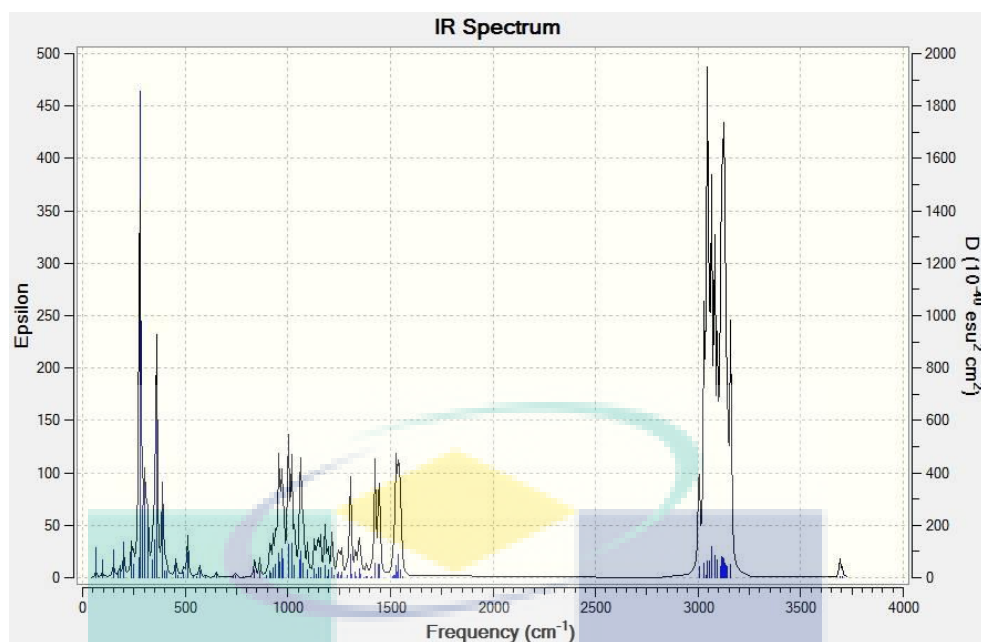


Figure 4.14. The stimulated IR spectrum

4.8 GCMS Analysis

In this study, five samples were tested by analyzing them via GCMS (**Figure 4.16** (a) – (e)). 10-hydroxypatchoulol with the molecule formula $C_{15}H_{26}O_2$ was not detected in any of the sample. Further research must be conducted in order to obtain the 10-hydroxypatchoulol. At this time, the proposed study cannot be continued because of the constraints in terms of raw material prices, which are quite expensive. Instead, this project focused on the C15 compound and information in the various C15 compound detected is tabulated in Table 4.1. Generally, seven C15 compounds were identified in all samples, namely (a) 1(2H)-Naphthalenone, octahydro-4,8a-dimethyl-6-(1-methylethenyl)-, (4.alpha.,4a.beta., 6.alpha., 8a.beta.)-, (b) 6-Isopropenyl-4,8a-dimethyl-1,2,3,5,6,7,8,8a-octahydro naphthalene-2, 3-diol, (c) 1,4-Methanoazulen-7-ol, decahydro-4,8,8,9-tetramethyl-, (+)-, (d) 1-Formyl-2,2,6-trimethyl-3-(3-methyl-but-2-enyl)-6-cyclohexene, (e) Alloaromadendrene oxide-(1), (f) Naphthalene, 2-(1,1-dimethylethyl)decahydro-4a-methyl-, and (g) 2-Benzyl-3-isopropyl-cyclopentanone as depicted in **Figure 4.17**. Sample one, three and five were constituted mainly by compound (a). Meanwhile, a part of compound (a), sample two was characterised with compound (b), (c) and (d). Finally, sample four was constituted by compound (a), (c) and (g). According to Table 4.1, it reveals the compound (a) is exists in all five samples.

However, it does not present as the highest percentage among the compound in the sample. But the existent of this compound in all sample suggest that the transformation process had occur on the patchoulol to this compound. Due to literature, this compound is a type of sesquiterpenes that has been found in the flowers, stems, and roots of *Tripleurospermum callosum* (Yasar et al., 2005). This plant is a species of the genus *Tripleurospermum* (family Compositae). Detailed information on physical properties of this compound is presented in Table 4.2.

The above result demonstrates that *Aspergillus niger* is capable of transforming patchoulol to various compound. However, in this study, the 1(2H)-naphthalenone, octahydro-4,8 a-dimethyl-6-(1-methylethenyl)-, (4.alpha.,4a.beta.,6.alpha.,8a.beta .)- was selected due to its present in all samples and at relatively high percentage. Figure 4.15 shows the study of the pathway involved in the process. It despite the formation of two double bonds. The first double bond was attached to CH₂ and the other double bond was attached to single atom oxygen. Furthermore, there was also the breakage process of the two rings in the patchoulol molecule to form two linear rings. Overall, two hydrogen atoms were separated from the patchoulol molecule.

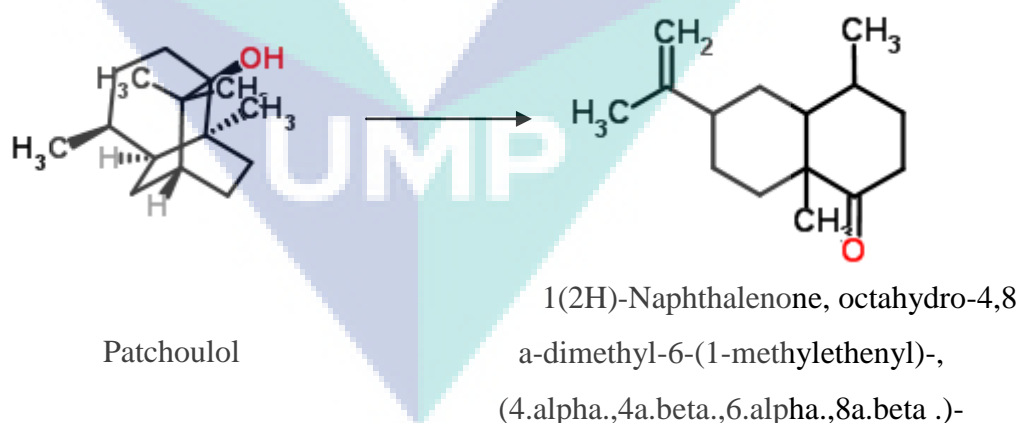


Figure 4.15. The study of the pathway involved in the process

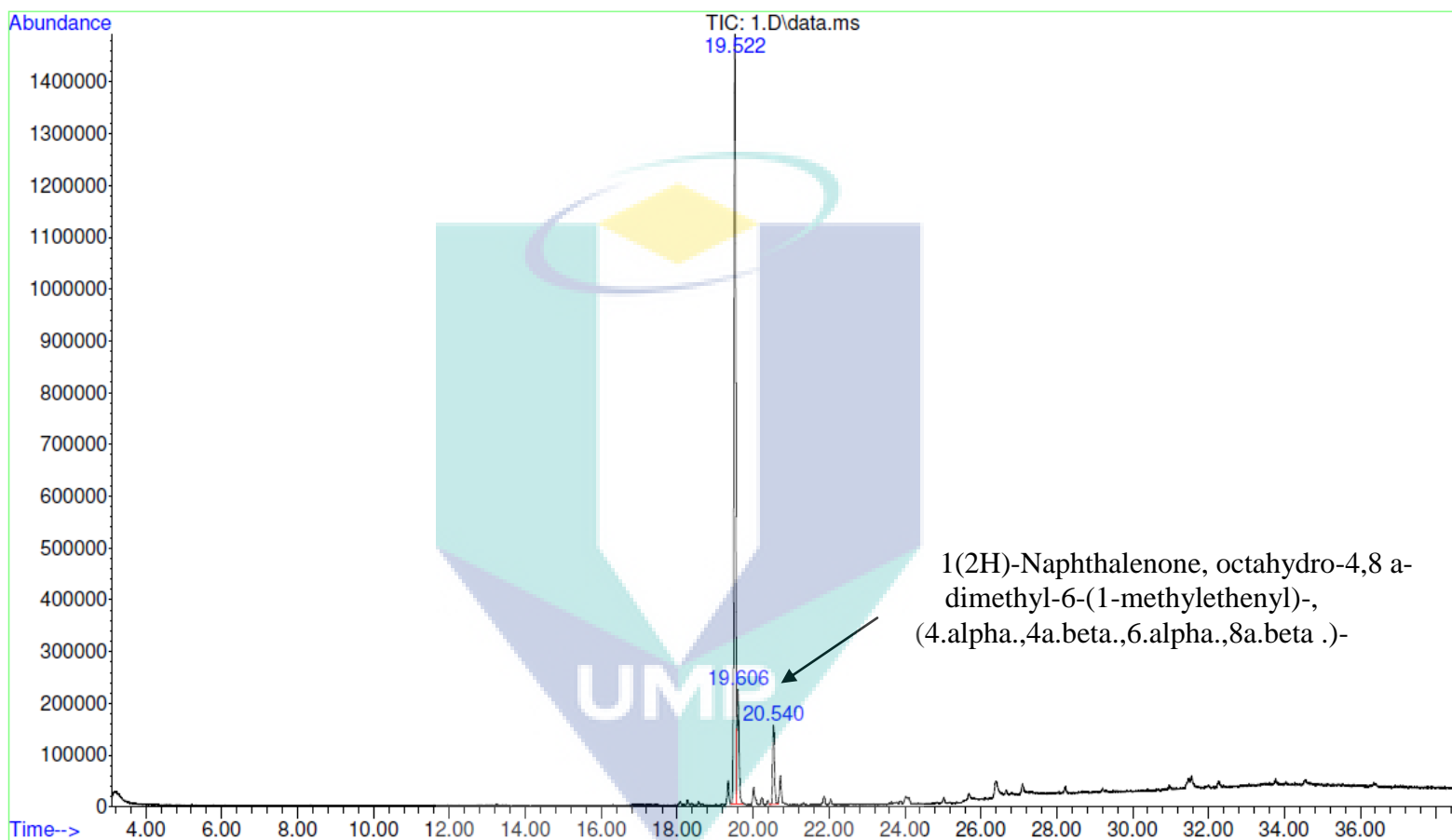


Figure 4.16: a) GCMS analysis of Sample 1

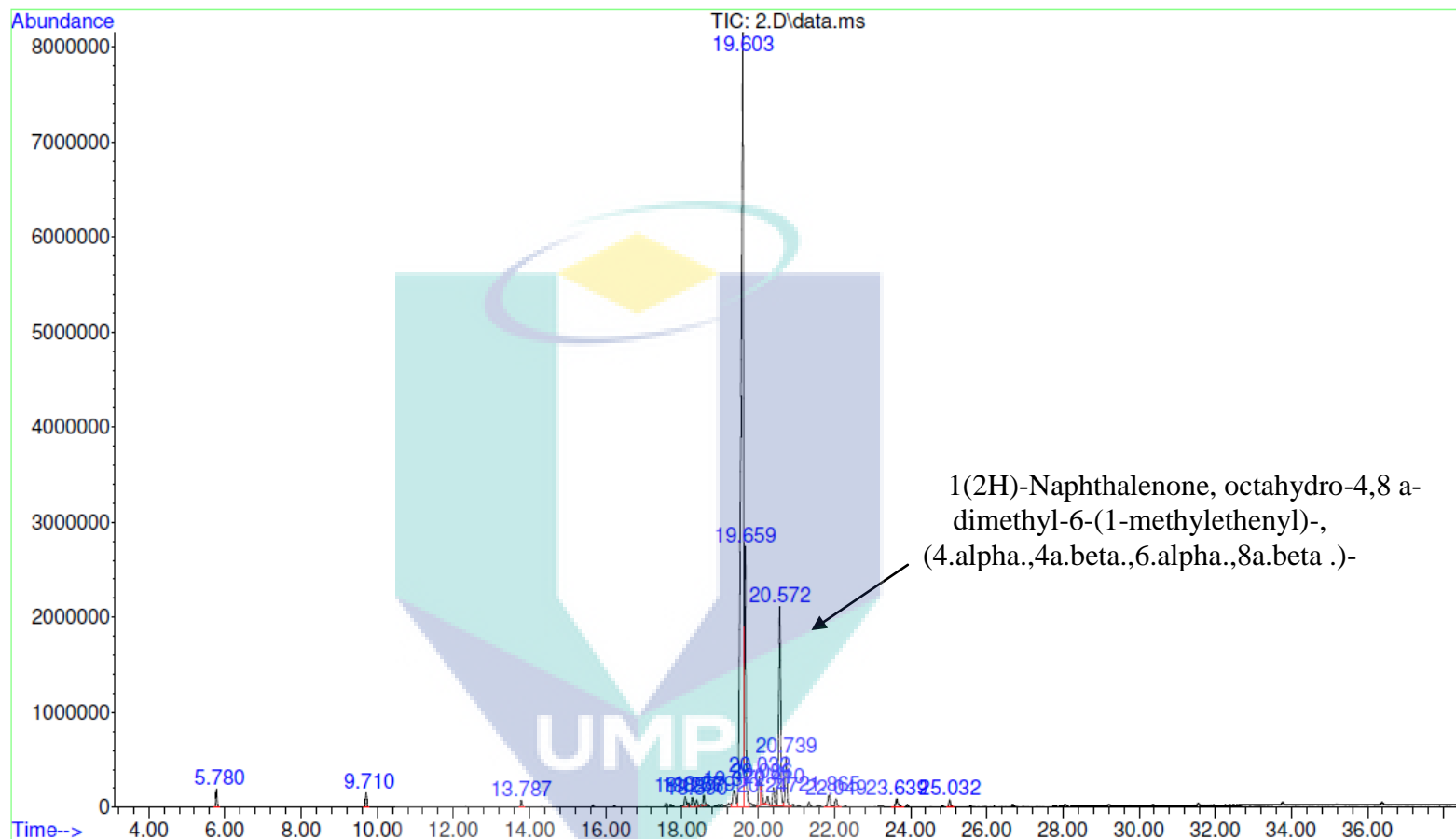


Figure 4.16. b) GCMS analysis of Sample 2

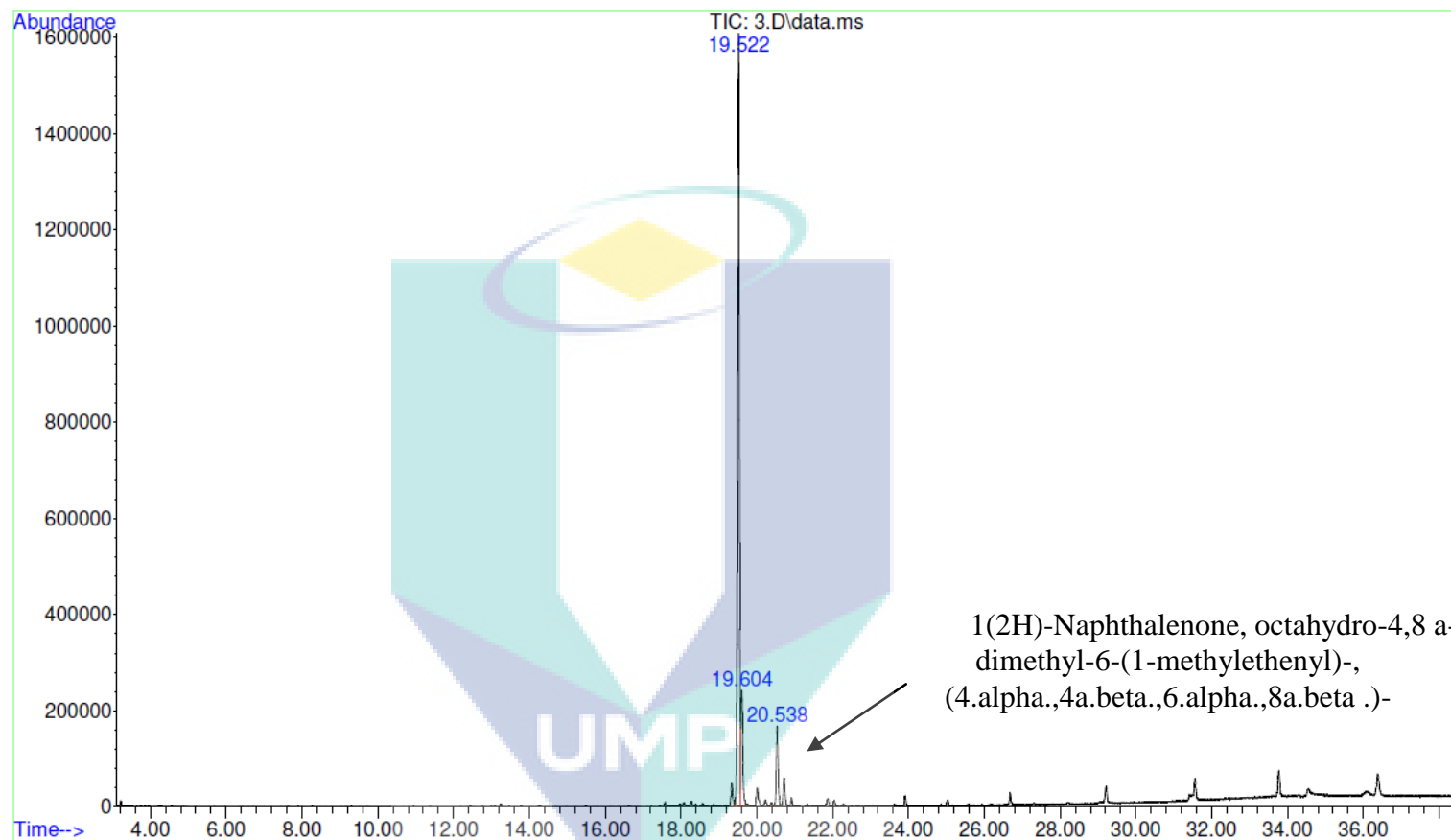


Figure 4.16. c) GCMS analysis of Sample 3

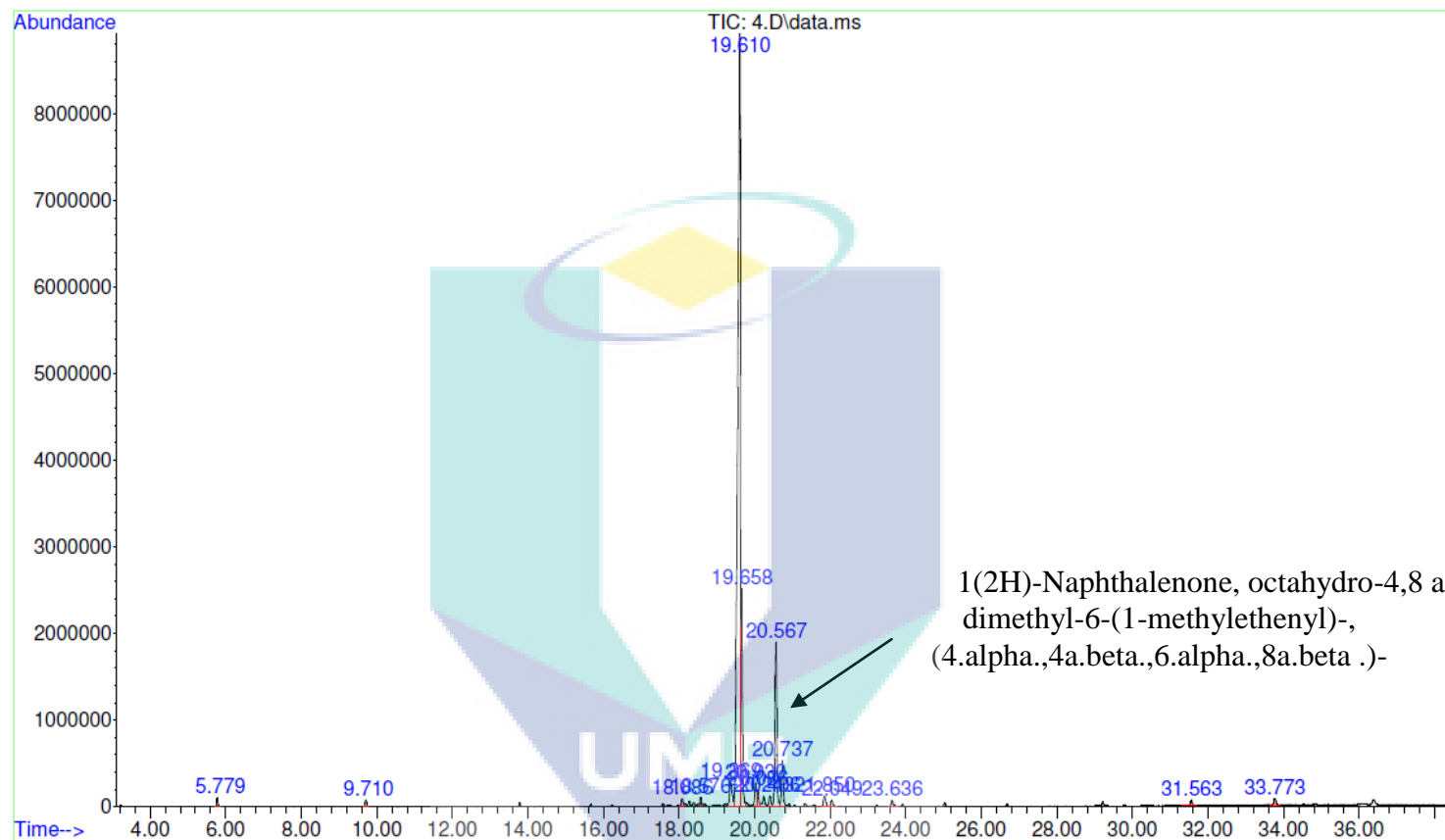


Figure 4.16. d) GCMS analysis of Sample 4

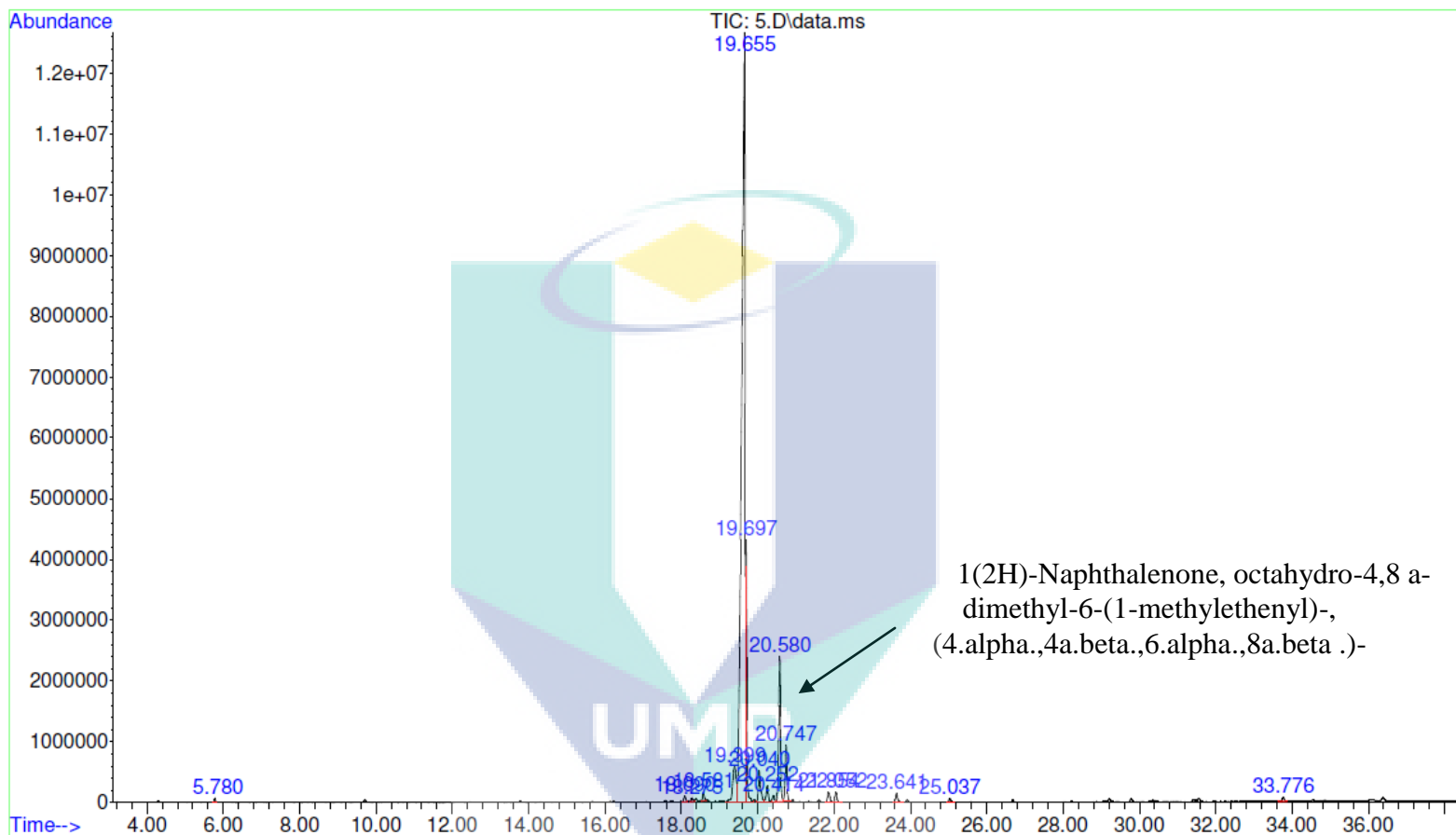


Figure 4.16. e) GCMS analysis of Sample 5

Table 4.1

List of C15 compounds detected in all five samples

Sample	C15	Chemical Formula	%	Retention time
1	<ul style="list-style-type: none"> 1(2H)-Naphthalenone, octahydro-4,8 a-dimethyl-6-(1-methylethenyl)-, (4.alpha.,4a.beta.,6.alpha.,8a.beta .)- 	C ₁₅ H ₂₄ O	9%	20.538
2	<ul style="list-style-type: none"> 6-Isopropenyl-4,8a-dimethyl-1,2,3,5,6,7,8,8a-octahydronaphthalene-2, 3-diol 1,4-Methanoazulen-7-ol, decahydro-4,8,8,9-tetramethyl-, (+)- 1-Formyl-2,2,6-trimethyl-3-(3-methyl-but-2-enyl)-6-cyclohexene 1(2H)-Naphthalenone, octahydro-4,8 a-dimethyl-6-(1-methylethenyl)-, (4.alpha.,4a.beta.,6.alpha.,8a.beta .)- Alloaromadendrene oxide-(1) Naphthalene, 2-(1,1-dimethylethyl)decahydro-4a-methyl- 	C ₁₅ H ₂₄ O ₂ C ₁₅ H ₂₆ O C ₁₅ H ₂₄ O C ₁₅ H ₂₄ O C ₁₅ H ₂₄ O C ₁₅ H ₂₈	0.34% 0.54% 1.54% 11.53% 0.46% 0.63%	18.387 18.579 20.031 20.573 22.048 23.639
3	<ul style="list-style-type: none"> 1(2H)-Naphthalenone, octahydro-4,8 a-dimethyl-6-(1-methylethenyl)-, (4.alpha.,4a.beta.,6.alpha.,8a.beta .)- 	C ₁₅ H ₂₄ O	8.26%	20.538
4	<ul style="list-style-type: none"> 1(2H)-Naphthalenone, octahydro-4,8 a-dimethyl-6-(1-methylethenyl)-, (4.alpha.,4a.beta.,6.alpha.,8a.beta .)- 2-Benzyl-3-isopropyl-cyclopentanon 1,4-Methanoazulen-7-ol, decahydro-4,8,8,9-tetramethyl-, (+)- 	C ₁₅ H ₂₄ O C ₁₅ H ₂₀ O C ₁₅ H ₂₆ O	10.05% 0.79% 0.42%	20.567 21.849 23.633
5	<ul style="list-style-type: none"> 1(2H)-Naphthalenone, octahydro-4,8 a-dimethyl-6-(1-methylethenyl)-, (4.alpha.,4a.beta.,6.alpha.,8a.beta .)- 	C ₁₅ H ₂₄ O	7.51%	20.579

Table 4.2

Chemical and physical properties of Compound 1

Type	Properties
Molecular formula	C ₁₅ H ₂₄ O
Molecular weight	220.350494
Density	0.937 g/cm ³
Boiling point	299.748 °C at 760 mmHg
Synonyms	6-Isopropenyl-4,8a-dimethyloctahydro-1(2H)-naphthalenone
IUPAC name	4,8a-dimethyl-6-prop-1-en-2-yl-2,3,4,4a,5,6,7,8-octahydronaphthalen-1-one

Source <http://pubchem.ncbi.nlm.nih.gov/summary/summary.cgi?cid=586719>

CSID:509991, <http://www.chemspider.com/Chemical-Structure.509991.html>

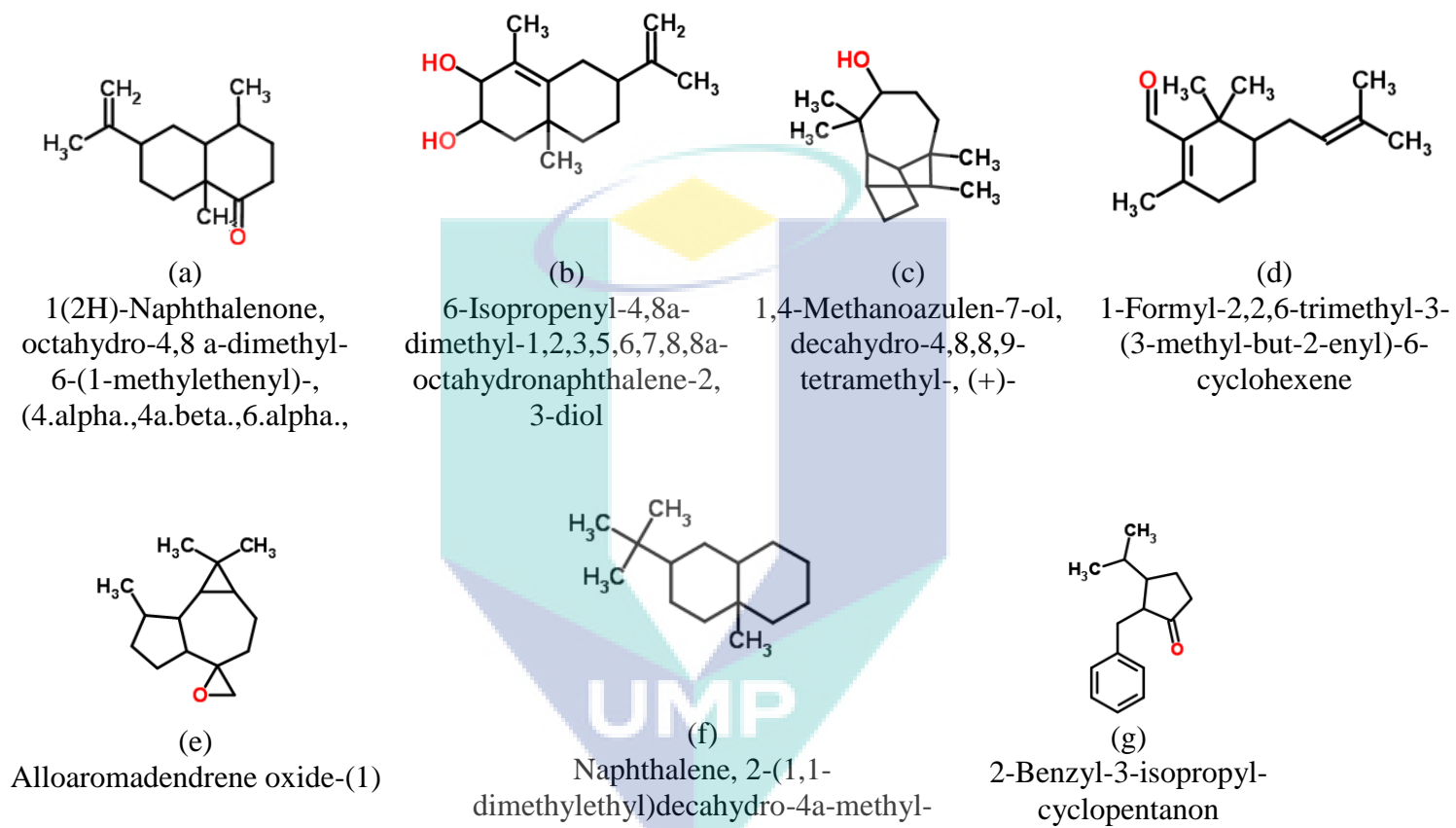


Figure 4.17. C15 compound detected in GCMS

4.9 Conclusion

This study involves both experiment and data simulation. From the simulation of data and literature review, it can be concluded that due to van der Waals interaction, patchoulol is tend to attract oxygen gas more than water thus produce the 10-hydroxypatchoulol. But, the presences of water have significantly affected the interaction between H41 and oxygen, where the interaction become stronger in the tertiary system. It shows the water system still be an important variable in the biotransformation process.

Unfortunately, experimental results did not yield the expected result. On the other hand, 1(2H)-Naphthalenone, octahydro-4,8 a-dimethyl-6-(1-methylethenyl)-, (4.alpha.,4a.beta.,6.alpha.,8a.beta .)- was produced in which two hydrogen have disappeared from the compound of patchoulol. Even though the expected result is failed to be reach, but the process still transform the patchoulol to a new compound that also benefit in the perfumery industry as the compound is also can be found in the *Tripleurospermum callosum* part of the plant (Yasar et al, 2005). Besides, the process also transforms the patchoulol to other six C15 compounds that the details on the single compound can be study in the further research.

CHAPTER 5

CONCLUSION AND RECOMMENDATION

5.1 Introduction

This chapter will summarise and discuss the topics from all chapters and conclude the lists of results attained and mentioned in chapter four. Recommendation of suggestions for future work from the study findings will also be included.

5.2 Overall Conclusion

This research has are two main objectives that cover the simulation and the experiment work. The overall objective is to study the molecular dynamic simulation of the biotransformation process of patchoulol to 10-hydroxy patchoulol. The molecular dynamic simulation worked involved three systems which investigated van der Waals interaction and hydrogen bonding. In relation to radial distribution analysis, it shows that the results from the pure system are in agreement in literature and theory. Because of that, the result from the pure system can be a reference to the following simulation in binary and tertiary systems. From the molecular dynamic simulation, it can be concluded that the patchoulol is more interested to the oxygen from the dissolved oxygen gas in producing the Van der Waals bond which initiates the formation of

hydroxyl group in patchoulol molecule. From this result, it can be suggested the oxygen gas can give the higher impact to the 10-hydroxypatchoulol production. The future researcher have to consider more on the oxygen supply and function of the fungi, the hydroxylase enzyme will act to catalyst the hydroxyl group formation in the patchoulol compound that will initiate the 10-hydroxypatchoulol production. Therefore, it can be concluded that the use of molecular dynamic simulation is able to increase the understanding and knowledge about the structure, interaction and intermolecular forces between molecules in a solution.

The sample from the biotransformation process has been analysed by FTIR and GCMS analysis. In FTIR, the changes in peak size and pattern have indicated that the chemical reaction has occurred and transformed the raw material. Basically, GCMS analysis did not indicate the presence of 10-hydroxypatchoulol. But with the emergence of various types of compounds in the data, it shows that *Aspergillus niger* is able to transform patchoulol to a variety of types of compound that may be useful in the perfume industry, medicine and so on. In this work, apart from converting the substrate to the 10-hydroxypatchoulol, this hydroxylation process have transformed the substrates to the new compound, 1(2H)-Naphthalenone, octahydro-4,8 a-dimethyl-6-(1-methylethenyl)-, (4.alpha.,4a.beta.,6.alpha.,8a.beta .)- compound with the molecular formula C₁₅H₂₄O.

5.3 Recommendation For Future Works.

There are several recommendations that should be considered as the extensive study from this work.

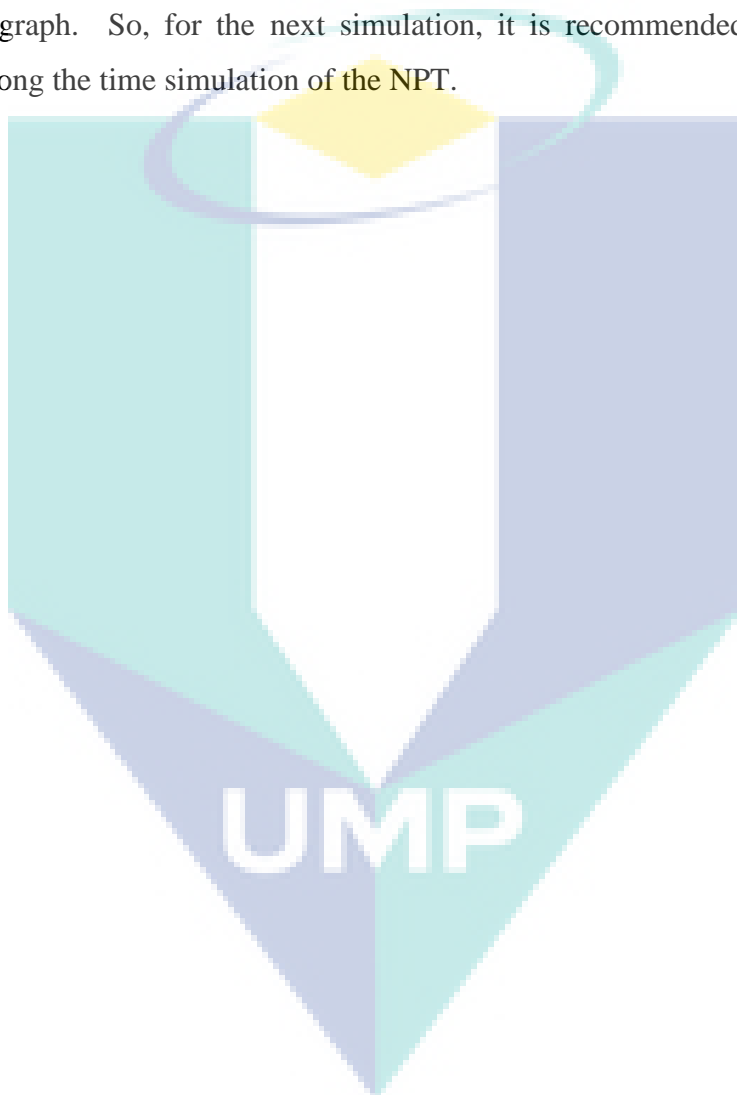
- (i) Simulation of enzyme that acts in the biotransformation process.

Biotransformation system involves the application of fungi that works with their enzyme and acts as the catalyst to the reaction. Theoretically, the enzyme will provide the active site to the substrates in order to generate a new product. For this research, however, the substrates involved were patchoulol and oxygen. Hence, the simulation of the enzyme can be a good addition in the simulation. This is because exact interaction and the structure changes can be further

investigated in the simulation. In this study, the enzyme that takes part in the process of hydroxylation is the hydroxylase.

- (ii) Increase more time simulation in NPT.

In this simulation, the simulations just took about 1000 ps in every NPT ensemble. The outcome was that the result was less equilibrated as showed in the graph. So, for the next simulation, it is recommended for researcher to prolong the time simulation of the NPT.



REFERENCES

- Abdulnour, Y., Toukmaji, and John, A. Board Jr.1996. Ewald summation techniques in perspective: a survey. *Computer Physics Communications*. 95 :73-92
- Adam, F., Abu, B.S.H., Mohd. Y. M. and Tajuddin, S.N.(2014) Molecular Dynamic Simulation of the Patchouli Oil Extraction Process. *Journal of Chemical & Engineering Data*, 59 (2): 183-188
- Ahmed Al-harrasi and Salim Al-Saidi., 2008. Phytochemical analysis of the essential oil from botanically certified Oleogum resin of *Boswellia sacra* (Omani Luban) *Molecules*. 13 :2181-2189
- Aleu, J., Hanson, J.R., Galan, R.H. and Collado, I.G. 1999. Biotransformation of the fungistic sesquiterpenoid patchoulol by *Botrytis cinera*. *J.Nat. Prod.* 62: 437-440
- Allen, M. P., and Tildesley, D. J. 1989, *Computer Simulation of Liquids*. Oxford: Clarendon Press.
- Allen, M.P. 2004. Introduction to Molecular Dynamics Simulation. *John von Neumann for Computing*. 23: 1-28
- Arunkumar S.,and Muthuselvam M.,2009.Analysis of phytochemical constituents and antimicrobial activities of Aloe vera L. against clinical pathogens. *World J. Agric. Sci.*5: 572-5
- Abdul, M.S.S., Abu, B.M.R., Adam, F. and Jama, P. (2013). Structures and hydrogen bonding recognition of mefenamic acid form i crystals in mefenamic acid/ ethanol solution. *International Journal Of Chemical Engineering And Application*.4(3): 124-128
- Buchcauer, G., and Baser, H. C. K. 2010. Handbook of essential oils , science, technology, and application. Taylor & Francis Group
- Barrat, J., and Hansen, J., 2003. *Basic concept for simple and complex liquid*. Press Syndicate Of The University Of Cambridge.
- Berthomieu, C., and Hienerwadel, R. 2009. Fourier transform infrared (FTIR) spectroscopy. *Photosynth Res.* 101:157–170
- Bluemke, W., and Schrader, J. 2001. Integrated bioprocess for enhanced production of natural flavors and fragrances by *Ceratocystis moniliformis*. *Biomol Eng.* 17(4-5):137-42.
- Buré, C. M., and Sellier, N. M. 2004. Analysis of the Essential Oil of Indonesian Patchouli (*Pogostemon cablin* Benth.) Using GC/MS (E1/C1). *Journal of Essential Oil Research*. 16 (1): 17–19.

- Baeurle and Stephan, A. 2009. Multiscale modeling of polymer materials using field-theoretic methodologies: A survey about recent developments. *Journal of Mathematical Chemistry*. 46 (2): 363–426.
- Brunk. E., and Ashari, N. 2012. Exercise for “molecular dynamic (MD) and Monte carlo (MC)”. (MD_MC_2012_Ex4_pdf)
- Chang, R. And Overby, J. 2011. *General Chemistry: The Essential Concepts*. McGraw-Hill Education; 6th edition
- Côté, A.S., Smith, B. and Philip, J.D. and Lindan. 2001. A Molecular Dynamics tutorial. *Daresbury Laboratory*.
<http://www.compsoc.man.ac.uk/~lucky/Democritus/Basic/Democritus.html>
- Chandler. 1987. *Introduction to modern stastical mechanics* .Oxford University press, Inc.
- Colthup, N.B., Daly, L.H., and Wiberly, S.E. 1975. *Introduction to infrared and Raman spectroscopy*. New York: Academic Press
- CSID:509991, <http://www.chemspider.com/Chemical-Structure.509991.html>
- Coates, J. 2000. *Interpretation of Infrared Spectra, A Practical Approach*. John Wiley & Sons Ltd, Chichester
- Colthup NB, Daly LH, Wiberly SE (1975) *Introduction to infrared and Raman spectroscopy*. Academic Press, New York
- DeKock, R.L., and Gray, H.B.(1989). *Chemical structure and bonding*. University Science Books.
- Dill, Ken A.; Bromberg, Sarina; Stigter, Dirk. 2003. *Molecular Driving Forces*. New York: Garland Science
- Allen, M.P. 2004. *Introduction to Molecular Dynamics Simulation*. *John von Neumann for Computing*. 23: 1-28
- Dung, N. X., Leclercq, P. A., Thai, T. H. and Moi, L. D. 1989. Chemical composition of patchouli oil of Vietnam. *Proceedings of the 11th International Congress of essential oils, fragrances and flavours*. *Chemistry analysis and structure*. 4: 99-102.
- Dalli, A. K., and Chakraborty, U. 2007. Characterization on antimicrobial compounds from a common fern, *Pteris biaurita*. *Indian Journal of Experimental Biology*. 45:285-290
- Dorland. *Dorland's Medical Dictionary for Health Consumers*. © 2007 by Saunders, an imprint of Elsevier, Inc.
- Douglas, F. 1999. GC/MS Analysis.
<http://www.scientific.org/tutorials/articles/gcms.html>

- Foong, L. N. 2008. *A Study on Microwave-Assisted Extraction of Patchouli Essential Oil: Effect of Hexane as Solvent*. Degree Thesis. Universiti Malaysia Pahang, Malaysia
- Gabler, R. 1978. *Electrical Interactions in Molecular Biophysics*. New York: Academic Press, Inc.
- Grimme, S., Diedrich, C., and Korth, M. 2006. The Importance of Inter- and Intramolecular van der Waals Interactions in Organic Reactions: the Dimerization of Anthracene Revisited. *Angew. Chem. Int. Ed.* 45(4): 625-629.
- Gabbar, H. A., and Suzuki, K. 2004. *The Design of a Practical Enterprise Safety Management System*. Kluwer Academic Publisher.
- Godfrey, T., and West, S. 1996. *Industrial Enzymology*. New York: Stockton Press
- Gibbs and Willard, J. 1902. *Elementary Principles in Statistical Mechanics*. New York: Charles Scribner's Sons.
- Guevara-Carrión, G., Hasse, H., and Vrabec, J., 2012. Topics in Current Chemistry. In: *Multiscale Molecular Methods in Applied Chemistry*. Springer, Heidelberg.
- Gopishetty, S. R., Louie, M.T., and Subramaniam, M.V. Microbial transformations of natural products. *Phytochemistry And Pharmacognosy*. Encyclopedia of Life Support Systems (EOLSS).
- Griffiths, P.; de Hasseth, J.A. (18 May 2007). *Fourier Transform Infrared Spectrometry* (2nd ed.). Wiley-Blackwell. ISBN 0-471-19404-2.
- Hajšlová, J., and Cajka, T. 2007. Gas chromatography–mass spectrometry (GC–MS)-Food Toxicants Analysis. Elsevier B.V
- Held, M. Schmid, A. Van Beilen, J.B. and Witholt, B. 2000. Biocatalysis. Biological systems for the production of chemicals. *Pure Appl. Chem.* 72(7): 1337–1343
- Hsu, C-P.S. 1997. *Handbook of instrumental technique for analytical chemistry : infrared spectroscopy*. Settle, F.A. Prentice Hall Ptr, Upper Saddle River, NJ 07458
- Hanson, J.R., Arantes, S.F., and Hitchcock, P.B. 1999. The microbiological hydroxylation of the sesquiterpenoid patchoulol by *Mucor plumbeus*. *Phytochemistry.* 52: 635-638.
- http://images.flatworldknowledge.com/averillfwk/averillfwk-fig11_005.jpg
- <http://pubchem.ncbi.nlm.nih.gov/summary/summary.cgi?cid=586719>
- Kostova, I., Ivanova, A., Dolcheror, I., Tsvetkova, I., and Kujungiev, A. 2002. GCMS analysis and antimicrobial activity of acidic fractions obtained from *Paeonia peregrina* and *Paeonia tenuifolia* Roots. *Z. Natuforsch;* 57C: 624 –628.

- Li, J. 2005. Basic molecular dynamics. Kluwer Academic Publishers.
- Lai, X., Su, Z., Chen, J., Li, Y., and He, J. 2014. Use of patchouli alcohol in preparation of drug against helicobacter pylori. *Patent Application Publication*. US 2014/0031434 A1.
- Jensen, B. 2011. Patchouli. (online)
<http://www.bojensen.net/EssentialOilsEng/EssentialOils23/EssentialOils23.htm>
- Li, J., Car, R., Tang, C., and Wingreen, N.S. Hydrophobic interaction and hydrogen-bond network for a methane pair in liquid water. *Proc. Natl. Acad. Sci. U.S.A.*, 104:2626-2630, 2007.
- Lynch, K.2013. Toxicology/DAU Testing by Mass Spectrometry. Slide. San Francisco. AACC Conference
- Lipkowitz, K. (1983), Molecular mechanics, by Ulrich Burkert and Norman L. Allinger, published by the American Chemical Society, 1982. *J. Comput. Chem.* 4: 605.
- Leach, A.R., *Molecular Modelling: Principles and Application*. Prentice Hall, 2 edition, 2001
- Machida, M., and Gomi, K. 2010. *Aspergillus: Molecular Biology and Genomics*: Caister Academic Press.
- Moura, A.F. and Freitas, L.C.G. 2003. Molecular Dynamics Simulation of the Sodium Octanoate Micelle in Aqueous Solution: Comparison of Force Field Parameters and Molecular Topology Effects on the Micellar Structure. *Brazilian Journal of Physics*, 34:64-72.
- MacKerell Jr., A. D., Bashford, D., Bellott, M., Dunbrack Jr, R. L., Evanseck, J. D., Field, M. J., Fischer, S., Gao, J., Guo, H., Ha, S., Joseph-McCarthy, D., Kuchnir, L., Kuczera, K., Lau, F. T. K., Mattos, C., Michnick, S., Ngo, T., Nguyen, D.T., Prodhom, B., Reiher, W.E., Roux, B., Schlenkrich, M., Smith, J. C., Stote, R., Straub, J., Watanabe, M., Wiórkiewicz-Kuczera, J., Yin, D., and Karplus, M. 1998. All-atom Empirical Potential for Molecular Modeling and Dynamics Studies of Proteins. *J. Phys. Chem.* 102: 3586-3616
- McHaney, R. 1991. Computer Simulation: A Practical Perspective. Academic Press.
- Matsumoto, M., Saito, S, Ohmine I. 2002. Molecular dynamics simulation of the ice nucleation and growth process leading to water freezing. *Nature*. 416(6879):409-13
- Mahanta, J.J., Chutia, M. and Sara, T.C. 2007. Study on Weed Flora and Their Influence on Patchoulol (*Pogostemon cablin* Benth.) Oil and Patchoulol. *Journal of Plant Science*. 2(1): 96-101.

- Näf, F., R. Decorzant, W. Giersch, and G. Ohloff. 1981. A Stereocontrolled Access to (\pm)-, (-)-, and (+)-Patchouli Alcohol. *Helvetica Chimica Acta*, 64(5): 1387–1397.
- Orphardt, C.E. 2003. Intermolecular force. *Virtual Chembook, Elmhurst College*.
<http://www.elmhurst.edu/~chm/vchembook/160Aintermolec.html>
- Pandey, A. 2004. Microbial Enzymes: Production and Applications: L-glutaminase. In: Concise Encyclopedia of Bioresource Technology. USA: Haworth Press, Binghamton.
- Podesta, M. 2002. Understanding the properties of matter. Taylor & Francis
- Rahman, A., Frank, and Stillinger, H. 1971. Molecular Dynamics Study of Liquid Water*. *The Journal Of Chemical Physics*. 55(7).
- Ramya, H. G., Palanimuthu, V., Rachna, S. 2013. An introduction to patchouli (*Pogostemon cablin* Benth.) – A medicinal and aromatic plant: It's importance to mankind.
Agric Eng Int: CIGR Journal. 15(2): 24. <http://www.cigrjournal.org>
- Sun, H. 1998. COMPASS: An ab Initio Force-Field Optimized for Condensed-Phase Applications Overview with Details on Alkane and Benzene Compounds. *J. Phys. Chem. B*. 102: 7338-7364
- Schuster, E., Dunn-Coleman, N., Frisvad, J., and van Dijck, P. 2002. On the safety of *Aspergillus niger* – a review. *Applied Microbiology and Biotechnology*. 59: 426-435.
- Simonich, S. 2015. GCMS- How does it work?
http://unsolvedmysteries.oregonstate.edu/MS_03
- Shipman, J., Wilson, J., Todd, A. (1993) An Introduction to Physical Science, 7th Ed., D. C. Heath.
- Shaikh, A.R., Tsuboi, H., Koyama, M., Endou, A., Takaba, H., Kubo, M., Del Carpio, c.a., Broclawik, E. and Miyamoto, A. (2001). Molecular Dynamics Simulation for Hydroxylation of Camphor by Cytochrome P450
- Suhara, Y., Itoh, S., Ogawa, M., Yokose, K., Sawada, T., Sano, T., Ninomiya, R. and Maruyama, H.B. 1981. Regio-selective 10-hydroxylation of Patchoulol, a Sesquiterpene, by *Pithomyces* species. *Applied and Environmental Microbiology*. 42(2):187-191
- Sigdel, S., Hui, G., Smith, T.J., Murell, J.C. and Lee, J-K. (2015) Molecular Dynamic Simulation to Rationalize Regioselective Hydroxylation of Aromatic Substrates By Soluble Methane Monooxygenase. *Bioorganic & Medical Chemistry Letters*. 25(7): 1611-1615

- Shishirkawde. 2011. Biotransformation.
<http://www.slideshare.net/shishirkawde/biotransformation-10417087>
- Tuckerman, M. 2010. *Statistical Mechanics, Theory and Molecular Simulation*. Oxford Graduate Texts
- Tuckerman, M. E., and Martyna, G.J. 2000. Understanding Modern Molecular Dynamics: Techniques and Application. *J. Phys. Chem. B.* 104: 159-178
- Thapa, S.K., and Adhikari, N.P. 2013. A Molecular Dynamics Study Of Oxygen Gas In Water At Different Temperatures. *International Journal of Modern Physics B.* (27) 1350023.
- Teisseire, P., Chemistry of patchouli oil. *Riv. Ital. Essenze Profumi Piante Offic. Aromi Saponi Cosmet.* (1973) 572-592
- Vasic-Racki, D., Liese, A., and Seelbach, K. 2006. History of Industrial Biotransformations – Dreams and Realities. WILEY-VCH Verlag GmbH & Co. KGaA, Weinheim.
- Vollhardt, K. P. C and Schore, N. E. 2007 *Organic Chemistry: Structure and Function*. New York: Bleyer, Brennan
- Yadav, S., Yadav, R.S.S., Yadava, S., and Yadav, K.D.S. 2011. stereoselective hydroxylation of ethylbenzene to (r)-1-phenylethanol using mycelia of *aspergillus niger* as catalyst. *Catalysis Communications.* 12(9):781-784
- Yu X.-D., Xie J.-H., Wang Y.-H., Li Y.-C., Mo Z.-Z., Zheng Y.-F., Su J.-Y., Liang Y.-e., Liang J.-Z., Su Z.-R., and Huang P. 2014. Selective Antibacterial Activity of Patchouli Alcohol Against *Helicobacter pylori* Based on Inhibition of Urease. *Phytother. Res.* 29.67–72,
- Yasar, A., Ucencu, O., Gulec, C., Inceer, H., Ayaz, S., and Yayl, N. 2005. GC-MS analysis of chloroform extracts in flowers, stems and roots of *Tripleurospermum callosum*. *Pharma Biol.* 43:108.
- Zumdahl, S. S., and Zumdahl, S.A. 2007. *Chemistry*. Houghton Mifflin.